Ride Quality and Drivability of a Typical Passenger Car subject to Engine/Driveline and Road Non-uniformities Excitations

Examensarbete utfört i Fordonssystem
vid Tekniska högskolan i Linköping
av

Neda Nickmehr

LiTH-ISY-EX--11/4477--SE

Linköping 2011

Ride Quality and Drivability of a Typical Passenger Car subject to Engine/Driveline and Road Non-uniformities Excitations

Examensarbete utfört i Fordonssystem
vid Tekniska högskolan i Linköping
av

Neda Nickmehr

LiTH-ISY-EX--11/4477--SE

Handledare: **Neda Nickmehr**
ISY, Linköpings universitet

Examinator: **Jan Åslund**
ISY, Linköpings universitet

Linköping, 7th June 2011

Avdelning, Institution
Division, Department
Division of vehicular system
Department of Electrical Engineering
Linköpings universitet
SE-58183Linköping, Sweden

Datum
Date
2011-06-07

Språk
Language
☐ Svenska/Swedish
■ Engelska/English
☐ _____

Rapporttyp
Report category
☐ licentiatavhandling
■ Examensarbete
☐ C-uppsats
☐ D-uppsats
☐ Övrigrapport
☐ _____

ISBN —

ISRN
LiTH-ISY-EX--11/4477--SE

Serietitel och serienummer ISSN
Title of series, numbering —
_____

URL för elektronisk version
http:\\ urn:nbn:se:liu:diva-69499

Title Ride Quality and Drivability of a Typical Passenger Car subject to Engine/Driveline and Road Non-uniformities Excitations

Författare Neda Nickmehr
Author

Sammanfattning
Abstract

The aim of this work is to evaluate ride quality of a typical passenger car. This requires both identifying the excitation resources, which result to undesired noise inside the vehicle, and studying human reaction t applied vibration. Driveline linear torsional vibration will be modelled by a 14-degress of freedom system while engine cylinder pressure torques are considered as an input force for the structure. The results show good agreement with the corresponding reference output responses which proves the accuracy of the numerical approach fourth order Runge-kutta. An eighteen-degree of freedom model is then used to investigate coupled motion of driveline and the tire/suspension assembly in order to attain vehicle body longitudinal acceleration subject to engine excitations. Road surface irregularities is simulated as a stationary random process and further vertical acceleration of the vehicle body will be obtained by considering the well-known quarter-car model including suspension/tire mechanisms and road input force. Finally, ISO diagrams are utilized to compare RMS vertical and lateral accelerations of the car body with the fatigue-decreased proficiency boundaries and to determine harmful frequency regions. According to the results, passive suspension system is not functional enough since its behaviour depends on frequency content of the input and it provides good isolation only when the car is subjected to a high frequency excitation. Although longitudinal RMS acceleration of the vehicle body due to engine force is not too significant, driveline torsional vibration itself has to be studied in order to avoid any dangerous damages for each component by recognizing resonance frequencies of the system. The report will come to an end by explaining different issues which are not investigated in this thesis and may be considered as future works.

Nyckelord
Keywords Ride quality, Driveline, Engine excitations, Road non-uniformities, Suspension System, Torsional vibration, Random process

Upphovsrätt

Copyright

Abstract

The aim of this work is to evaluate ride quality of a typical passenger car. This requires both identifying the excitation resources, which result to undesired noise inside the vehicle, and studying human reaction to applied vibration. Driveline linear torsional vibration will be modeled by a 14-degress of freedom system while engine cylinder pressure torques are considered as an input force for the structure. The results show good agreement with the corresponding reference output responses which proves the accuracy of the numerical approach fourth order Runge-kutta. An eighteen-degree of freedom model is then used to investigate coupled motion of driveline and the tire/suspension assembly in order to attain vehicle body longitudinal acceleration subject to engine excitations. Road surface irregularities is simulated as a stationary random process and further vertical acceleration of the vehicle body will be obtained by considering the well-known quarter-car model including suspension/tire mechanisms and road input force. Finally, ISO diagrams are utilized to compare RMS vertical and lateral accelerations of the car body with the fatigue-decreased proficiency boundaries and to determine harmful frequency regions.

According to the results, passive suspension system is not functional enough since its behavior depends on frequency content of the input and it provides good isolation only when the car is subjected to a high frequency excitation. Although longitudinal RMS acceleration of the vehicle body due to engine force is not too significant, driveline torsional vibration itself has to be studied in order to avoid any dangerous damages for each component by recognizing resonance frequencies of the system. The report will come to an end by explaining different issues which are not investigated in this thesis and may be considered as future works.

Acknowledgments

This work has been carried out at vehicular system division, ISY department, Linköping University, Sweden. The thesis would not have been possible without the support of many people and division laboratory facilities. I wish to express my gratitude to my examiner and supervisor, Dr. Jan Åslund and PhD student Kristoffer Lundahl who were abundantly helpful and offered invaluable assistance, support and guidance. Special thanks also to my bachelor supervisor professor Farshidianfar for sharing the literature and invaluable assistance. I would like to express my love and gratitude to my beloved parents **Maryam** and **Ahmad** for their understanding and endless love, through the duration of my master study.

Linköping, May 2011

Neda Nickmehr

Table of Contents

1 Chapter 1 1

1.1 Background 1

1.2 Objective 2

1.3 Assumptions and Limitations 2

1.4 Outline 3

2 Chapter 2 5

2.1 Driveline and vehicle Modeling 5

2.2 Road Surface Irregularities 5

2.3 Human Response to vibration 5

3 Chapter 3 7

3.1 Introduction 7

3.2 Driveline components 7

3.2.1 Engine, flywheel and the main excitation torque 7

3.2.2 Clutch Assembly 18

3.2.3 Gearbox 19

3.2.4 Cardan (propeller) shaft and universal (Hooke's) joints 19

3.2.5 Differential and final drive system 20

3.2.6 Damping in the whole driveline system 21

3.3 Overall driveline model 21

3.4 Torsional vibration 22

4 Chapter 4 23

4.1 Introduction 23

4.2 Mathematical model and system matrices 23

4.3 Summary of Modal analysis 25

4.4 Natural frequencies 27

5 Chapter 5 29

5.1 Introduction 29

5.2 Mathematical model for forced vibration of the driveline system 29

5.3 Time responses of driveline at clutch and driving wheels 30

5.4 Power spectral densities of time histories 34

6 Chapter 6 37

6.1 Introduction 37

6.2 Coupled vibration of driveline and the vehicle body 37
6.3 Tire model and longitudinal force 37
6.4 18-degrees of freedom system for whole vehicle model and its equations of motion 38
6.5 Time response of the system 42
6.6 Studying the influence of stiffness and damping coefficients 46
7 Chapter 7 49
7.1 Introduction 49
7.2 Quarter-car model and performance of suspension system 49
7.3 Road roughness classification by ISO and the recommended single-sided vertical amplitude power spectral density 53
7.4 Typical passenger car driver RMS acceleration to an average road roughness 54
8 Chapter 8 57
8.1 Introduction 57
8.2 International Standard ISO 2631-1:1985 57
8.3 Results and Discussion 58
8.4 Thesis conclusion 60
8.5 Future works 60
9 References 63
10 Appendix 65
10.1 LTI object 65
10.2 Driveline Modeling MATLAB code 65
10.3 Power spectral density function 68
10.4 Vehicle modeling MATLAB codeATLAB code 70

Figures

Figure 1-1, the ride dynamic system 1
Figure 3-1, Front-engine rear-wheel-drive vehicle driveline [3] 7
Figure 3-2, Main engine parts [1] 8
Figure 3-3, Original System of a crank [3] 8
Figure 3-4, Equivalent system of crankshaft and its compact model [3] 9
Figure 3-5, output torque of a four-stroke single-cylinder engine [1] 9
Figure 3-6, Line diagram of cylinders arrangement 10
Figure 3-7, engine torque in the case of four cylinders 10
Figure 3-8, 10 seconds pressure recording from cylinder 1 11
Figure 3-9, 10 seconds pressure recording from cylinder 2 12
Figure 3-10, Crank mechanism 13
Figure 3-11, Torque output of cylinder 1, total and fluctuating part, during 10 seconds and one working cycle 14
Figure 3-12, Torque output of cylinder 2, total and fluctuating part, during 10 seconds and one working cycle 15
Figure 3-13, Output torques from 4 cylinders in the same plot 16
Figure 3-14, Compact crankshaft model for a four-cylinder engine 17
Figure 3-15, PSD for output torque from cylinder 1 17
Figure 3-16, PSD for output torque from cylinder 2 18
Figure 3-17, Clutch system [22] 18
Figure 3-18, Gearbox model [3] 19
Figure 3-19, Hooke's (cardan) joints [1] 20
Figure 3-20, propeller shafts and universal joints mathematical model [3] 20
Figure 3-21, Final drive system and its equivalent model [3] 21
Figure 3-22, Damped torsional vibration mathematical model of driveline system [3] 22
Figure 5-1, Driveline model 29
Figure 5-2, Time response at the clutch, using different methods of solution: Black-> Modal analysis, Blue-> ODE45, Green-> self-written Runge-Kutta code with nonzero initial conditions and yellow-> with zero initial conditions 31
Figure 5-3, zoomed version of figure 5.2 in order to see the instability of modal analysis and ODE45 solutions 31
Figure 5-4, Time response at the clutch with the aid of Runge-Kutta method 32
Figure 5-5, Time response at the driving wheels 33
Figure 5-6, Power spectral density of the time response at the clutch 34
Figure 5-7, Power spectral density of the time response at the driving wheels 35
Figure 6-1, tire model [3] 38
Figure 6-2, overall vehicle model [3] 39
Figure 6-3, Total engine excitation torques after applying filtration 44
Figure 6-4, torsional velocity vibration of driving wheels due to engine excitation torques by using table 6.1 data values 44
Figure 6-5, zoomed version of Figure 6-4 between seconds 8 to 9 45

Figure 6-6, Longitudinal velocity vibration of the vehicle body and axle due to engine excitation torques by using table 6-1 data values 45
Figure 6-7, zoomed version of Figure 6-6 46
Figure 6-8, torsional velocity of driving wheels with low damping 47
Figure 6-9, Longitudinal velocities of vehicle body and axle with low damping 48
Figure 6-10, Longitudinal velocities of vehicle body and axle with low suspension system stiffness 48
Figure 7-1, Two-degrees of freedom model vehicle 49
Figure 7-2, Transmissibility as a function of frequency ratio for a single-degree of freedom system 51
Figure 7-3, Modified quarter-car model including seat displacement 51
Figure 7-4, Measured vertical acceleration of a passenger car seat traveling at 80 Km/hr over an average road 54
Figure 7-5, vehicle body vertical acceleration subject to an average road roughness with 80 Km/hr traveling speed 55
Figure 8-1, ISO 2631-1:1985 "fatigue-decreased proficiency boundary": vertical acceleration limits as a function of frequency and exposure time [4] 57
Figure 8-2, ISO 2631-1:1985 "fatigue-decreased proficiency boundary": longitudinal acceleration limits as a function of frequency and exposure time [4] 58
Figure 8-3, vehicle body vertical acceleration due to road excitation in comparison with ISO ride comfort boundaries 58
Figure 8-4, Measured longitudinal acceleration of a passenger car body due to engine excitation torques 59

Tables

Table 3-1, Engine properties 10
Table 4-1, Typical values for equivalent parameters of a vehicle driveline [3] 24
Table 4-2, Undamped natural frequencies of whole driveline model using typical parameter values for a passenger car 27
Table 4-3, first five natural modes of driveline system 28
Table 6-1, Overall vehicle properties [3] 43
Table 7-1, Tire/suspension properties [3] 50
Table 7-2, Classification of road roughness proposed by ISO [4] 53

1 Chapter 1

Introduction

1.1 Background

Ride quality is an important parameter for car manufacturers, which clarifies the transmission level of *unwanted* noises and vibrations from vehicle body to the passengers. The term *unwanted* is defined according to human response to vibration which is different from one person to another and will be described more in the next chapters. Increasing customer demands for more comfortable cars and better ride quality, not only requires "full understanding of human response to excitation", but also it is needed to study "different sources which may result to vibration of vehicle body", and "dynamic behavior of the automobiles".

In order to provide better realization of ride behavior [1], it is useful to show the ride dynamic system as follows (Figure 1-1):

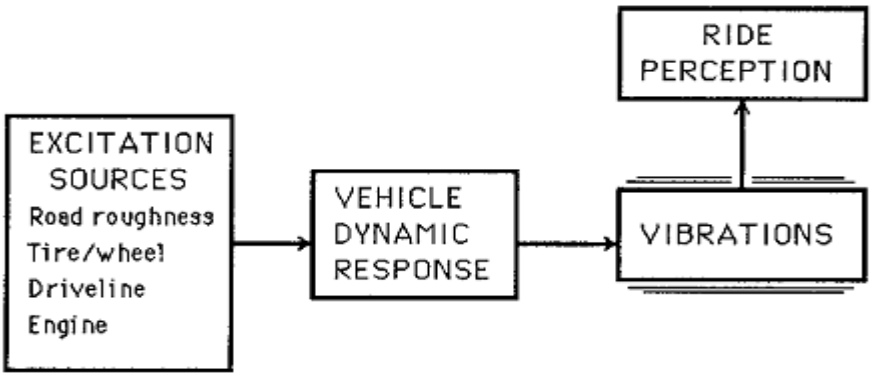

Figure 1-1, the ride dynamic system

According to Figure 1-1, there are four different excitation sources that may be divided into two categories: 1) road surface irregularities and 2) on-board origins which result from rotating parts (engine, driveline and non-uniformities (imbalances) of tire/wheel).

Since the days of first vehicles, the attempts have been made to isolate the car body from road roughness[1], and the car suspension system is responsible for this duty. Road profile is a random function which acts as an input to suspension system, furthermore theory of stochastic processes and power spectral densities have been utilized in the literatures to model this random signal. The two degrees of freedom model (2-DOF) known as a quarter-car model is used to simulate suspension system and vehicle body [2]. The goal is to optimize the suspension system parameters to decrease the undesired effects on the vehicle body (Chapter 7) according to ride comfort criterion that may be selected.

Driveline is one of the considerable sources of noise and vibration for any type of automobiles, which is composed of everything from the engine to the driven wheels. Driveline torsional oscillations fall into two broad categories: "gear rattle" and "driveline vibration". Idle gear rattle is a consequence of gear tooth impacts, and driveline vibrations are noises which come from the driveline system parts such as engine, clutch and universal

[1] roughness is described by the elevation profile along the wheel tracks over which the vehicle passes [1]

joints, while the vehicle is in motion at different running situations [3], we are interested in the driveline system vibration in three aspects: 1) finding system natural frequencies in order to avoid coincidence with forced frequencies and resonance occurrence, 2) to determine forced response subject to engine oscillatory torque and universal joints and 3) transient response. It should be noted that some components of driveline such as universal (Hooke's) joints result to nonlinear behavior of the system, and in addition the torsional vibration of driveline can be coupled with the horizontal and vertical motions of vehicle body and rear axle, these phenomenon may cause the complication of the system.

Modeling the system (quarter car model or driveline) and obtaining the response, it's time to evaluate ride quality of the system. Hence it is necessary to specify ride comfort limits. Various methods have been developed over the years for assessing human tolerance to vibration [4] which will be more explained in chapter 8.

1.2 Objective

The goal of this thesis is divided into two major parts:
1- To model the driveline and engine fluctuating torque in order to find free and forced responses of the system and furthermore studying the sensitivity of driveline behavior by changing design parameters. The attempt is made to simulate driveline as a 14-degrees-of-freedom (DOF) system and the whole vehicle as an 18-DOF mechanism and at last determining the horizontal acceleration of sprung mass (vehicle body) due to engine torque using Runge-kutta numerical method. Acceleration time history is then converted to frequency domain using power spectral density tool in order to compare with ride comfort diagrams.
2- To use quarter car model and obtain driver response subject to road random irregularities with the aid of random process theory. In this part of the report, the importance of the suspension system to decrease the undesired motions will be illustrated.

1.3 Assumptions and Limitations

In this project a lumped-parameter model is used for studying the torsional vibration of driveline system which assumed to be a set of inertia disks linked together by torsional, linear and massless springs [3]. A normal four cylinder rear drive passenger car will be considered and the system parameter values such as sprung and unsprung masses, all the stiffness and damping coefficients have been chosen according to references [3] and [4] and different vehicle companies database. It should also be noted that this work is based on the PhD thesis by **El-Adl Mohammed Aly Rabeih** which is done in 1997.

The engine fluctuating torque (as will be described later) consists of two major parts: gas pressure torque and inertia torque[1] which are come from cylinder gas pressure and reciprocating components of engine, respectively. however in the current report, we will only study the effects of the pressure torque since there is no useful data for the mass of reciprocating parts, furthermore the cylinders pressure are measured in the vehicular system engine Laboratory for a four-stroke four-cylinder engine with the firing order of 1-3-4-2. Moreover the nonlinear torque which is resulted by Hook's joints has been introduced in this thesis while defining the response of the system subject to this couple requires strong nonlinear method which is beyond the aim of this work.

In order to investigate the road surface influences, three assumptions have been included:

[1] Especially in high speed vehicles, the inertia torque is very important!

- The road profile is assumed to be a stationary ergodic random process, however in reality the road's profiles are non-stationary functions.
- the amplitude distribution of the road roughness is assumed to be Gaussian
- The car has a constant speed and travels on a straight line.

1.4 Outline

The thesis is composed of ***8 chapters***. This introductory chapter is followed by a short literature review of what has been done so far associated to this work. In *chapter 3*, driveline system and its different parts have been modeled as well as relations of converting cylinders pressure to the torques which are delivered by crankshaft. *Chapter 4* included of mathematical simulation of driveline, and modal analysis to find natural frequencies of the system. *Chapter 5* consists of introducing different methods of obtaining forced response of 14-degrees of freedom system. In *chapter 6* the whole vehicle model has been described and horizontal vibration of the vehicle body and rear axle is obtained subject to driveline torsional oscillations. Besides, the parameter values will be changed in order to study the sensitivity of the system to stiffness and damping coefficients. *Chapter 7* consists of using quarter-car model to define the response of driver to road non-uniformities which is an input to the system. The report will be ended by *chapter 8* which has included international standard ISO for evaluation of human exposure to whole-body vibration [4] and calculating RMS vertical and horizontal accelerations of our model to compare with ride comfort criteria. Moreover the conclusion section and future work suggestions are the last parts of the final chapter.

2 Chapter 2

Previous work

2.1 Driveline and vehicle Modeling

During the last four decades and from the early days of automotive industry, the attempts have been made to reach the desired ride comfort and quieter vehicles. Since driveline torsional behavior is one of the major resources of unwanted vibrations in the cars, significant researches have been done by different car companies and university scientists in order to gain an acceptable model for driveline system and its components structure. Skyes and Wyman in 1971, and Ergun in 1975 were among the first people who calculated natural frequencies of a conventional automobile driveline system theoretically and experimentally, respectively [3]. Reik in 1990 studied the main vibration sources of driveline system and he considered the gas pressure torque and its effects [5]. Zhanqi *et al* in 1992, [6], constructed a mathematical model including torsional, vertical and vehicle fore-aft vibrations to study the coupling of those vibrations together, he also has investigated the influences of different parameter values on the response of the vehicle chassis and axle. Significant experimental measurements of system behavior and principal modes have been done by different researchers in the years 1980-1990 [7]. El-Adl Mohammed Aly Rabeih has done a complete research in 1997 concerning the *driveline* and *compelete vehicle* free and forced vibration modelings, sensitivity analysis of *driveline* and *suspension system* parameter values. he used runge-kutta numerical method in order to find displacement and velocity time histories at different points of the model [3]. In the last decade, more investigations are focused on the nonlinearity in driveline system such as gear rattle, backlash, and bahvior of the system during clutch engagement.

2.2 Road Surface Irregularities

The health, protection, ride comfort and performance of both driver and passengers in automobiles are influenced by the type of the surface, over which the vehicle moves. Earlier researches in the automotive industry included of subjecting mathematical models to deterministic inputs, however in real situation surface profiles are rarely simple forms. A significant effort has been done between the years 1950-1970 in order to find the spectrum of road roughness [10]. Furthermore attempts by various organizations have been done over the years to divide the road surface irregularities into different classes, the international organization for standardization (ISO) has presented this classification (A-H) based on the power spectral density [4].

A huge amount of reports during the last four decades have included studies about passive, semi-active and active suspension systems and vibration isolations in automobiles as well as different optimizations methods to define optimum parameter values of suspension system subject to random excitation from the road [13].

2.3 Human Response to vibration

Significant investigations have been conducted to acquire ride comfort limitations. There are different standards to evaluate drivability and ride quality of a vehicle which are mentioned

in references [4] and [17]. According to ISO 2631-1:1985, four parameters have trivial influences on obtaining human response to vibration which are intensity, frequency, direction and exposure time. In this work, these criterions will be used to study the ride comfort of the desired model.

3 Chapter 3

Description of driveline and torsional phenomena

3.1 Introduction

In this chapter, torsional models of driveline system and its components are defined, since driveline torsional vibration due to engine torque excitations is one of the main reasons of undesired noise in the vehicles. Further, the necessary relations in order to obtain oscillatory engine torques from cylinder pressures time histories are introduced.

3.2 Driveline components

The driveline function is to transmit mechanical energy of the engine to the wheels and that will be occurred through different parts. A classical front-engine rear-wheel-drive vehicle driveline is illustrated in Figure 3-1, Front-engine rear-wheel-drive vehicle driveline[3]. The most common components of the system are engine, flywheel, clutch, gearbox, propeller (or Cardan) shaft and universal joints, differential and rear axle assembly and tires. According to the goal of the thesis and in order to simplify the analysis of driveline vibration, a lumped parameter model is used for the whole driveline system. However from the vibration theory, it is known that in the real world the systems are distributed, and therefore cannot be modeled as point masses. Although, utilizing this simple simulation has some advantages and the most important one is the ability of estimating natural frequencies and the forced response of the system subject to different excitations without complicated mathematics. In the following sections, each part is described in more detail and an appropriate model will be suggested.

3.2.1 Engine, flywheel and the main excitation torque

Engine is the primary power source on a vehicle. Rotating behavior of the engine and discrete strokes during its working cycle result to torsional vibration excitation of the driveline.

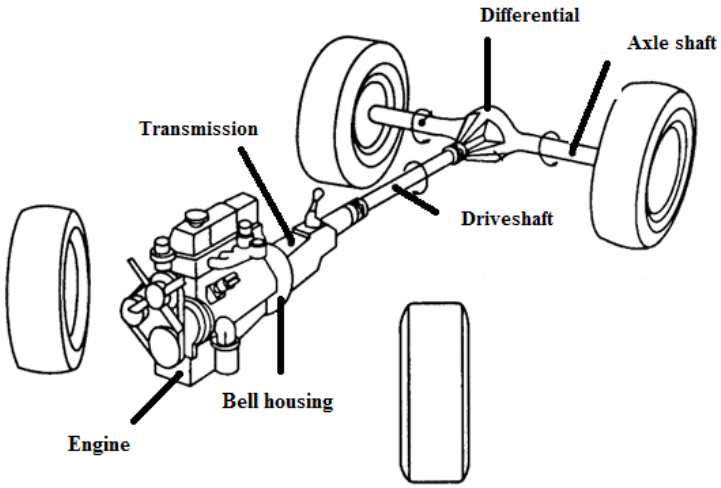

Figure 3-1, Front-engine rear-wheel-drive vehicle driveline [3]

The main parts of the engines are: cylinder, piston, connecting rod and crankshaft[1] which are shown in Figure 3-2, Main engine parts. The crankshaft rotates by pushing the piston up and down in the cylinder area, there are two dead points (at extreme down and up positions) where the pressure on the piston will have no effects to force the crankshaft to turn, a ***stroke*** is called to the movement of piston from one dead center to another dead center. Four-stroke engine consists of induction, compression, power and exhaust steps, more description of engine parts and strokes function can be found in the books of motor vehicle technology and it is not the aim of this thesis.

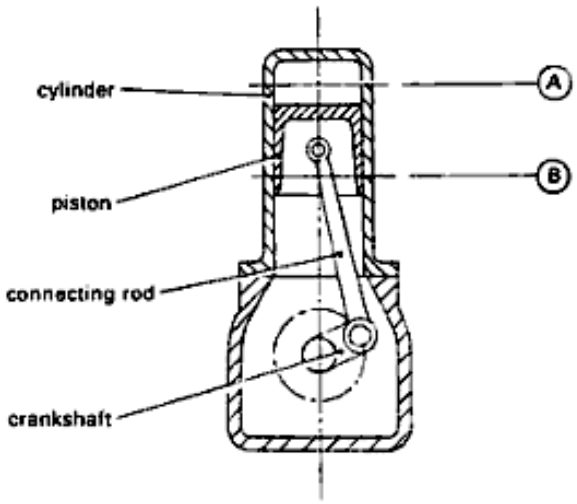

Figure 3-2, Main engine parts [1]

Since we are interested in torsional vibration of the driveline, the rotational dynamics of the engine will be simulated by taking into account the crankshaft system which is shown in Figure 3-3:

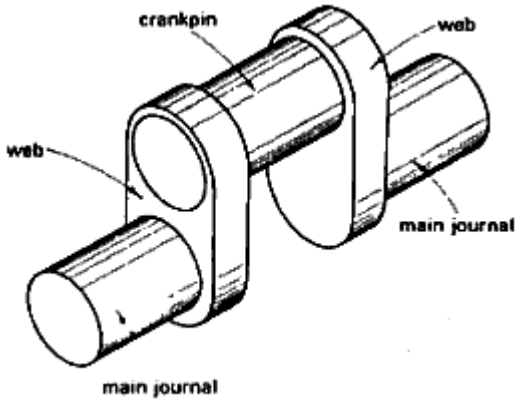

Figure 3-3, Original System of a crank [3]

The compact crankshaft system can be modeled as follows (Figure 3-4), where the rotational J_w (journal+ crank pin+ webs) and reciprocating parts J_r (piston+ connecting rod+ piston pin) are composed together as one final inertia disk[2] J_1.

[1] The crankshaft (crank) is the part of an engine which translates reciprocating linear piston motion into rotation, crankshaft connects to flywheel.

[2] It should be noted that the engine mounts, which are important tools to decrease the unwanted effects of engine vibration on the other pieces and to isolate the engine from the external excitations, will not be considered here and their suitable influence can be perused in the next studies.

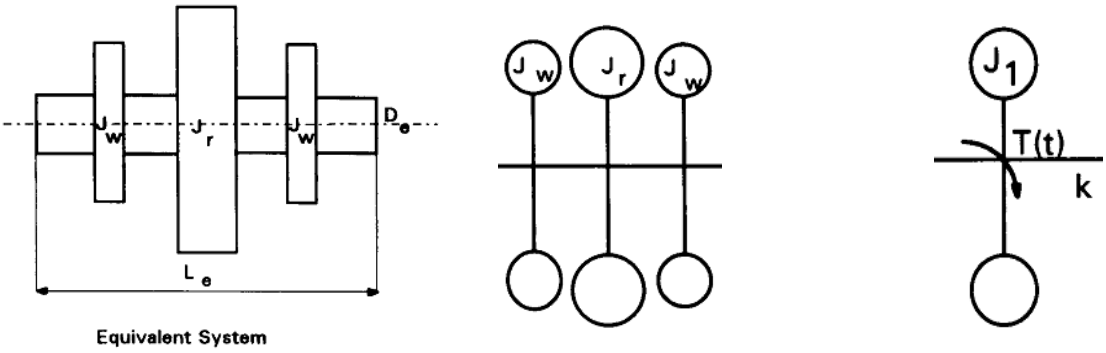

Figure 3-4, Equivalent system of crankshaft and its compact model [3]

In the above figure, $T(t)$ is the engine excitation torque, and k is the equivalent torsional stiffness which is calculated in reference [3].

Because of the cyclic operation of a piston engine, the torque which is delivered at the crankshaft is oscillatory and consists of a steady-state component (mean torque) plus superimposed torque fluctuations $T(t)$[1] (Figure 3-5):

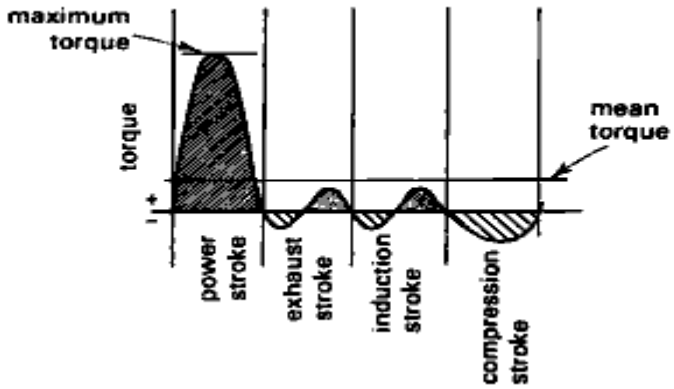

Figure 3-5, output torque of a four-stroke single-cylinder engine [1]

Concerning to practical issues, there are always more than one cylinder which are arranged to have their power strokes in succession [20], the most common case is to have four cylinders. the firing order of the engine illustrates the order in which the cylinders act, *in this thesis we will consider four-stroke four-cylinder engine with firing order 1-3-4-2*, consequently we will have 720 degrees per cycle of operation for this kind of engine and each stroke takes 180 degrees. Figure 3-6 shows a simplified line-diagram of the cylinders and cranks,

[1] Moreover, the torsional vibration of the crankshaft due to longitudinal torque on the moving part of the engine, is of particular importance because many crankshafts have failed subject to this torque.

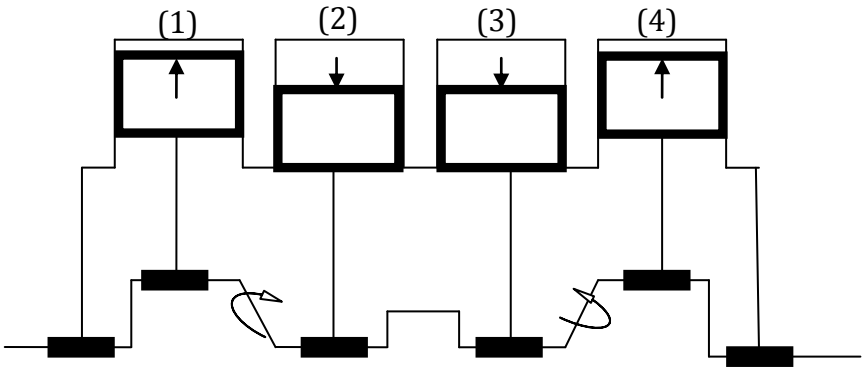

Figure 3-6, Line diagram of cylinders arrangement

As it is seen in the above figure, pistons move in pairs: 1&4 and 2&3. The measured pressures in engine laboratory are associated to cylinders 1 and 2 and the assumption of this work is that: cylinders 1 & 4, and 2 & 3 have the same pressure distributions, respectively. The following graph presents the expected torque for a four cylinder engine.

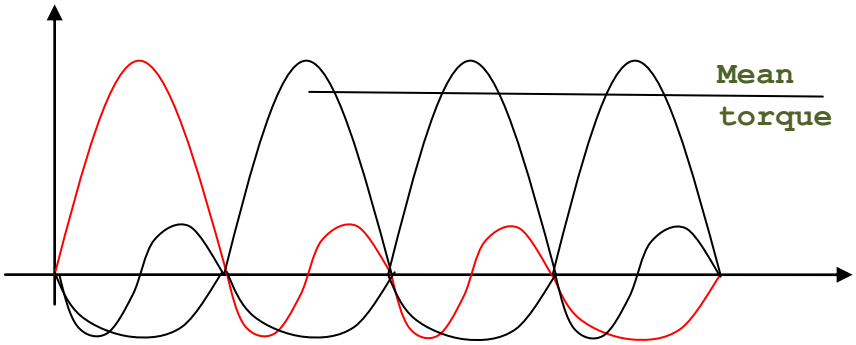

Figure 3-7, engine torque in the case of four cylinders

Each cylinder excitation torque[1] formed from two main parts[2]: *gas-pressure torque* {$Tg(t)$} and *inertia torque*, however as it is also mentioned in section 1.3, in this report we will study only the influence of the gas-pressure. Gas-pressure torque itself composed of harmonics[3] and steady-value, while the steady-value (mean value) will not excite torsional vibration; it is omitted in the calculations.

Figure 3-8 and Figure 3-9 show the cylinders 1 and 2 pressures time history {$p_{g1}(t)$ & $p_{g2}(t)$} respectively, in addition the characteristics of the LAB engine are given in Table 3-1,

Table 3-1, Engine properties

Num. of strokes	Num. of cylinders	Piston Diameter, m	Crank radius, m	Connecting rod length, m	Mean Torque[4], N.m	Engine speed, RPM, rad/sec	Expected fluctuating torque fundamental frequency[5]
4	4	**0.086**	**0.043**	**0.043*4**	**100**	**2000** **ω=209.4395**	**104.72 rad/s** **or 16.66 Hz**

[1] which causes torsional vibration
[2] the friction torque is assumed to be small compared to these two main components
[3] which repeats themselves every complete working cycle, the interval of repetition is two revolutions of the crankshaft (4π) and the period is $4\pi/\omega$ [3]
[4] The useful engine mean torque is the steady part of cylinders net torque which is measured by a sensor at flywheel point, this value is normally provided by the engine manufacturer
[5] Refer to page 12

In this stage, the relations of converting cylinder pressure to delivered torque by the crankshaft are presented. In addition the mean value of calculated torque will be subtracted from the total torque in order to find the fluctuating part,

- Applying force on the piston (F_p) in Figure 3-10, Crank mechanism = Gas pressure $\{p(t)\}$ * piston area (A_p).

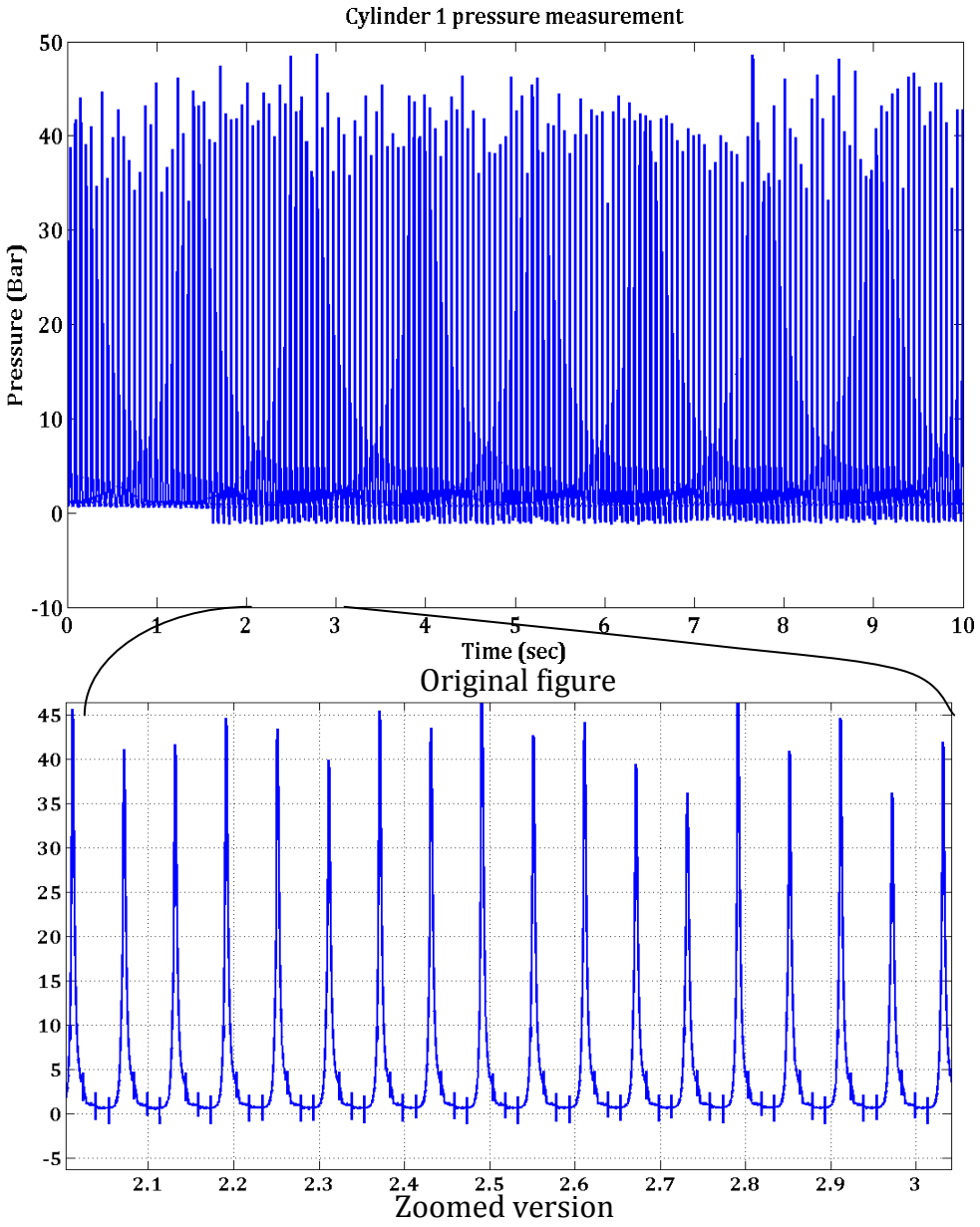

Figure 3-8, 10 seconds pressure recording from cylinder 1

- Gas torque $\{Tg(t)\}= F_p$ * $dx_p/d\varphi$ where crank angle $\varphi = \omega t$ and ω is the constant crankshaft speed, furthermore x_p denotes the piston displacement
- According to Figure 3-10, Crank mechanism, it is possible to derive the expression for $dx_p/d\theta$ [21],
- In the above figure, r is the crank radius and l is the connecting rod length (these values have been provided in Table 3-1).

- Piston displacement in terms of crank angle can be estimated[1] in the following form:

$$x_p \approx r(1 - cos\omega t) + \frac{r^2}{2l}\sin^2 \omega t \qquad 3.1$$

Therefore, the differentiation of x_p with respect to $\theta = \omega t$ is[2]:

$$\dot{x}_p = r \sin\theta + \frac{r^2}{l}\sin\theta \cos\theta \qquad 3.2$$

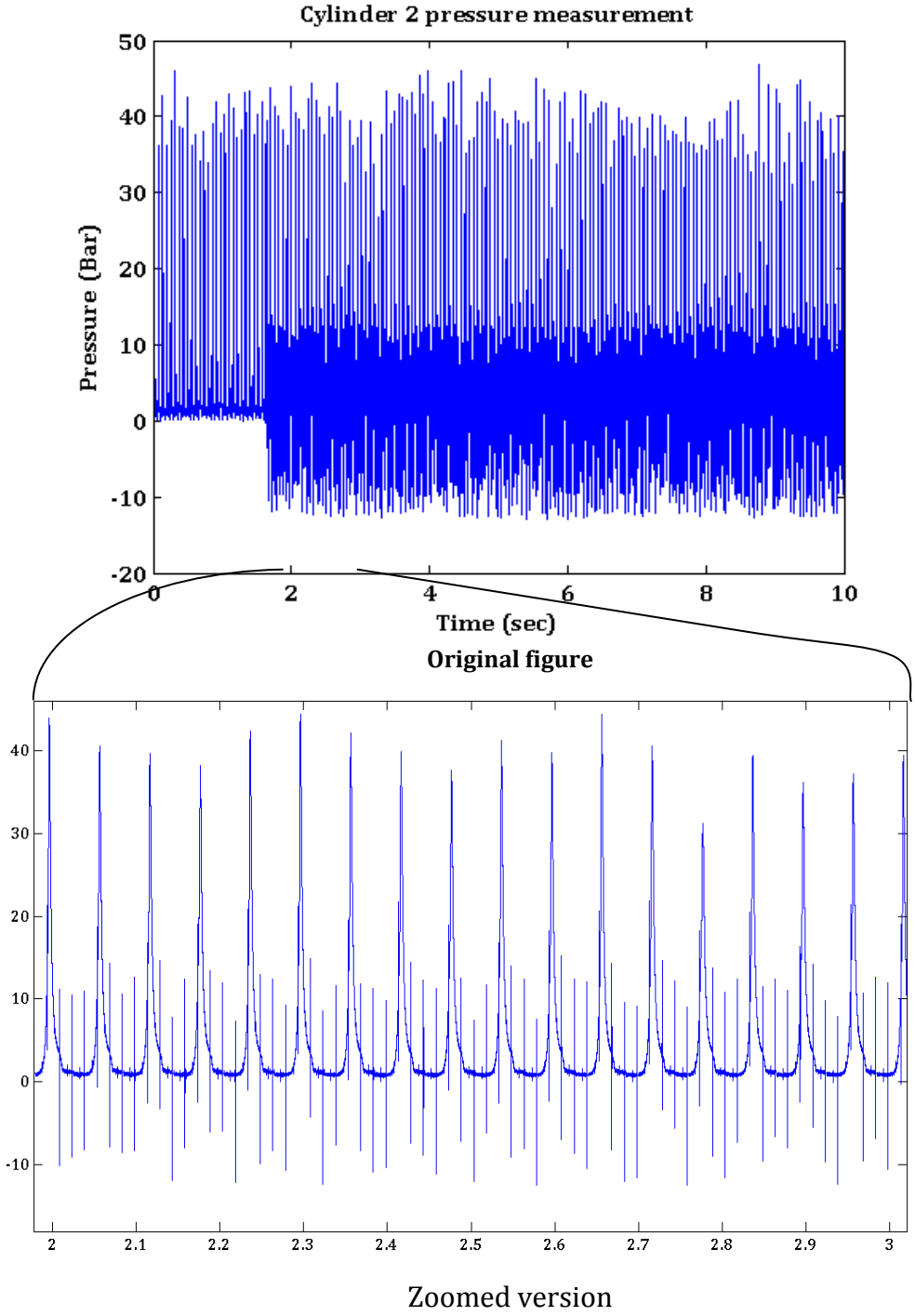

Figure 3-9, 10 seconds pressure recording from cylinder 2

[1] The exact expression is available in reference [23][21]

[2] It should be noted that $\frac{r}{l} = \frac{1}{4}$

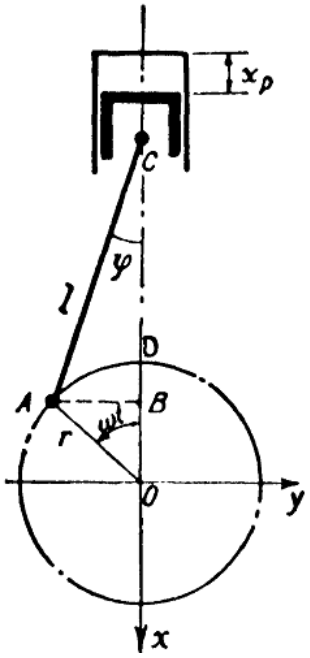

Figure 3-10, Crank mechanism

- Finally, the associated torque due to combustion, $T_g(t)$ is

$$T_g(t) = p_g\, A_p\, \dot{x}_p \qquad 3.3$$

Figure 3-11 and Figure 3-12 show the total torque outputs (in 10 seconds and in one working cycle as well) and their fluctuating parts from cylinders 1 and 2 respectively.
As it was expected, the computed torque in one working cycle is similar to what was demonstrated previously (Figure 3-5) for a four-cylinder four-stroke engine. In Figure 3-11 and Figure 3-12, different strokes are clearly distinguishable. Cylinders 3 and 4 output torques are equal to cylinders 1 and 2 outputs, *according to the assumption which was made before*. The noises which are seen in the plots are removable using filter commands, the necessity of using filtration and the associated MATLAB commands will be described more in detail in the next chapters. Finally to check the correctness of presented torque calculations from the measured output pressures of cylinders 1&2, it is functional to find the mean value for summation of torque 1, torque 2, torque 3 and torque 4 {$T_{g1}(t)$, $T_{g2}(t)$, $T_{g3}(t)$, and $T_{g4}(t)$}. We expect that this mean value have to be around the value which was set during experiment, 100N.m: with the aid of MATLAB command mean (torque1+torque2+torque3 +torque 4) = 109.5114, which seems acceptable according to 100 N.m.

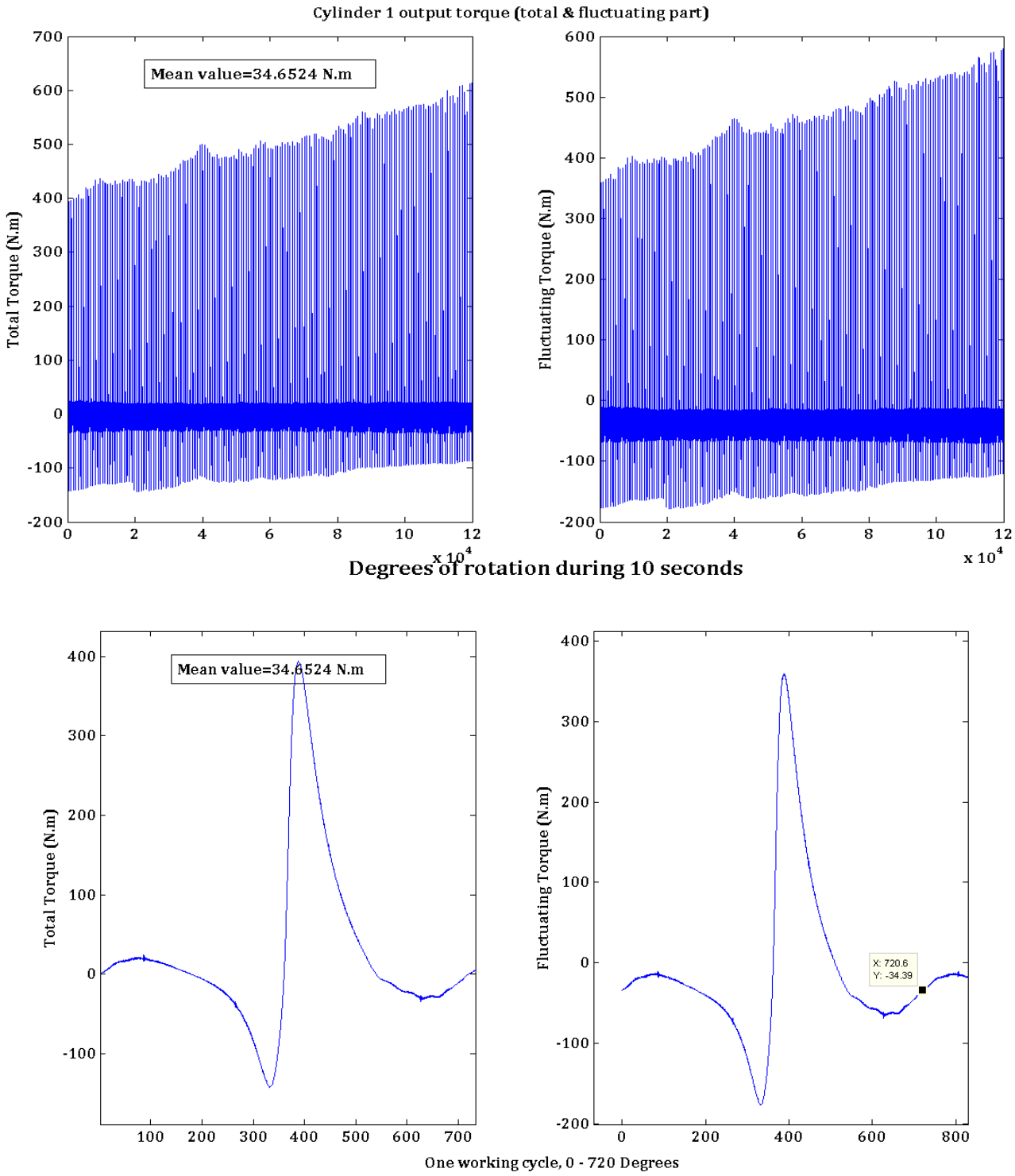

Figure 3-11, Torque output of cylinder 1, total and fluctuating part, during 10 seconds and one working cycle

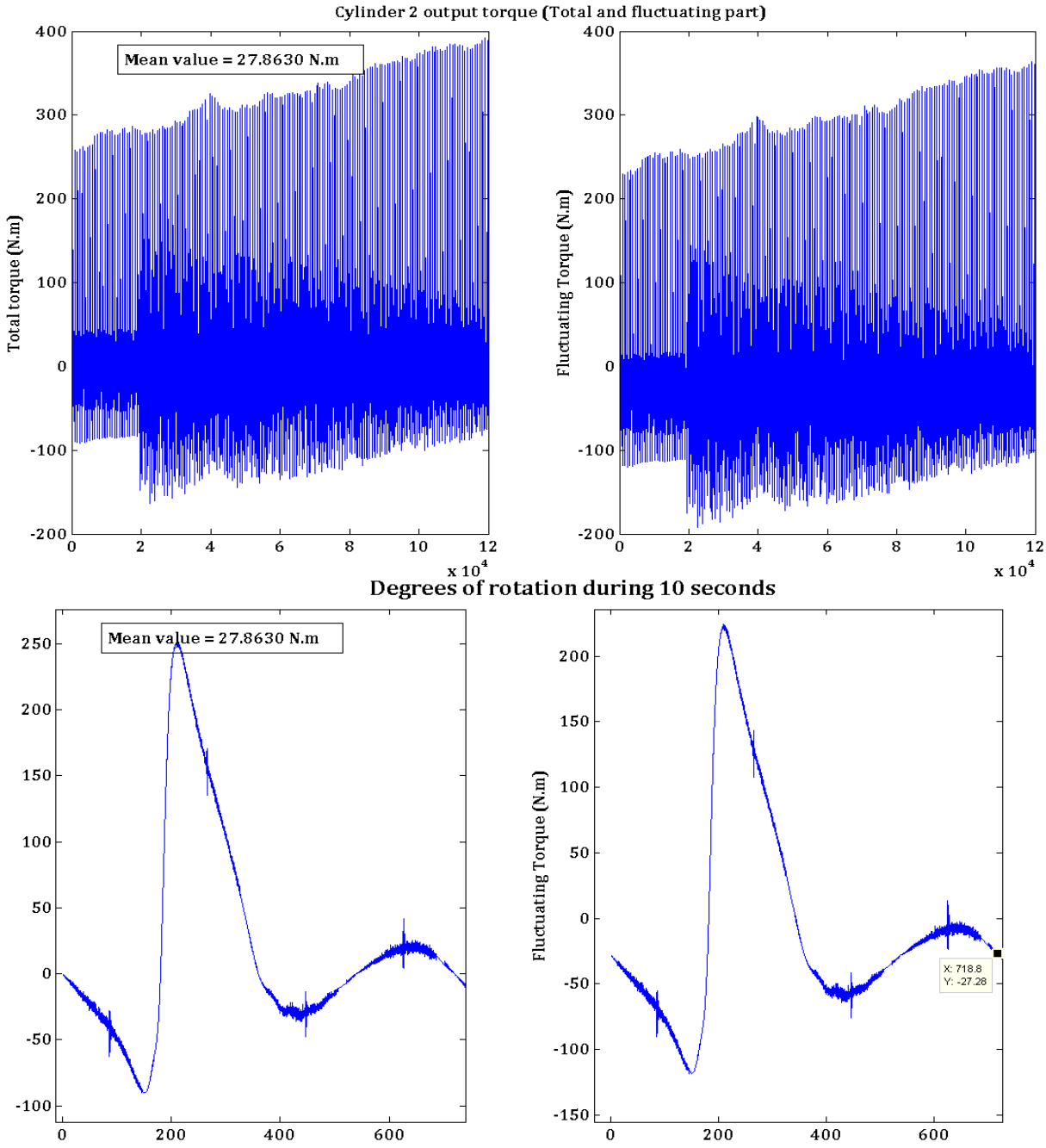

Figure 3-12, Torque output of cylinder 2, total and fluctuating part, during 10 seconds and one working cycle

It would be useful to plot cylinders output torques in one graph (Figure 3-13): $T_{g1}(t)$, $T_{g2}(t)$, $T_{g3}(t)$, and $T_{g4}(t)$.

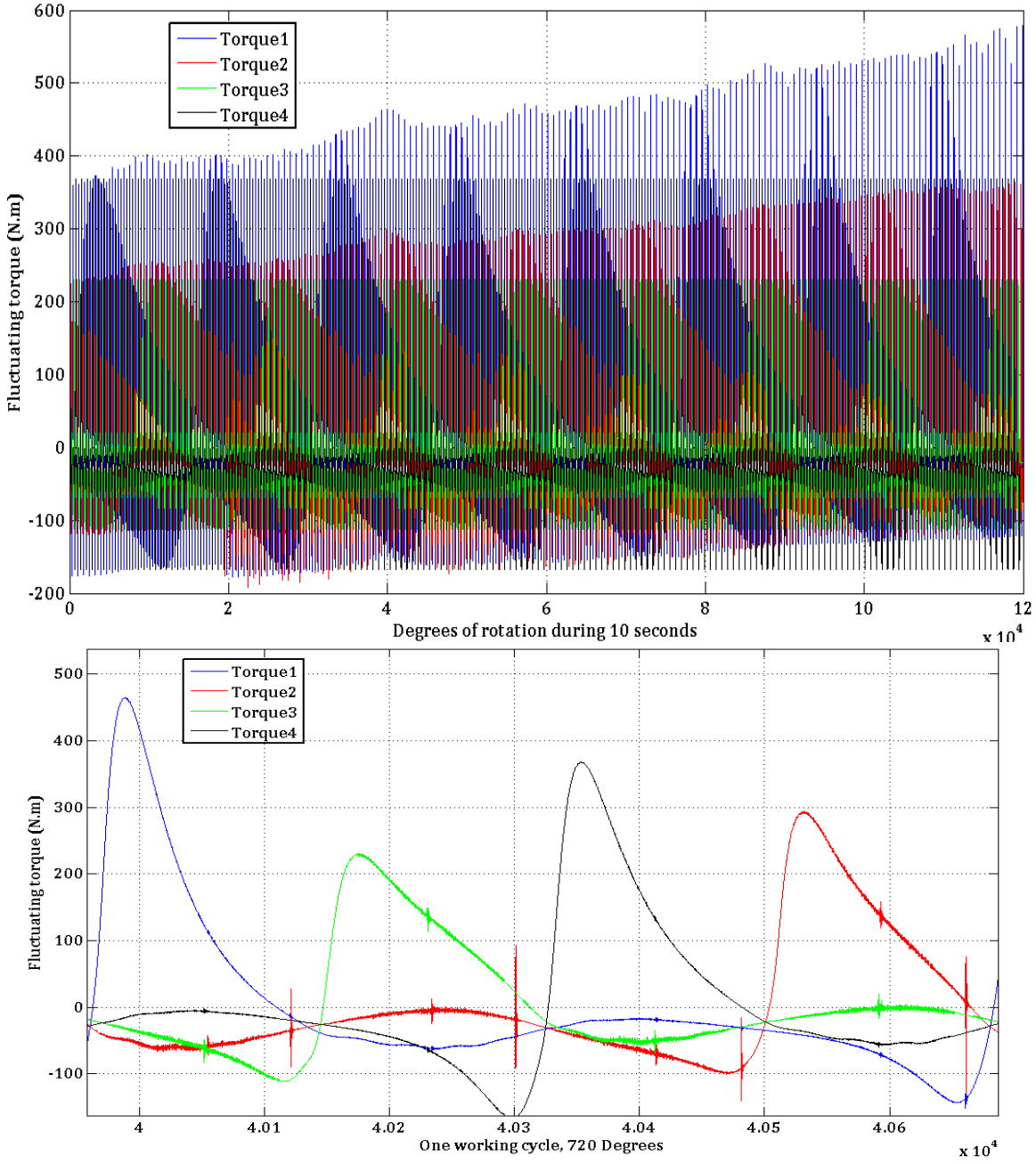

Figure 3-13, Output torques from 4 cylinders in the same plot[1]

The driveline system is subjected to these input excitation torques which are shown in Figure 3-14. This figure represents compact crankshaft model of a four-cylinder engine [3]. It should be noted that J_d is the torsional damper and J_f is the flywheel mass moments of inertia, respectively. Function of the flywheel is to decrease the magnitude of angular accelerations produced by input excitation torques $T_{g1}(t)$, $T_{g2}(t)$, $T_{g3}(t)$, and $T_{g4}(t)$.

[1] This diagram is similar to Figure 3-7

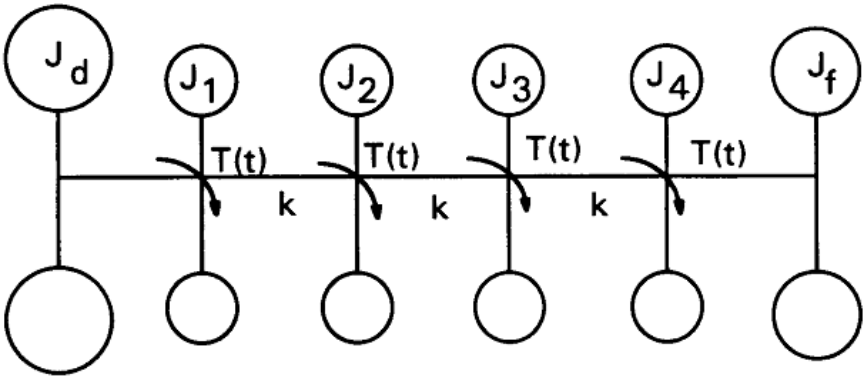

Figure 3-14, Compact crankshaft model for a four-cylinder engine

Furthermore, to see the excitation (forced) frequencies[1] which are associated to the above torques, the power spectral densities of the cylinder 1 and cylinder 2 time histories, in Figure 3-13, are obtained using MATLAB commands and are demonstrated in the following figure.

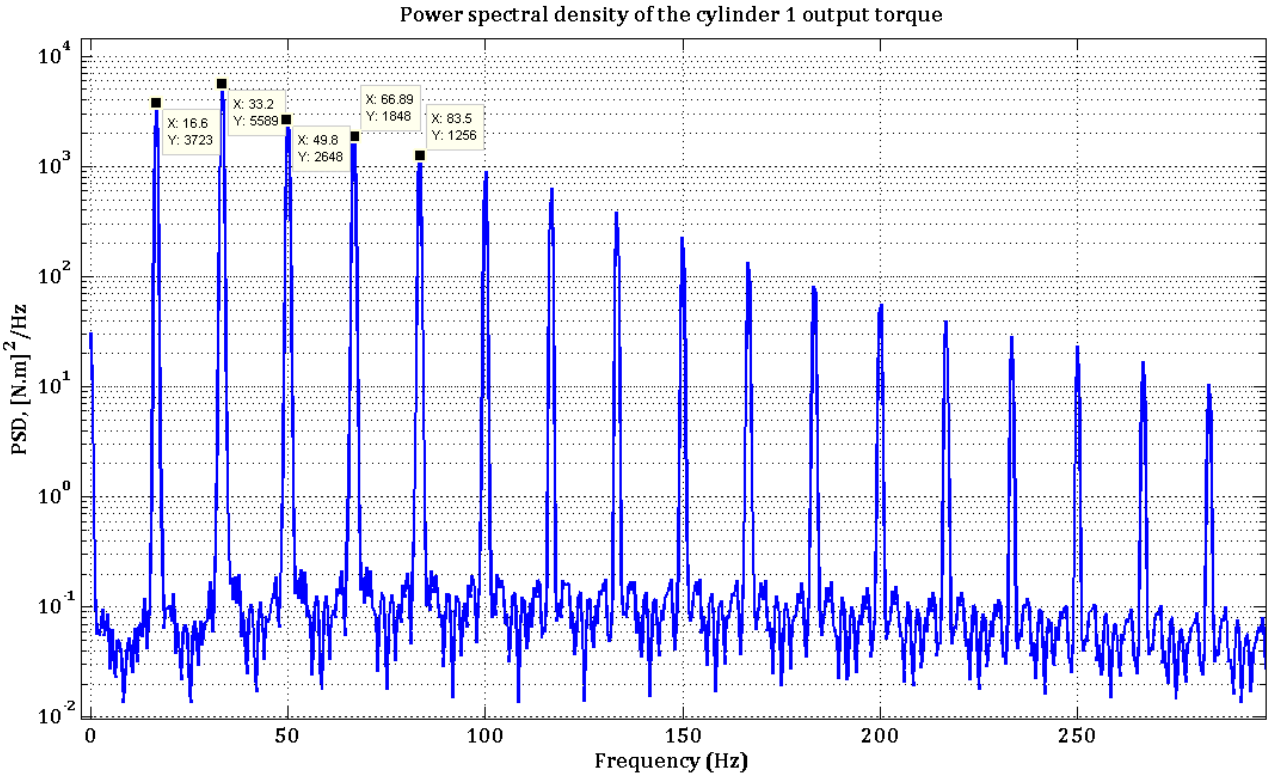

Figure 3-15, PSD for output torque from cylinder 1

[1] fundamental frequency (refer to Table 3-1)and its multiplications

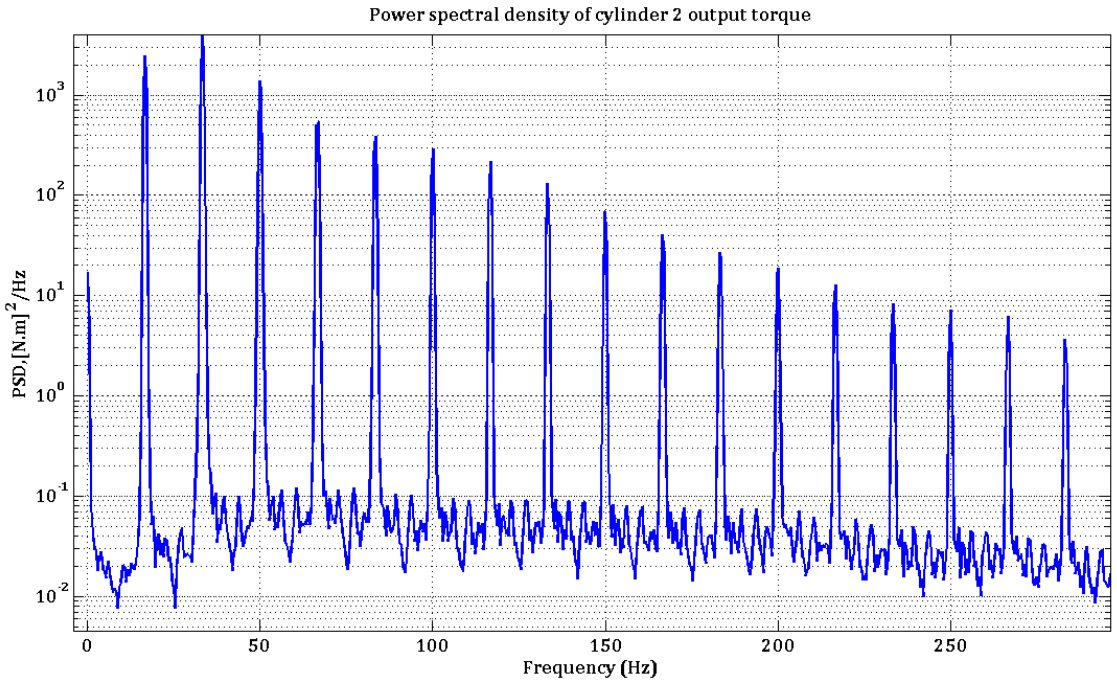

Figure 3-16, PSD for output torque from cylinder 2

According to Figure 3-15 and Figure 3-16, as it was expected from Table 3-1, Engine properties, the first (fundamental) frequency is *almost equal to 16.6 Hz* (half engine speed[1]) and the next excitation frequencies are 33.2, 50, 66.9, 83 … Hz.

3.2.2 Clutch Assembly

We have the clutch system (Figure 3-17) after flywheel which is made of two different components, clutch disk and clutch mechanism[22]:

Figure 3-17, Clutch system [22]

[1] Therefore as it will be seen in chapter 5, resonance happens when half engine speed or half multiple of engine speed is equal to one of the natural frequency of the system

The major duties of the clutch assembly are to join and disjoin the gearbox with the engine, to transmit engine power to the input shaft, and to supply isolation from the oscillatory engine torque oscillations. This function is achieved by two mechanisms rotationally connected by an elastic and dissipative system which can rotate together (Figure 3-17, Clutch system), The first system is the clutch disc and rings connected to the flywheel, and the second is the clutch hub connected to the input shaft via spline backlash [22]. Two different working conditions can be considered for clutch: 1-clutch behavior during the steady state running (linear action) and 2- clutch treatment during engagement (nonlinear phenomenon[1]), however in this work we simply model the clutch system as an inertia disc together with the flywheel which is connected to the gearbox via a spring and a damper [3] and it is shown in the driveline overall model in section 3.3.

3.2.3 Gearbox

The third component in the driveline system is the gearbox which consists of various helical gears in order to provide the ability of changing the speed ratio between the engine and driving wheels for driver of the car. We have two major groups of the gearboxes: manual and automatic. Since the dynamic model of gearbox mechanism is related to the purpose of the study and concerning the aim of this thesis, which is analysis of the driveline torsional behavior, therefore modeling of gears and carrying shafts as a simple torsional vibratory system is the primary interest of this step of the report. The following mathematical model is suggested for the torsional vibration of driveline, where the model included an equivalent inertia disc for each of the gear that transmits torque. it should be noted that the inertia of each disc contains also the inertia of the idling gears which results to the reduction of the driving gear speed.

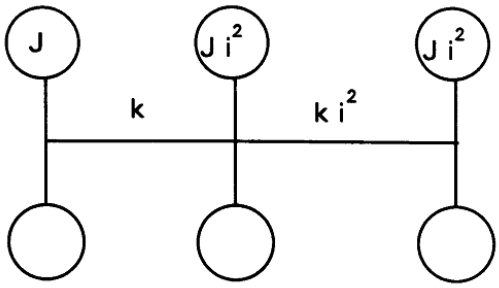

Figure 3-18, Gearbox model [3]

3.2.4 Cardan (propeller) shaft and universal (Hooke's) joints

Cardan shaft transmits the engine torque from the differential to the wheels. Since the engine gearbox shaft, cardan shaft and back axle are not in line, a universal joint, which is shown in Figure 3-19, has to be used in order to attach them. The Hooke's joint suffer from one important problem: even when the input shaft has a constant speed, the output shaft rotates at a variable speed. We know that velocity change means acceleration and concerning Newton's law, acceleration results to force. Therefore a secondary couple will be created and it is nonlinear. The magnitude of this produced torque is proportional to the torque

[1] One of the most important purposes of torsional vibration of the driveline is during clutch engagement in manual gear box mechanisms. The study of this topic is too complex and beyond the goal of this report.

which is applied on the driveline and the Hooke's joint angle, thus the variation of the driveline excitation torque will cause new torque[1] fluctuation.

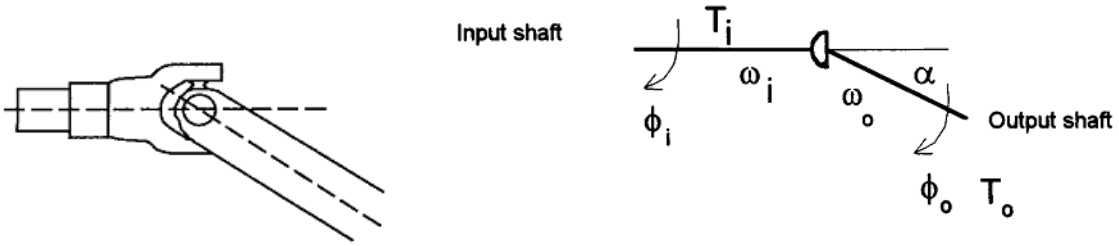

Figure 3-19, Hooke's (cardan) joints [1]

In order to find a simple model for propeller shaft and universal joints in the whole driveline system, we assume that the mass moment of inertia of the joints is much larger than the propeller shaft, therefore the system is regarded as an elastic massless shaft (like a spring) between two inertias [3]. Moreover, the generated torque by the joints will be applied on the two ends of the cardan shaft as it is shown in Figure 3-20, propeller shafts and universal joints mathematical model,

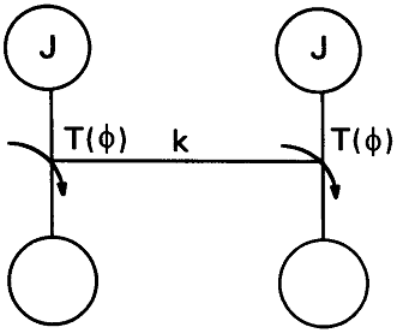

Figure 3-20, propeller shafts and universal joints mathematical model [3]

3.2.5 Differential and final drive system

A differential is a mechanism in automobiles, usually but not necessarily including gears, which has the ability of transmitting torque and rotation through three shafts, normally it receives one input and provides two outputs. the differential also allows each of the driving roadwheels to rotate at different speeds. Final drive system consists of differential and two similar shafts which are connected to the wheels, and a simple model for that, is demonstarted in the following figure:

[11] The derivation of the vibratory torque which is generated by universal joints is completely described in [3].

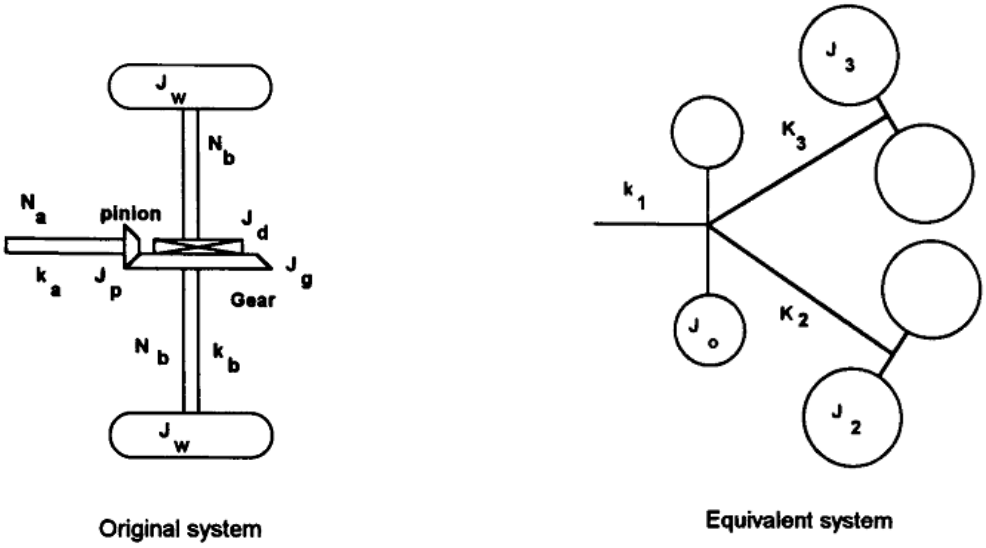

Figure 3-21, Final drive system and its equivalent model [3]

3.2.6 Damping in the whole driveline system

Damping is a resisting force which acts on the vibrating body and may arise from different sources such as friction between dry sliding surfaces, friction between lubricated surfaces, air or fluid resistance, electric damping, and internal friction due to imperfect elasticity. Regarding the damping type, the mathematical model is different and may depend on the velocity of the motion, material, viscosity of the lubricant and etc... The cases, in which the friction forces are proportional to velocity, are named as viscous damping. In the current driveline system, we will only consider the effects of viscous damping in different components[1] and other kinds of damping are neglected. The equivalent viscous torsional damping coefficients are given in reference [3].

3.3 Overall driveline model

As it was described before, the overall torsional model for driveline system is based on discretisation and lumped masses are used. The suggested 14-degrees of freedom linear model for a four-cylinder rear-drive passenger car is shown in Figure 3-22 which composed of inertia discs and massless torsional springs and viscous dampers.

[1] Crankshaft, engine, clutch disc, gearbox, propeller shaft and differential units, and tires.

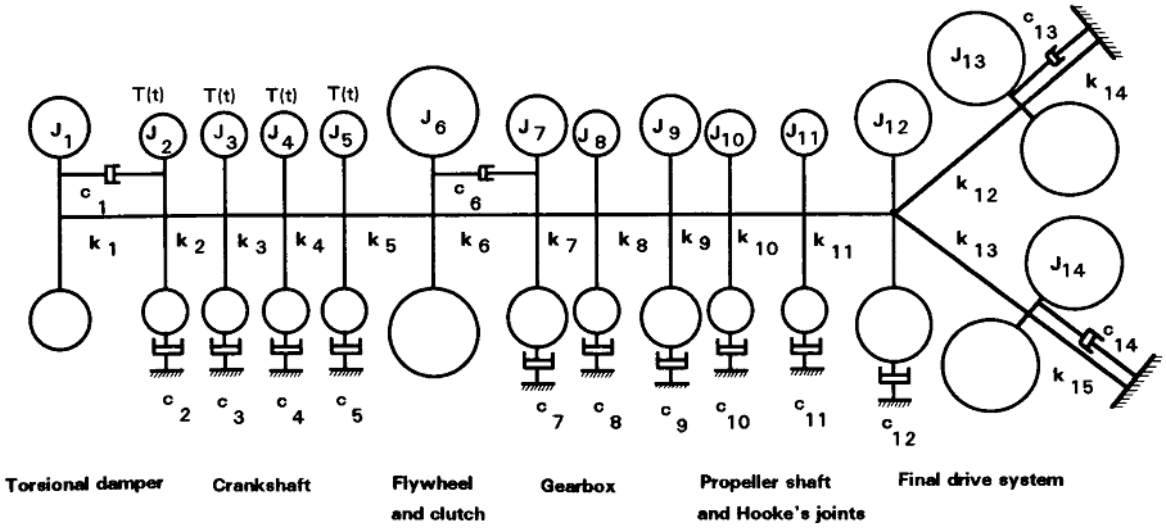

Figure 3-22, Damped torsional vibration mathematical model of driveline system [3]

This model is used throughout this thesis in order to study the free and forced vibration of driveline and whole vehicle.

3.4 Torsional vibration

There are different excitation sources (linear and nonlinear) for the torsional vibration of the driveline model which is shown in Figure 3-22, Damped torsional vibration mathematical model of driveline system. However as it was mentioned in section 3.2.1, engine torque oscillations[1] (linear behavior), is the main reason of torsional vibration. Studying the nonlinear purposes such as Hooke's joints is beyond the scope of this thesis. It should be noted that torsional vibration is in primary interest since firstly, it may cause harmful effects on the different parts of the system and secondly, it will be coupled with the whole body motions of the vehicle and results to longitudinal vibration which is investigated in the next chapters.

[1] due to different strokes

4 Chapter 4

Undamped natural frequencies of the overall driveline system

4.1 Introduction

This chapter includes solving driveline differential equations of motion in order to find natural frequencies of the system. To avoid resonance, which is a harmful phenomenon for mechanical systems, it is necessary to obtain natural frequencies of the structure. Modal analysis is used to study undamped model of the driveline system.

4.2 Mathematical model and system matrices

The governing differential equation for torsional vibration of the overall driveline system (14-degrees of freedom) which is shown in Figure 3-22, is

$$\mathbf{M}\ddot{\mathbf{x}} + \mathbf{C}\dot{\mathbf{x}} + \mathbf{K}\mathbf{x} = \mathbf{F}(t) \qquad 4.1$$

where $\mathbf{M}$, $\mathbf{C}$, $\mathbf{K}$ and $\mathbf{F}(t)$ are the *symmetric* mass moment of inertia[1], torsional damping, stiffness, and applying force (engine fluctuating torque) matrices, respectively and finally $\mathbf{x}(t)$ is the 14-dimensional column vector of generalized coordinates. In Table 4-1, parameter values are given for mass moment of inertia, stiffness and damping coefficients of different components in driveline. In order to obtain the system matrices for this multi-degrees of freedom system, two methods have been described in vibration theory books [21]: Newton's procedure and energy method, the closer one applies Newton's laws on the free body diagram of each component and it is straightforward but time consuming, while the energy method is based on Lagrange's equations and more practical for large systems. In this thesis Newton's method is utilized and the inertia, stiffness and damping matrices have been determined as follows:

[1] Since we have torsional vibration, **M** matrix is briefly called inertia matrix

Table 4-1, Typical values for equivalent parameters of a vehicle driveline [3]

Equivalent stiffness coefficient (N/m or N.m/rad)		Equivalent moment of inertia ($kg.m^2$)		Equivalent system damping coefficient (N.s/m or N.m.s/rad)	
Parameter	**Value**	**Parameter**	**Value**	**Parameter**	**Value**
k_1	0.2e6	J_1	0.3	c_1	3
k_2	1e6	J_2	0.03	c_2	2
k_3	1e6	J_3	0.03	c_3	2
k_4	1e6	J_4	0.03	c_4	2
k_5	1e6	J_5	0.03	c_5	2
k_6	0.05e6	J_6	1.0	c_6	4.42
k_7	2e6	J_7	0.05	c_7	1
k_8	1e6	J_8	0.03	c_8	1
k_9	0.1e6	J_9	0.05	c_9	1
k_{10}	0.1e6	J_{10}	0.02	c_{10}	1.8
k_{11}	0.2e6	J_{11}	0.02	c_{11}	1.8
k_{12}	0.5e6	J_{12}	0.3	c_{12}	2
k_{13}	0.5e6	J_{13}	2	c_{13}	10
k_{14}	0.2e6	J_{14}	2	c_{14}	10
k_{15}	0.2e6				

$$\mathbf{K} = \begin{bmatrix}
k_1 & -k_1 & 0 & 0 & 0 & 0 & 0 & 0 & 0 & 0 & 0 & 0 & 0 & 0 \\
-k_1 & k_1+k_2 & -k_2 & & & & & & & & & & & 0 \\
0 & -k_2 & k_2+k_3 & -k_3 & & & & & & & & & & 0 \\
0 & & -k_3 & k_3+k_4 & -k_4 & & & & & & & & & 0 \\
0 & & & -k_4 & k_4+k_5 & -k_5 & & & & & & & & 0 \\
0 & & & & -k_5 & k_5+k_6 & -k_6 & & & & & & & 0 \\
0 & & & & & -k_6 & k_6+k_7 & -k_7 & & & & & & 0 \\
0 & & & & & & -k_7 & k_7+k_8 & -k_8 & & & & & 0 \\
0 & & & & & & & -k_8 & k_8+k_9 & -k_9 & & & & 0 \\
0 & & & & & & & & -k_9 & k_9+k_{10} & -k_{10} & & & 0 \\
0 & & & & & & & & & -k_{10} & k_{10}+k_{11} & -k_{11} & & 0 \\
0 & & & & & & & & & & -k_{11} & k_{11}+k_{12}+k_{13} & -k_{13} & -k_{12} \\
0 & & & & & & & & & & & -k_{13} & k_{13}+k_{15} & 0 \\
0 & 0 & 0 & 0 & 0 & 0 & 0 & 0 & 0 & 0 & 0 & -k_{12} & 0 & k_{12}+k_{14}
\end{bmatrix}$$

$$\mathbf{C} = \begin{bmatrix} c_1 & -c_1 & 0 & 0 & 0 & 0 & 0 & 0 & 0 & 0 & 0 & 0 & 0 & 0 \\ -c_1 & c_1+c_2 & & & & & & & & & & & & 0 \\ 0 & & c_3 & & & & & & & & & & & 0 \\ 0 & & & c_4 & & & & & & & & & & 0 \\ 0 & & & & c_5 & & & & & & & & & 0 \\ 0 & & & & & c_6 & -c_6 & & & & & & & 0 \\ 0 & & & & & -c_6 & c_6+c_7 & & & & & & & 0 \\ 0 & & & & & & & c_8 & & & & & & 0 \\ 0 & & & & & & & & c_9 & & & & & 0 \\ 0 & & & & & & & & & c_{10} & & & & 0 \\ 0 & & & & & & & & & & c_{11} & & & 0 \\ 0 & & & & & & & & & & & c_{12} & & 0 \\ 0 & & & & & & & & & & & & c_{13} & 0 \\ 0 & 0 & 0 & 0 & 0 & 0 & 0 & 0 & 0 & 0 & 0 & 0 & 0 & c_{14} \end{bmatrix}$$

$$\mathbf{M} = \begin{bmatrix} J_1 & 0 & 0 & 0 & 0 & 0 & 0 & 0 & 0 & 0 & 0 & 0 & 0 & 0 \\ 0 & J_2 & & & & & & & & & & & & 0 \\ 0 & & J_3 & & & & & & & & & & & 0 \\ 0 & & & J_4 & & & & & & & & & & 0 \\ 0 & & & & J_5 & & & & & & & & & 0 \\ 0 & & & & & J_6 & & & & & & & & 0 \\ 0 & & & & & & J_7 & & & & & & & 0 \\ 0 & & & & & & & J_8 & & & & & & 0 \\ 0 & & & & & & & & J_9 & & & & & 0 \\ 0 & & & & & & & & & J_{10} & & & & 0 \\ 0 & & & & & & & & & & J_{11} & & & 0 \\ 0 & & & & & & & & & & & J_{12} & & 0 \\ 0 & & & & & & & & & & & & J_{13} & 0 \\ 0 & 0 & 0 & 0 & 0 & 0 & 0 & 0 & 0 & 0 & 0 & 0 & 0 & J_{14} \end{bmatrix}$$

Now to find undamped natural frequencies of the system, the right hand side of equation 4.1 and damping matrix are set to be zero. it should be mentioned that, since the damping matrix is not a linear combination of the inertia and stiffness matrices ($\mathbf{C} \neq \alpha\mathbf{M} + \beta\mathbf{K}$), it is not possible to use modal analysis[1] to decouple the equations, therefore *undamped* natural frequencies are to be determined, however they are almost the same with damped frequencies which are provided in reference [3].

4.3 Summary of Modal analysis

Modal analysis is a procedure to find the natural frequencies of the system by decoupling the system differential equations of the motion which is given in equation 4.1. The problem is that when the equations are coupled, it is not possible to solve them separately at the same

[1] which is described in section 4.3

time. There are different types of coupling: static coupling[1] and dynamic coupling[2], according to the mass and stiffness matrices which are already given, we have static coupling in driveline system of equations. It is also useful to mention that the selection of coordinate system influences on the existence or nonexistence of the coupling.
As it is known from vibration theory [21], we can substitute $\mathbf{x} = \mathbf{X}e^{i\omega t}$ [3] in the equations of motion (equation 4.1), and further we reach to the following expression:

$$-\omega^2\mathbf{M}\mathbf{X}e^{i\omega t} + \mathbf{K}\mathbf{X}e^{i\omega t} = \mathbf{0} \qquad 4.2$$

By removing the scalar value $e^{i\omega t}$,

$$-\omega^2\mathbf{M}\mathbf{X} + \mathbf{K}\mathbf{X} = \mathbf{0} \qquad 4.3$$

In order to solve equation 4.3, it is converted to the form $\mathbf{A}\mathbf{X} = \lambda\mathbf{X}$ which is the familiar form for Eigen-value problems. To do so, both sides of relation 4.3 are multiplied by the term $\mathbf{K^{-1}}$ from the left as follows:

$$-\omega^2\mathbf{K^{-1}}\mathbf{M}\mathbf{X} + \mathbf{K^{-1}}\mathbf{K}\mathbf{X} = \mathbf{0} \qquad 4.4$$

or

$$-\omega^2\mathbf{K^{-1}}\mathbf{M}\mathbf{X} + \mathbf{I}\mathbf{X} = \mathbf{0} \qquad 4.5$$

and finally we obtain:

$$\mathbf{K^{-1}}\mathbf{M}\mathbf{X} = 1/\omega^2\mathbf{X} \qquad 4.6$$

in this case $\mathbf{A} = \mathbf{K^{-1}}\mathbf{M}$ and $\lambda = 1/\omega^2$. Therefore the natural frequencies of the multi-degrees of freedom system are the inverse of the positive square roots of the Eigen-values of matrix **A**. It is possible to find these values by using eig command in MATLAB. In order to determine the corresponding mode shape[4] $\mathbf{X_i}$ for each frequency ω_i , the following equation has to be solved:

$$\mathbf{K^{-1}}\mathbf{M}\mathbf{X_i} = 1/\omega_i^2\,\mathbf{X_i} \qquad 4.7$$

using these mode shapes, we can form the modal vectors matrix that is the base of modal equations[5] for modal analysis[6]. however (as it was noted in previous section) in the current system, this method of solution is not usable to attain the forced response of driveline mechanism since the damping matrix is un-proportional and the above procedure do not decouple the equations which are coupled by damping coefficients. Although, in the next

[1] When the stiffness matrix is not diagonal
[2] When the mass matrix is not diagonal
[3] Since we know that the response of the undamped vibratory system, **x** will be sinusoidal, therefore it can be shown by exponential form
[4] finding the mode shapes of one mechanical system provides the information about the positions at which large displacement will occur and therefore, it would be possible to represent a solution to attenuate the harmful vibration
[5] Modal equations are n independent relations for an n-degree of freedom system which are solvable separately, the new coordinate are called principal coordinates.
[6] More description is available in vibrations book [21]

chapter, forced response of the system is determined using both modal analysis and numerical method, and the precision of the solutions is studied according to reference [3], in order to see the inaccuracy of modal method and to evaluate the precision of numerical method.

4.4 Natural frequencies

Resonance is a harmful phenomenon which happens in mechanical systems, this results to failure of the mechanism and is very dangerous in the case of passenger cars. As it is known, resonance occurs when natural frequencies of the system coincident with the forced frequencies, therefore in order to avoid this unwanted situation, it is necessary to know natural frequencies of the system (using the method of previous section for a multi-degree of freedom system). Moreover we will find the mode shapes of driveline to be aware about the positions which have considerable vibration amplitude.

Among the undamped natural frequencies for torsional vibration of the whole driveline model Table 4-2, the first six frequencies are important while they are in operating range of the driveline system.

Table 4-2, Undamped natural frequencies of whole driveline model using typical parameter values for a passenger car

Mode number	1	2	3	4	5	6	7	8	9	10	11	12	13	14
Natural Frequency (Hz)	4.03	9.416	12.585	50.856	109.682	139.041	427.421	432.407	679.986	838.878	955.638	1421.383	1730.087	1845.537

These values have a very good agreement with the damped natural frequencies for the system, which are given in [3]- table 5.2. However there are fewer calculations in the case of finding undamped frequencies for the vibratory systems. Further, the first five mode shapes of the system are obtained as in Table 4-3.

Table 4-3, first five natural modes of driveline system

1st Mode	2nd Mode	3rd Mode	4th Mode	5th Mode
1.0000	0	-1.9806	1.0000	-2.8087
0.9990	0	-1.9621	0.8468	-0.8078
0.9982	0	-1.9579	0.8136	-0.3961
0.9986	0	-1.9535	0.7779	0.0212
0.9983	0	-1.9487	0.7398	0.4383
0.9981	0	-1.9435	0.6994	0.8491
0.9799	0	-1.5969	-1.5362	1.0000
0.9794	0	-1.5879	-1.5882	0.9919
0.9785	0	-1.5698	-1.6873	0.9616
0.9686	0	-1.3836	-2.5919	0.4299
0.9586	0	-1.1956	-3.4436	-0.1426
0.9535	0	-1.1009	-3.8342	-0.4221
0.8337	-1	1	0.0972	0.0022
0.8337	1	1	0.0972	0.0022

In addition, the second mode only includes the driving wheels vibration (with a common frequency) and other components of the system are in rest, therefore it can be concluded that the 2nd mode has been never excited by any excitation torques.

5 Chapter 5

Steady-state Response of linear driveline model due to engine fluctuating torque

5.1 Introduction

In this chapter, forced response of driveline model subject to the engine cylinder pressure input torques is determined, using the same system of differential equations as chapter4, however now excitation forces exist in the right hand side of the equations. According to the final solutions, the results of Runge-kutta numerical method provide desired accuracy.

5.2 Mathematical model for forced vibration of the driveline system

In order to obtain forced response of the linear damped system, again we consider the main differential matrix equation for torsional vibration of the driveline mechanism (Figure 5-1):

$$\mathbf{M}\ddot{\mathbf{x}} + \mathbf{C}\dot{\mathbf{x}} + \mathbf{K}\mathbf{x} = \mathbf{F}(t) \qquad 5.1$$

here the force matrix is a column vector as follows:

$$\begin{bmatrix} 0 & T_{g1}(t) & T_{g2}(t) & T_{g3}(t) & T_{g4}(t) & 0 & 0 & 0 & 0 & 0 & 0 & 0 & 0 & 0 \end{bmatrix}^{-1} \qquad 4.2$$

where $T_{g1}(t)$, $T_{g2}(t)$, $T_{g3}(t)$ and $T_{g4}(t)$ are engine fluctuation torques from different cylinders which are given in Figure 3-13. the applying forces are not sinusoidal but periodic.

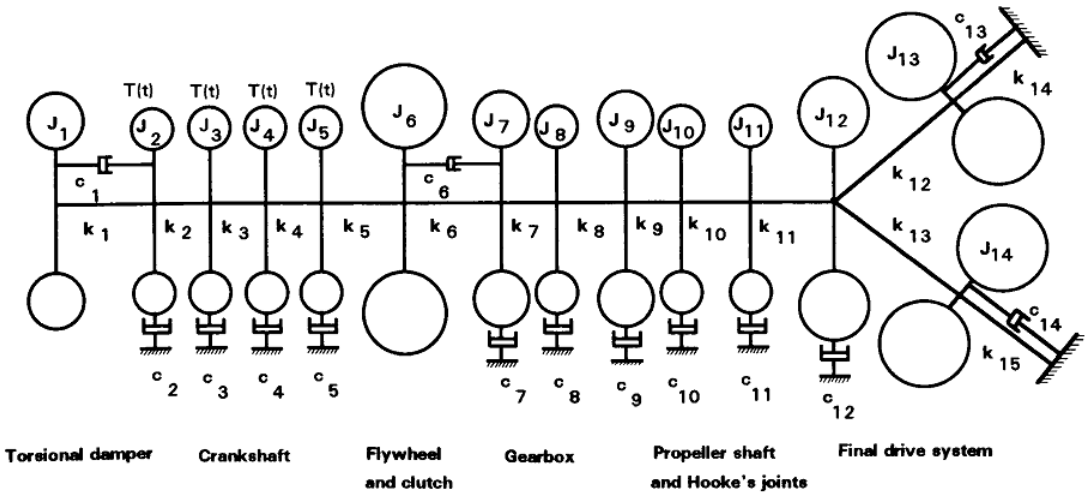

Figure 5-1, Driveline model

5.3 Time responses of driveline at clutch and driving wheels

Steady-state response of the equation 5.1 is found using 3 methods in this section: Modal analysis as an analytical method, and 2 numerical procedures[1]: ode45 function in MATLAB and self-written fourth order Runge-Kutta method. Although the excitation forces are not exactly similar to reference [3][2], there is a good agreement between the responses from numerical methods that have been utilized here and the results which are given in [3], however the Modal analysis answer is not satisfactory. In the following paragraphs, a brief description is provided for each of the three solution methods:

- *Modal analysis*
  I. Decoupling the system of differential equations 5.1, by using Modal procedure in section 4.3. In addition, the modal forces have to be obtained.
  II. Finding the forced response of each independent equation using `lsim`[3] function in MATLAB, the associated command is given in Appendix 10.1. m(1,j),c(1,j)and k(1,j)are read from modal inertia, damping and stiffness matrices respectively. The big assumption is that damping matrix will be decoupled through modal process.
  III. The obtained solution is represented in Figure 5-2 for clutch torsional displacement together with the solutions from the numerical methods. The output result from modal analysis is not correct in the amplitude value, and also it is unstable (which is more clear in Figure 5-3). All the corresponding matlab codes are attached in **appendix** 10.210.2.
- ode 45 function
  I. MATLAB software includes a series of functions which are called solvers in order to solve ordinary differential equations of each order, they use Runge-Kutta numerical method with variable time step to find the solution of the equations. ode 23, ode 45 and ode 113 are the most famous functions of these solvers. In this thesis ode 45 is used to find the forced response of the 14-degrees of freedom driveline system. To do so, first it is necessary to convert the equations of the motion to a set of first order differential equations (this form is named state-variable form or Cauchy form), this new form[4] is saved in a separate function.
  II. The second step is to manipulate the force data in order to use them as an input for the system.
  III. Finally the command
  [T,Y]=ode45(@(t,z)sde(t,z,t1,F),[0,10],[zeros(14,1).zeros(14,1)])is written to find the solution for the system of equations in the desired time interval [0,10] with zero intial postions and velocities, there are two problems that this method suffers from: ”a little unstability which appears in Figure 5-2” and ”it is vey time consuming[5]”.

[1] However the base of both numerical methods is Runge-kutta method.
[2] He has used sinusoidal terms to simulate the engine torques and the solution is obtained using Modal analysis method.
[3] According to MATLAB help, `lsim` is an useful function in this software which is able to determine the vibratory system response to any arbitrary point data input as
[4] 28 first order differential equations
[5] For 10 seconds, it took around 2 days to find the answer

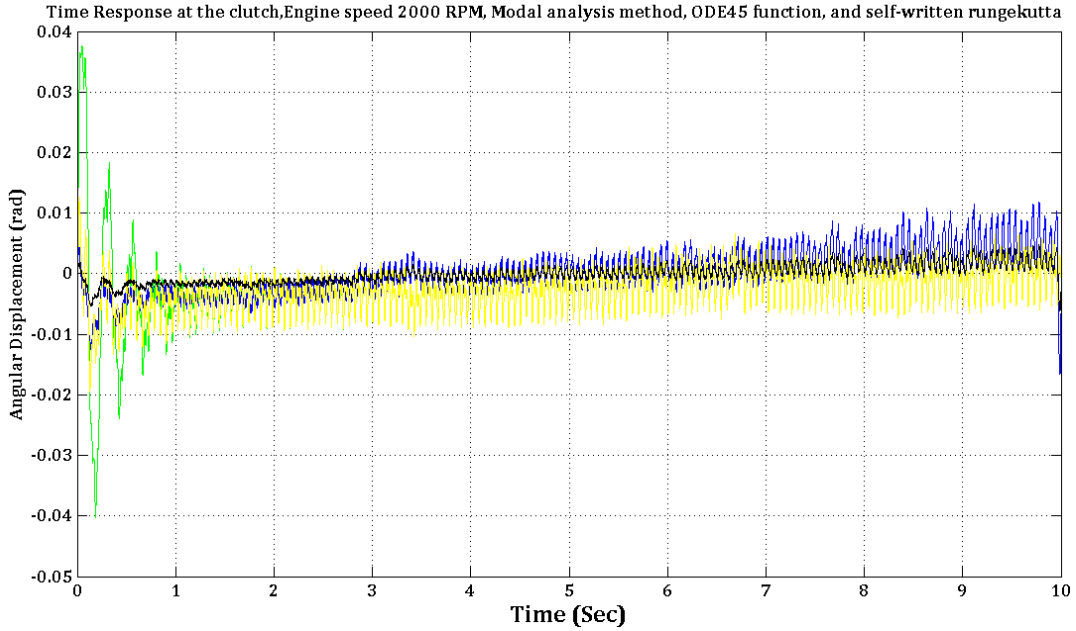

Figure 5-2, Time response at the clutch, using different methods of solution: Black-> Modal analysis, Blue-> ODE45, Green-> self-written Runge-Kutta code with nonzero initial conditions and yellow-> with zero initial conditions

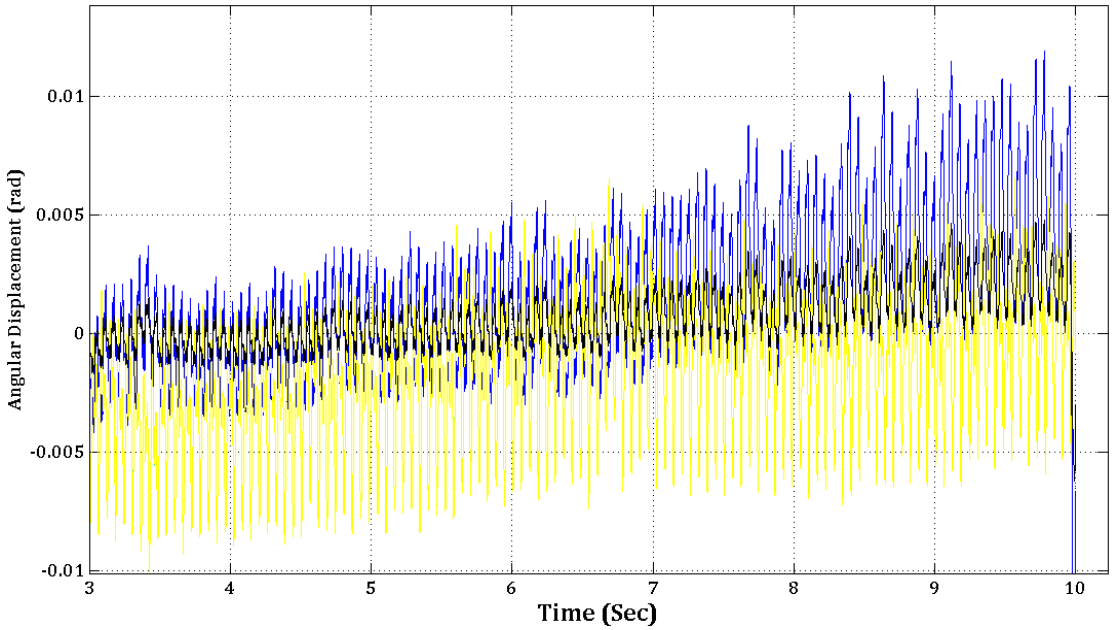

Figure 5-3, zoomed version of figure 5.2 in order to see the instability of modal analysis and ODE45 solutions

- *Self-written Runge-Kutta code*

I. In order to improve the calculations time, a MATLAB m-file is written to find the solutions for a system of fourteen second order differential equations using numerical method which is called *Runge-Kutta*[1], in this work the fourth order *Runge-Kutta* will be utilized which means that the error per step is on the order of h^5, while the total accumulated error has order h^4.

[1] From Wikipedia -> In numerical analysis, the **Runge–Kutta methods** are an important family of implicit and explicit iterative methods for the approximation of solutions of ordinary differential equations. These techniques were developed around 1900 by the German mathematicians C. Runge and M.W. Kutta.

II. For this method we have to do the same manipulations like the previous procedure to convert all the 14 second order equations to 28 first order equations (State-variable form).

III. The final result is shown in Figure 5-2, which has not only less instability[1] in comparison with ode 45 function solution, but also it takes a few minutes to obtain the answer which is very valuable regarding the computer program efficiency. Another point which is important is that, according to Figure 5-4, there is no difference in the response of the system, either we consider zero intial velocities or when a non-zero matrix[2] is set to be as initial velocities.

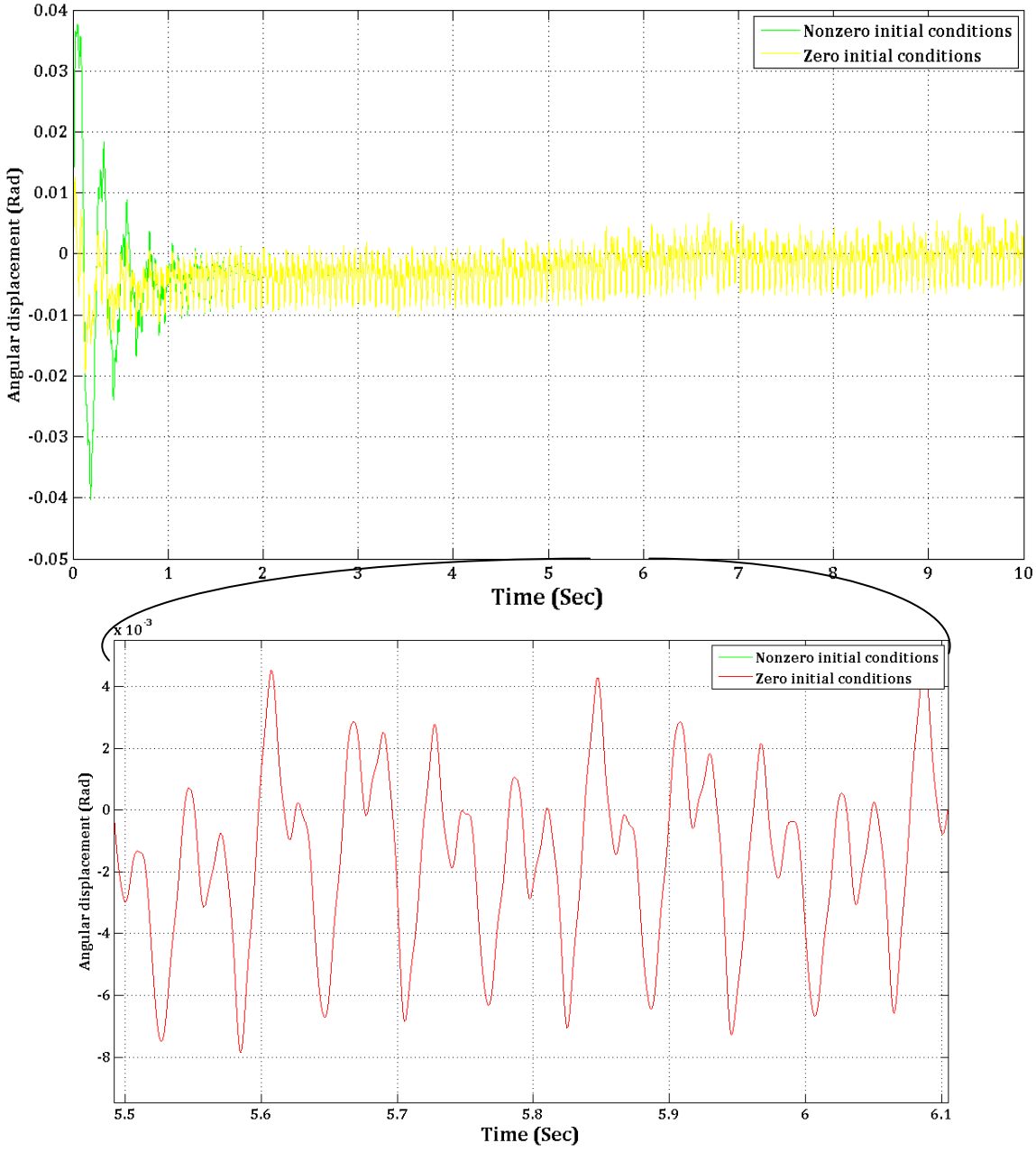

Figure 5-4, Time response at the clutch with the aid of Runge-Kutta method

[1] displacement vibrates around zero position which is preferable

[2] We are studying steady-state running and the force data are not from a period of starting and stopping the engine, we have only picked 10 seconds of running engine.

In comparison with the clutch response, which is given in reference [3], smaller amplitude is achieved here because the engine excitation force do not include the generated torque due to reciprocating components, however the FFT plot contains the same frequencies.

Angular vibration of the driving wheels has also significant importance since it may produce longitudinal vibration of the vehicle body[1], therefore the displacement plots are presented in Figure 5-5 by using the last method.

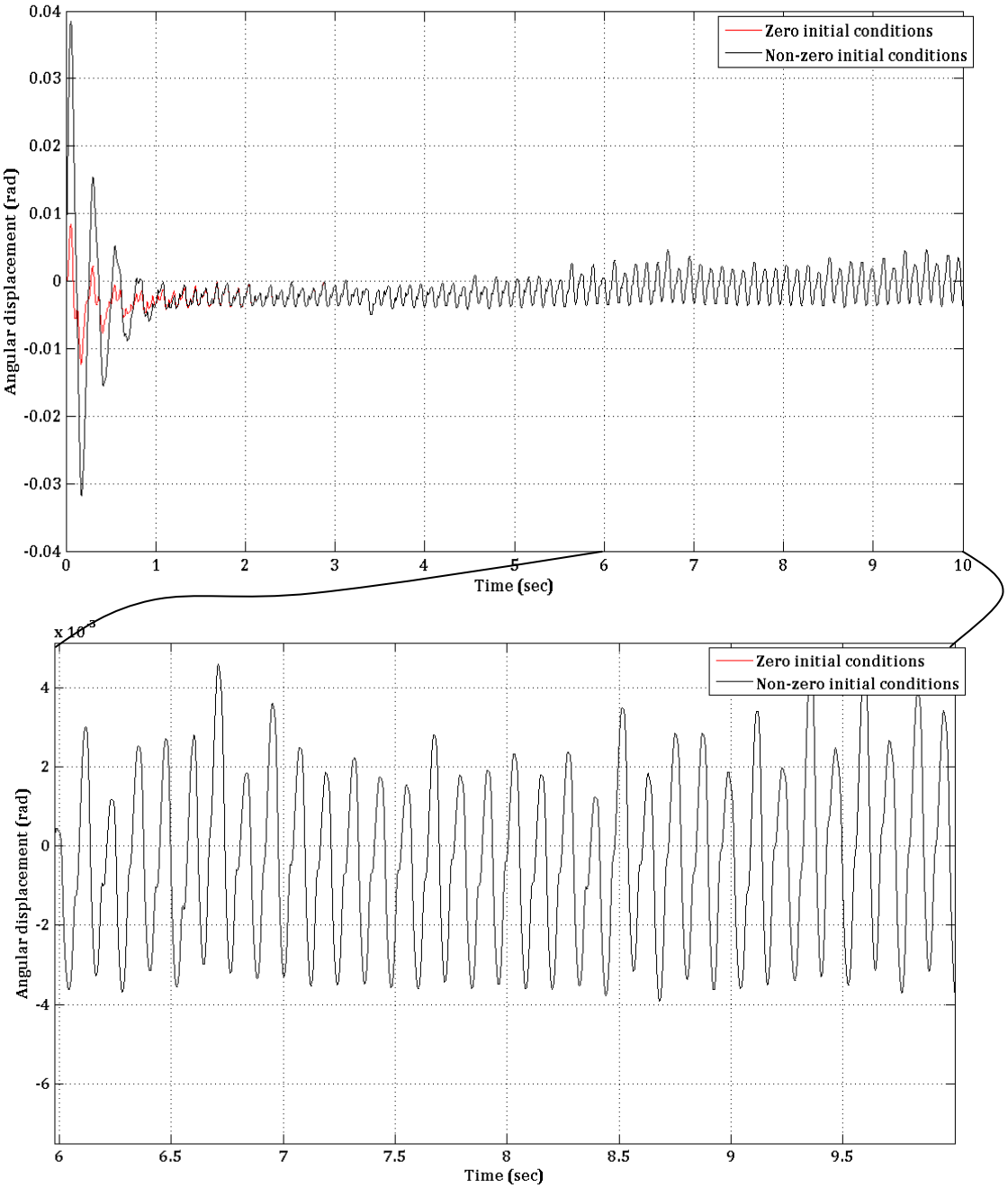

Figure 5-5, Time response at the driving wheels

[1] this will be described more in chapter 6

As it was expected the amplitude is smaller compare to clutch response, since between clutch and driving wheels there are number of components that reduce and damp the effects of engine excitation torque, moreover the response plot is almost stable.

5.4 Power spectral densities of time histories

We are always interested in the responses of the mechanical systems in frequency domain in order to find harmful frequencies which are within the operating range of the machine. Power spectral density is a tool to obtain Fourier transform of random signal time histories [4]. After determining time responses of clutch and driving wheels in the previous section, it would be useful to plot PSD diagrams. we expect to see frequencies of the applying force which are different for different engine speeds (in this report for 2000 RPM, according to Figure 3-16, 16.6 Hz is the fundamental frequency of the engine excitation torque and further we have 33.2, 50, 66.9, 83 … Hz) since the natural frequencies of the driveline are known, it is obvious that high amplitudes will occur if applying force frequencies coincident with the natural frequencies of the system. There are different built-in functions in MATLAB to attain power spectral densities of random signals. PSD function is used in this thesis which is attached in appendix 10.310.2. Figure 5-6 and Figure 5-7 show the PSDs of clutch response and driving wheels[1], respectively.

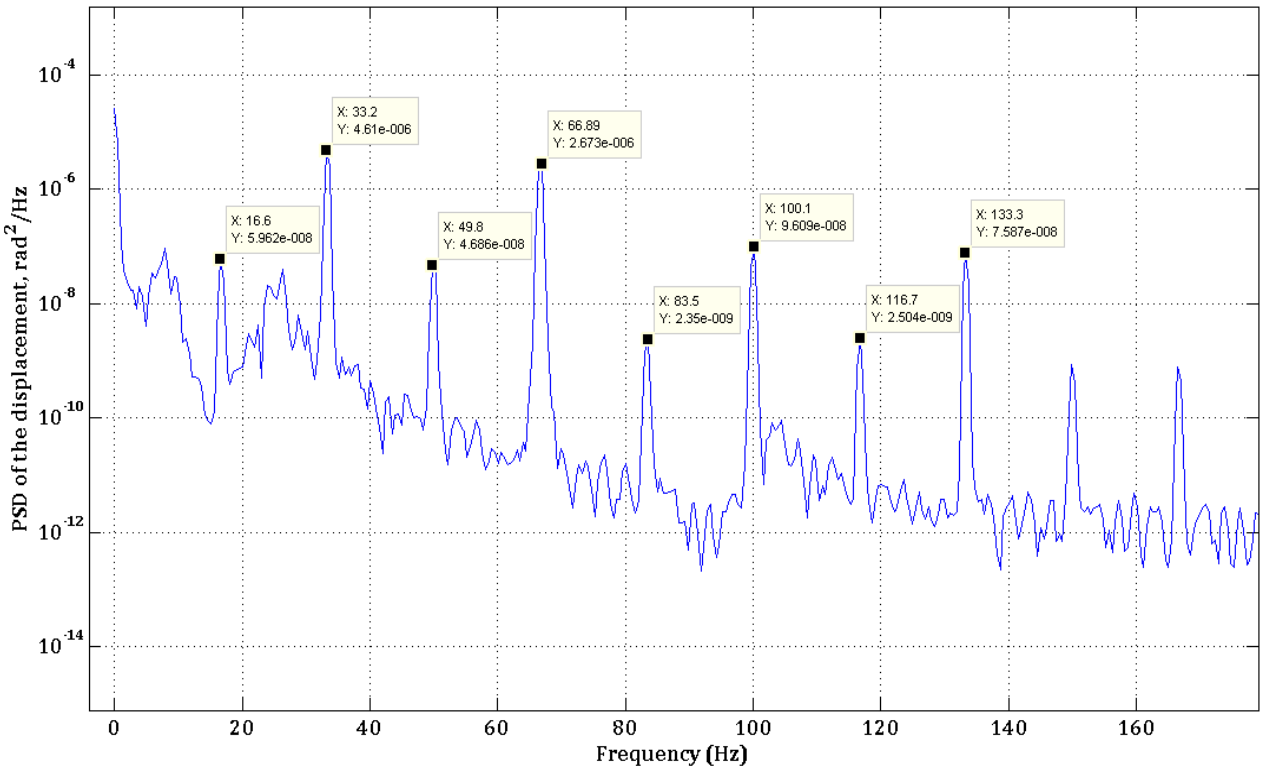

Figure 5-6, Power spectral density of the time response at the clutch

As it was expected all the forcing frequencies have created sharp peaks in the frequency domain of the system response.

[1] In this section only the PSD diagrams have been obtained for the time domain results from the Runge-Kutta numerical method.

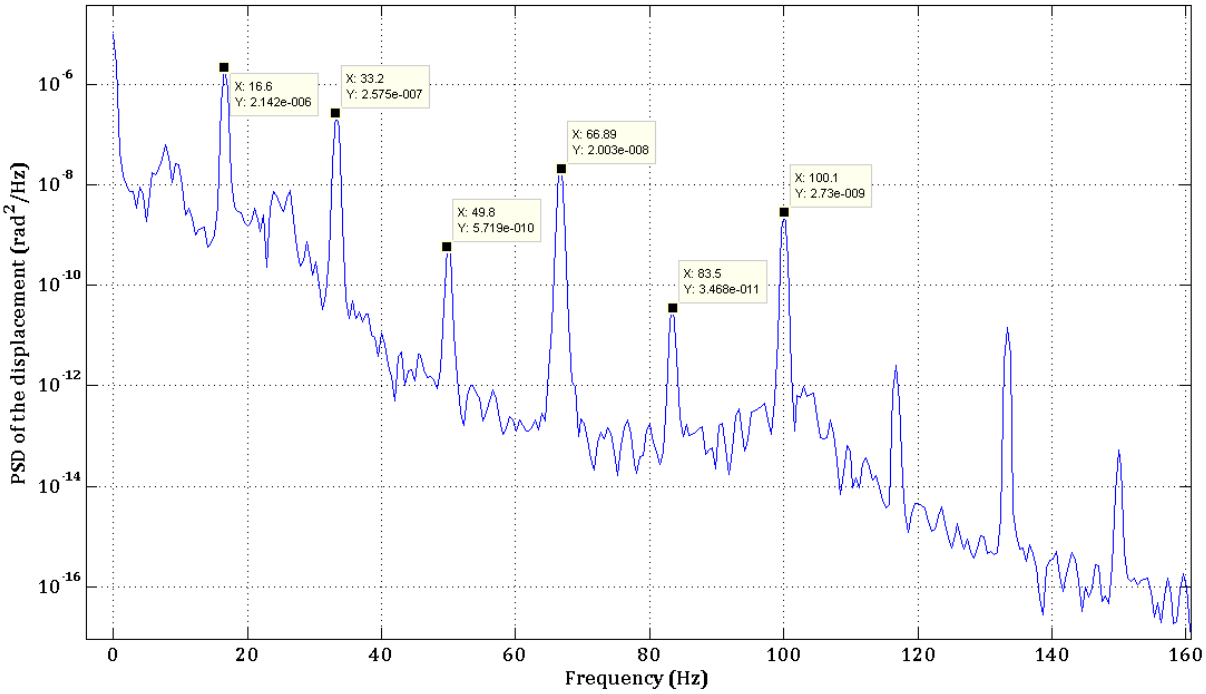

Figure 5-7, Power spectral density of the time response at the driving wheels

There are two important points that have to be mentioned at the end of this chapter:

I. Since the engine speed is not constant in a car, therefore the forcing frequencies are not fixed and in addition, even at the constant engine speed, there exist more than one excitation frequency. as a result, the problem of controlling driveline system becomes complicated and it is not possible to use passive control method.

II. On the other hand, while the response of the system is predictable, it is feasible to find an optimization technique to decrease the unwanted effects as well as achieving active algorithm to control the output vibrations.

6 Chapter 6

Vibration of the whole vehicle system due to torsional vibration of the driveline

6.1 Introduction

The main goal of this thesis, as it was mentioned in section 1.1, is to reduce the effects of unwanted vibrations on the automobiles passengers. So far, we have studied the engine fluctuation torques from different cylinders, as the main excitation source of driveline, while failure of each component of driveline system can result to a dangerous occurrence. furthermore it was noted that driveline vibration beside road surface irregularities is the main reason of undesired noises inside the passenger cars, accordingly it is necessary to obtain the vehicle body response due to driveline vibration in order to use the RMS acceleration of the vehicle body (sprung mass of the car) through ride comfort diagrams and study the drivability of a specific car.

6.2 Coupled vibration of driveline and the vehicle body

Torque fluctuations at the driving axle will result to variation of the drive forces at the ground and therefore may generate longitudinal vibrations in the vehicle. Hence torsional vibration of the driveline is coupled with the vibrations of the vehicle body. In order to achieve the response of sprung mass subject to engine excitations, first the whole vehicle should be modeled which is the aim of the following sections.

6.3 Tire model and longitudinal force

The whole vehicle model is divided into two main parts: *driveline part* which consists of all the components between engine and differential and *tire-suspension-body system* part. This section is devoted to tire modeling.

One powertrain component which is, most of the time, simplified in both old and new torsional models of the automobiles, is the influence of the tires. However tires are the most important element in the quest to get a car to handle well, since they are the only link between the vehicle and the ground. By the efforts of Pacejka [23], Delft University of Technology has significantly contributed to tire research. In this thesis, Pacejka principles are used to gain a model for tire which consists of longitudinal and vertical stiffness and damping coefficients, two different inertias are taken into account in order to have more accurate model: one for the wheel and the other for the tire tread bands [3], all the necessary properties for the calculations are given in Table 6-1. It should be noted that, an ideal tire/wheel assembly is considered here, although practically the imperfections in the manufacturing of tires, wheels, hubs, brakes and other parts of the rotating assembly, may cause to three main groups of irregularities: mass imbalance, dimensional variations and stiffness variations which are more described in reference [1].

Using the 2-degrees of freedom model for tire in Figure 6-1, according to Pacejka formula, the total longitudinal force relation is found to be:

$$F_l = -A_r(k_{14}z_1 + c_{14}\dot{z}_1) - R(k_{13}\theta_t + c_{13}\dot{\theta}_t) \qquad 6.1$$

where A_r is the coefficient of tire rolling resistance which is available in the database, and all other parameters are demonstrated in Figure 6-1, the corresponding values are provided in Table 6-1. The above expression shows that if the tire has an oscillatory rotational/vertical movement, then the longitudinal tire/road contact force will be various which result to longitudinal vibration of the vehicle body and this is not desired in a large scale according to ride comfort criteria.

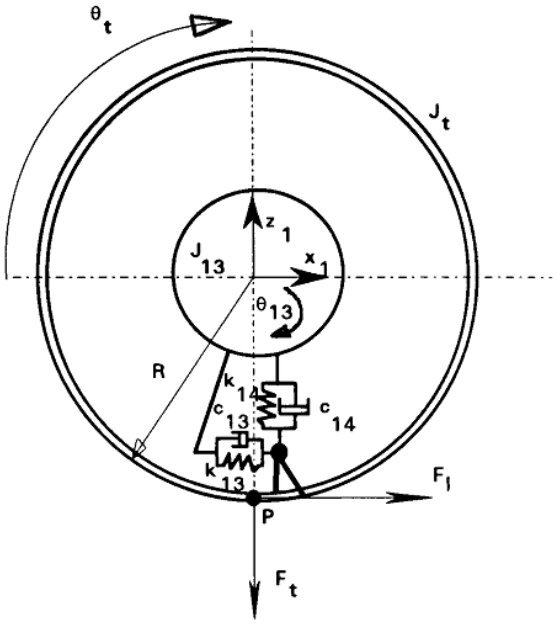

Figure 6-1, tire model [3]

6.4 18-degrees of freedom system for whole vehicle model and its equations of motion

In order to achieve an overall model including torsional vibration of driveline coupling with tire, suspension and vehicle body motion, first we consider the substructure which includes sprung (vehicle body) and unsprung masses, m_b and m_u respectively (Figure 6-2), moreover it is assumed that vehicle body motion is limited in longitudinal and vertical directions by suspension system characteristics. The second substructure as it was already explained is driveline from torsional damper to differential (12-degrees of freedom) and it is shown in Figure 6-2 as well.

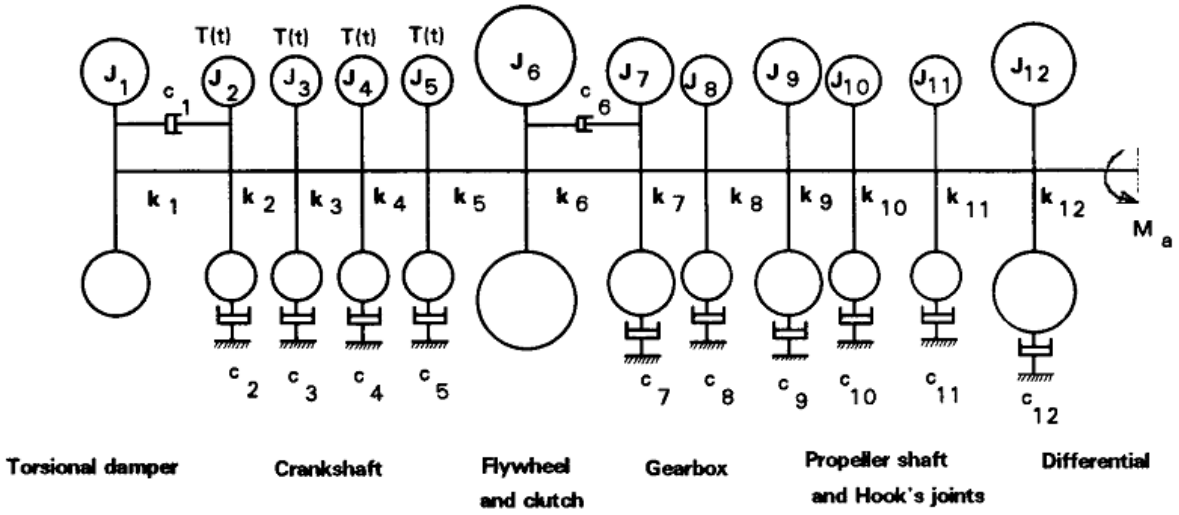

Driveline substructure (12-degrees of freedom)

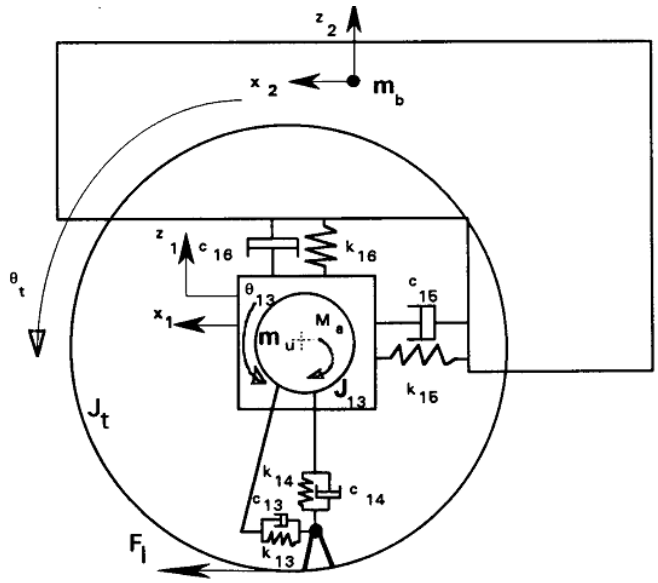

Tire, suspension and vehicle body substructure (6-degrees of freedom)

Figure 6-2, overall vehicle model [3]

According to the above figure, two substructures are related to each other by a torque named M_a which is equal to:

$$M_a = k_{12}(\theta_{13} - \theta_{12}) \qquad 6.2$$

furthermore, while it is supposed that two wheels have the same movements in Figure 6-2, it would be reasonable to regard them as single wheel.
Now we follow the same Newton procedure as section 4.2 in order to attain differential equations of motion for the overall 18-degrees of freedom system. Mass, stiffness and damping matrices in equation 6.3 are given in equations 6.4, 6.5 and 6.6 respectively.

$$\mathbf{M}\ddot{\mathbf{x}} + \mathbf{C}\dot{\mathbf{x}} + \mathbf{K}\mathbf{x} = \mathbf{F}(t) \qquad 6.3$$

where $\mathbf{K} = \begin{bmatrix} \mathbf{K}_1 & \mathbf{K}_2 \\ \mathbf{K}_3 & \mathbf{K}_4 \end{bmatrix}$

$$\mathbf{K_1}^{12\times12} =$$

$$\begin{bmatrix}
k_1 & -k_1 & 0 & 0 & 0 & 0 & 0 & 0 & 0 & 0 & 0 & 0 \\
-k_1 & k_1+k_2 & -k_2 & & & & & & & & & 0 \\
0 & -k_2 & k_2+k_3 & -k_3 & & & & & & & & 0 \\
0 & & -k_3 & k_3+k_4 & -k_4 & & & & & & & 0 \\
0 & & & -k_4 & k_4+k_5 & -k_5 & & & & & & 0 \\
0 & & & & -k_5 & k_5+k_6 & -k_6 & & & & & 0 \\
0 & & & & & -k_6 & k_6+k_7 & -k_7 & & & & 0 \\
0 & & & & & & -k_7 & k_7+k_8 & -k_8 & & & 0 \\
0 & & & & & & & -k_8 & k_8+k_9 & -k_9 & & 0 \\
0 & & & & & & & & -k_9 & k_9+k_{10} & -k_{10} & 0 \\
0 & & & & & & & & & -k_{10} & k_{10}+k_{11} & -k_{11} \\
0 & 0 & 0 & 0 & 0 & 0 & 0 & 0 & 0 & 0 & -k_{11} & k_{11}+k_{12}+k_{13}
\end{bmatrix}$$

$$\mathbf{K_2}^{12\times6} =$$

6.4

$$\begin{bmatrix}
0 & 0 & 0 & 0 & 0 & 0 \\
0 & 0 & 0 & 0 & 0 & 0 \\
0 & 0 & 0 & 0 & 0 & 0 \\
0 & 0 & 0 & 0 & 0 & 0 \\
0 & 0 & 0 & 0 & 0 & 0 \\
0 & 0 & 0 & 0 & 0 & 0 \\
0 & 0 & 0 & 0 & 0 & 0 \\
0 & 0 & 0 & 0 & 0 & 0 \\
0 & 0 & 0 & 0 & 0 & 0 \\
0 & 0 & 0 & 0 & 0 & 0 \\
0 & 0 & 0 & 0 & 0 & 0 \\
-k_{12} & 0 & 0 & 0 & 0 & 0
\end{bmatrix}$$

$$\mathbf{K_3}^{6\times12} = \text{transpose}\left(\mathbf{K_2}^{12\times6}\right)$$

$$\mathbf{K_4}^{6\times6} =$$

$$\begin{bmatrix}
k_{12} & -R^2k_{13} & 0 & -A_rRk_{14} & 0 & 0 \\
0 & 0 & 0 & -A_rRk_{14} & 0 & 0 \\
0 & Rk_{13} & k_{15} & A_rk_{14} & -k_{15} & 0 \\
0 & 0 & 0 & k_{14}+k_{16} & 0 & -k_{16} \\
0 & 0 & -k_{15} & 0 & k_{15} & 0 \\
0 & 0 & 0 & -k_{16} & 0 & k_{16}
\end{bmatrix}$$

,

$$\mathbf{C} = \begin{bmatrix} \mathbf{C_1} & \mathbf{C_2} \\ \mathbf{C_3} & \mathbf{C_4} \end{bmatrix}$$

where

$$\mathbf{C_1}^{12\times12} =$$

6.5

$$\begin{bmatrix} c_1 & -c_1 & 0 & 0 & 0 & 0 & 0 & 0 & 0 & 0 & 0 & 0 \\ -c_1 & c_1+c_2 & & & & & & & & & & 0 \\ 0 & & c_3 & & & & & & & & & 0 \\ 0 & & & c_4 & & & & & & & & 0 \\ 0 & & & & c_5 & & & & & & & 0 \\ 0 & & & & & c_6 & -c_6 & & & & & 0 \\ 0 & & & & & -c_6 & c_6+c_7 & & & & & 0 \\ 0 & & & & & & & c_8 & & & & 0 \\ 0 & & & & & & & & c_9 & & & 0 \\ 0 & & & & & & & & & c_{10} & & 0 \\ 0 & & & & & & & & & & c_{11} & 0 \\ 0 & 0 & 0 & 0 & 0 & 0 & 0 & 0 & 0 & 0 & 0 & c_{12} \end{bmatrix}$$

$$\mathbf{C_2}^{12\times6} = \mathbf{C_3}^{6\times12} \rightarrow \text{Zero matrices}$$

$$\mathbf{C_4}^{6\times6} =$$

$$\begin{bmatrix} 0 & -R^2c_{13} & 0 & -A_rRc_{14} & 0 & 0 \\ 0 & 0 & 0 & -A_rRc_{14} & 0 & 0 \\ 0 & Rc_{13} & c_{15} & A_rc_{14} & -c_{15} & 0 \\ 0 & 0 & 0 & c_{14}+c_{16} & 0 & -c_{16} \\ 0 & 0 & -c_{15} & 0 & c_{15} & 0 \\ 0 & 0 & 0 & -c_{16} & 0 & c_{16} \end{bmatrix}$$

and finally the stiffness matrix is defined as follows:

$$\mathbf{M} = \begin{bmatrix} \mathbf{M_1} & \mathbf{M_2} \\ \mathbf{M_3} & \mathbf{M_4} \end{bmatrix}$$

where

$$\mathbf{M_1}^{12\times12} = \qquad 6.6$$

$$\mathbf{M} = \begin{bmatrix} J_1 & 0 & 0 & 0 & 0 & 0 & 0 & 0 & 0 & 0 & 0 & 0 \\ 0 & J_2 & & & & & & & & & & 0 \\ 0 & & J_3 & & & & & & & & & 0 \\ 0 & & & J_4 & & & & & & & & 0 \\ 0 & & & & J_5 & & & & & & & 0 \\ 0 & & & & & J_6 & & & & & & 0 \\ 0 & & & & & & J_7 & & & & & 0 \\ 0 & & & & & & & J_8 & & & & 0 \\ 0 & & & & & & & & J_9 & & & 0 \\ 0 & & & & & & & & & J_{10} & & 0 \\ 0 & & & & & & & & & & J_{11} & 0 \\ 0 & 0 & 0 & 0 & 0 & 0 & 0 & 0 & 0 & 0 & 0 & J_{12} \end{bmatrix}$$

$$\mathbf{M}_2{}^{12\times6} = (\mathbf{M}_3{}^{6\times12})^{\mathrm{T}} \rightarrow \text{Zero matrices} = 0_{12\times6}$$

$$\mathbf{M}_4{}^{6\times6} =$$

$$\begin{bmatrix} J_t + J_{13} & J_t & 0 & 0 & 0 & 0 \\ J_t & J_t & 0 & 0 & 0 & 0 \\ 0 & 0 & m_u & 0 & 0 & 0 \\ 0 & 0 & 0 & m_u & 0 & 0 \\ 0 & 0 & 0 & 0 & m_b & 0 \\ 0 & 0 & 0 & 0 & 0 & m_b \end{bmatrix}$$

It is useful to denote that **C** and **K** matrices in the above expression contain terms associated to tire/road contact force which has been obtained already.

6.5 Time response of the system

This section is devoted to solve the differential equations of 18-degrees of freedom system subject to engine fluctuation torques. In order to avoid nonlinearity we ignore the effects of Hook's joints and we only consider the excitation torques from the engine. Also, steady-state running is regarded, and studying the system behavior during clutch engagement (transient running) is beyond the aim of this report.

In contrast with the differential equations for the 14-degrees of freedom driveline mechanism which was solved in section 5.3, the current stiffness and damping matrices are not symmetric, as a result finding the time response of the system is more difficult and time consumable. Considering the excitation torques data from *Figure 3-13, Output torques from 4 cylinders in the same plot*, again the solution of the system has been obtained via fourth order Runge-kutta method and by substituting the given data in Table 6-1 [3] in equation 6.1 and in its associated matrices.

Table 6-1, Overall vehicle properties [3]

Equivalent stiffness coefficient (N/m or N.m/rad)		Equivalent moment of inertia (kg or kg.m^2)		Equivalent system damping coefficient (N.s/m or N.m.s/rad)	
Parameter	**Value**	**Parameter**	**Value**	**Parameter**	**Value**
k_1	0.2e6	J_1	0.3	c_1	3
k_2	1e6	J_2	0.03	c_2	2
k_3	1e6	J_3	0.03	c_3	2
k_4	1e6	J_4	0.03	c_4	2
k_5	1e6	J_5	0.03	c_5	2
k_6	0.05e6	J_6	1.0	c_6	4.42
k_7	2e6	J_7	0.05	c_7	1
k_8	1e6	J_8	0.03	c_8	1
k_9	0.1e6	J_9	0.05	c_9	1
k_{10}	0.1e6	J_{10}	0.02	c_{10}	1.8
k_{11}	0.2e6	J_{11}	0.02	c_{11}	1.8
k_{12}	1e4	J_{12}	0.3	c_{12}	2
k_{13}	0.5e6	J_{13}	4	c_{13}	4000
k_{14}	0.4e6	J_t	0.12	c_{14}	600
k_{15}	1e8	m_u	180 (for both wheels)	c_{15}	100000
k_{16}	9e4	m_b	1800	c_{16}	4000
Typical tire radius in a normal passenger car		30 cm	rolling friction coefficient: The force resisting the motion when a body rolls on a surface is called the rolling resistance or rolling friction, some typical rolling coefficient are provided in www.engineeringtoolbox.com/rolling-friction		0.03

In order to reduce the computer efforts and upcoming difficulties due to instability for solving the second order differential equations of 18-degrees of freedom vehicle system, the cylinders pressures embedded noises are filtered[1] before converting to torques and consequently applying as an input to the system, the associated MATLAB commands are attached in appendix 10.210.1, cut-off frequency is chosen depending on the degree of filtration and 1000 Hz is suitable for our study, the filtered version of the torques time histories, which were shown in Figure 3-13, are demonstrated in Figure 6-3,

[1] We used an order n low-pass digital Butterworth filter with normalized cutoff frequency ω_n. Butterworth filters sacrifice roll-off steepness for monotonicity in the pass- and stop-bands.

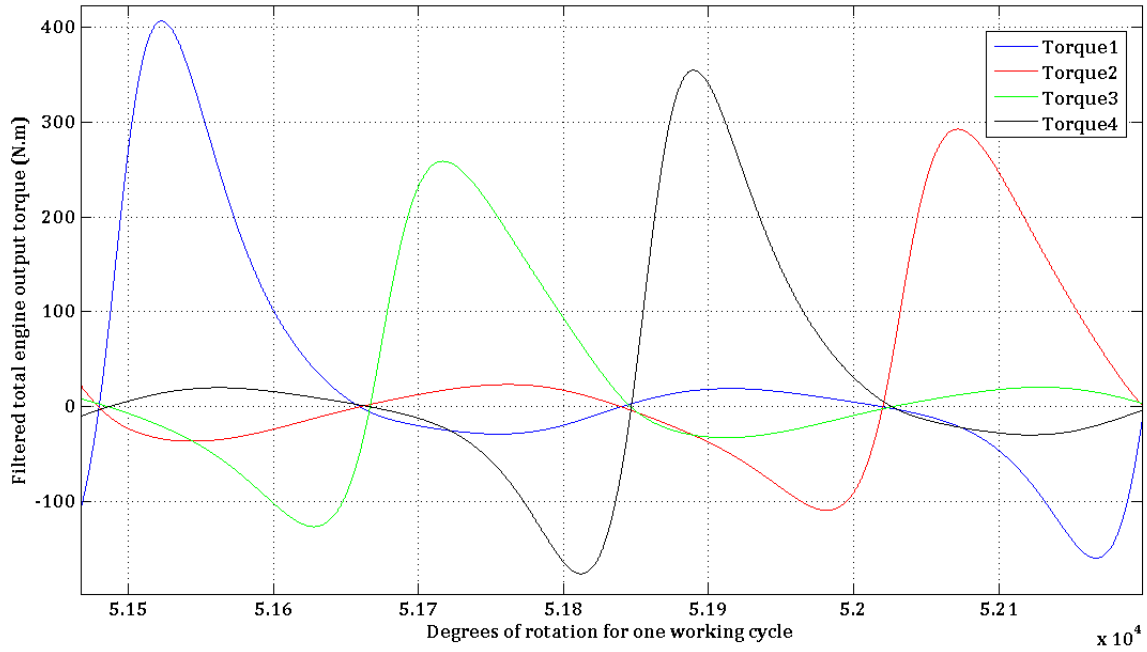

Figure 6-3, Total engine excitation torques after applying filtration

It is clear that the mean value of the torques summation should not change after filtration and remain around the experiment set value (100 N.m). Here we have 93.12 N.m which is meaningful. In the following plots, torsional vibration of driving wheels and longitudinal oscillations of the vehicle body and axle are represented for the nominal values which are given in Table 6-1. Zero initial displacements and velocities are used to determine the solution of equations.

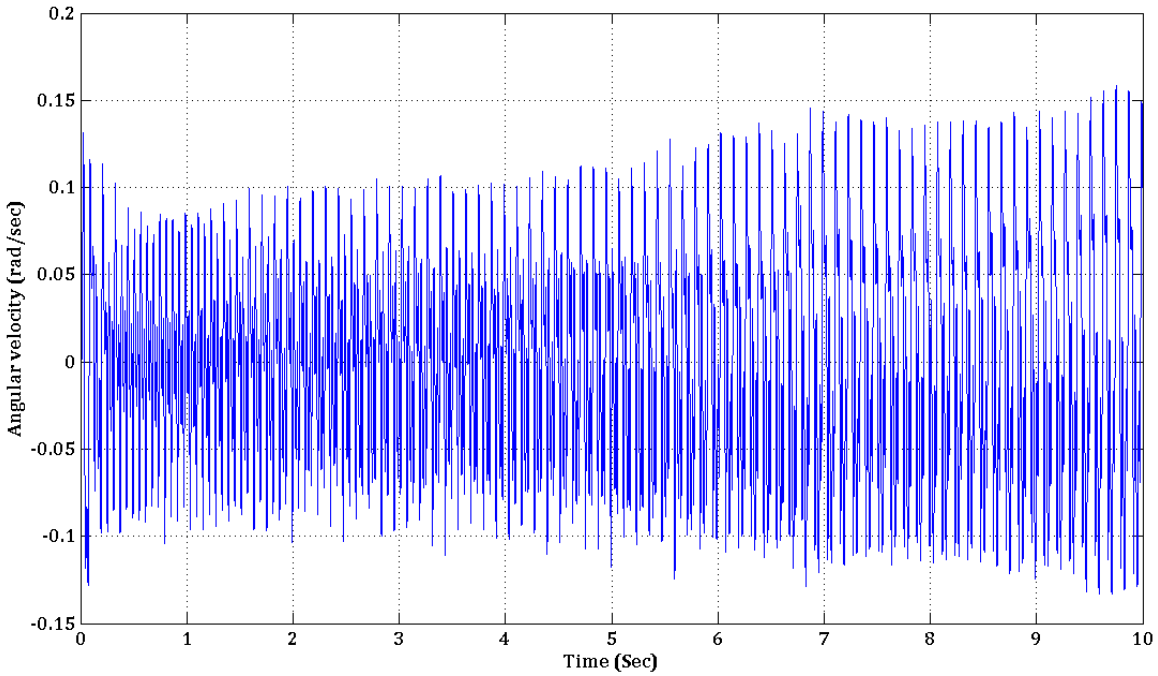

Figure 6-4, torsional velocity vibration of driving wheels due to engine excitation torques by using table 6.1 data values

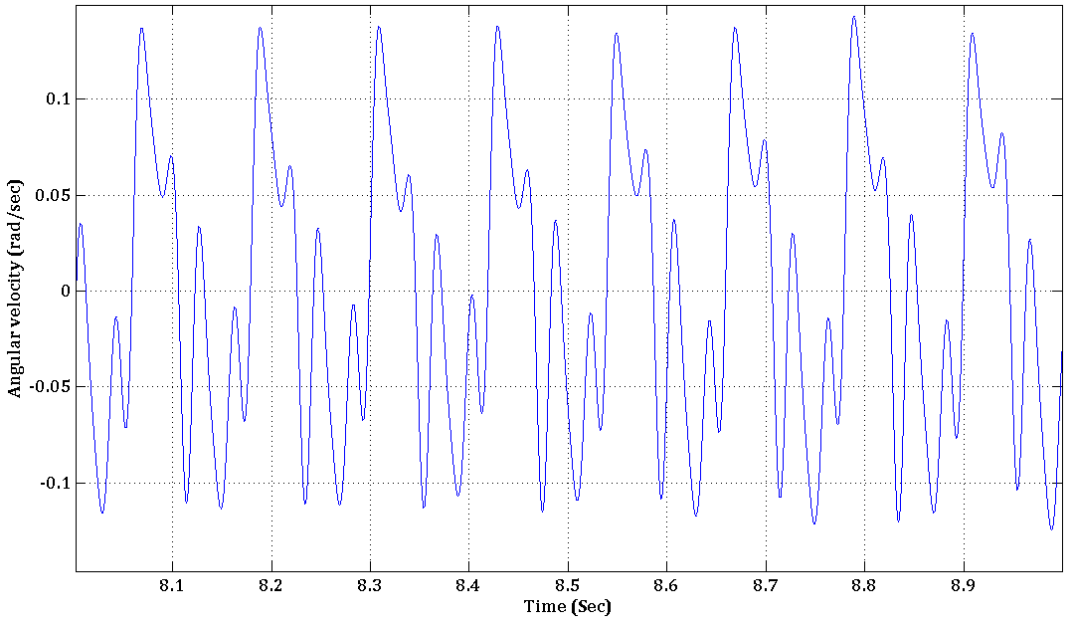

Figure 6-5, zoomed version of Figure 6-4 between seconds 8 to 9

The result became stable in the second five seconds. To have a better look one second has picked out and zoomed in Figure 6-5.

According to Figure 6-5, there is a good agreement between the amplitude of torsional velocity in our result and reference [3] (Fig 8.5), however due to different input force, the frequency content is dissimilar.

As it was earlier denoted number of times, vehicle body vibration in every direction (sprung-mass) is very important in the level of ride comfort and we need vehicle body accleration to go through drivability diagrams, hence firstly it is necessary to obtain the plots in Figure 6-6:

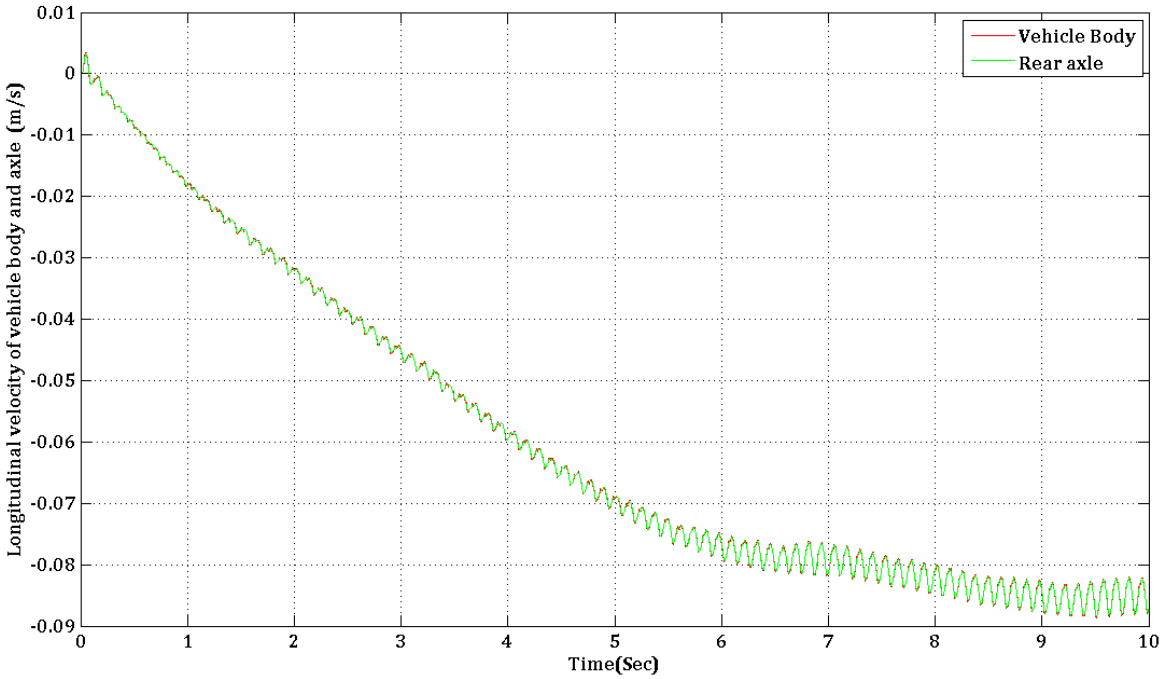

Figure 6-6, Longitudinal velocity vibration of the vehicle body and axle due to engine excitation torques by using table 6-1 data values

From the above figure, it takes considerable seconds for achieving stable results. Huge amount of input data to the system and thirty six differential equations that have to be processed at the same time is one reason, the last three seconds is almost stable which is zoomed in Figure 6-7. Accordingly fourth order Runge-kutta approach is not that powerful to solve this system and as a future work another predictor corrector numerical method has to be used to study this kind of systems. Again the results agree with reference [3].

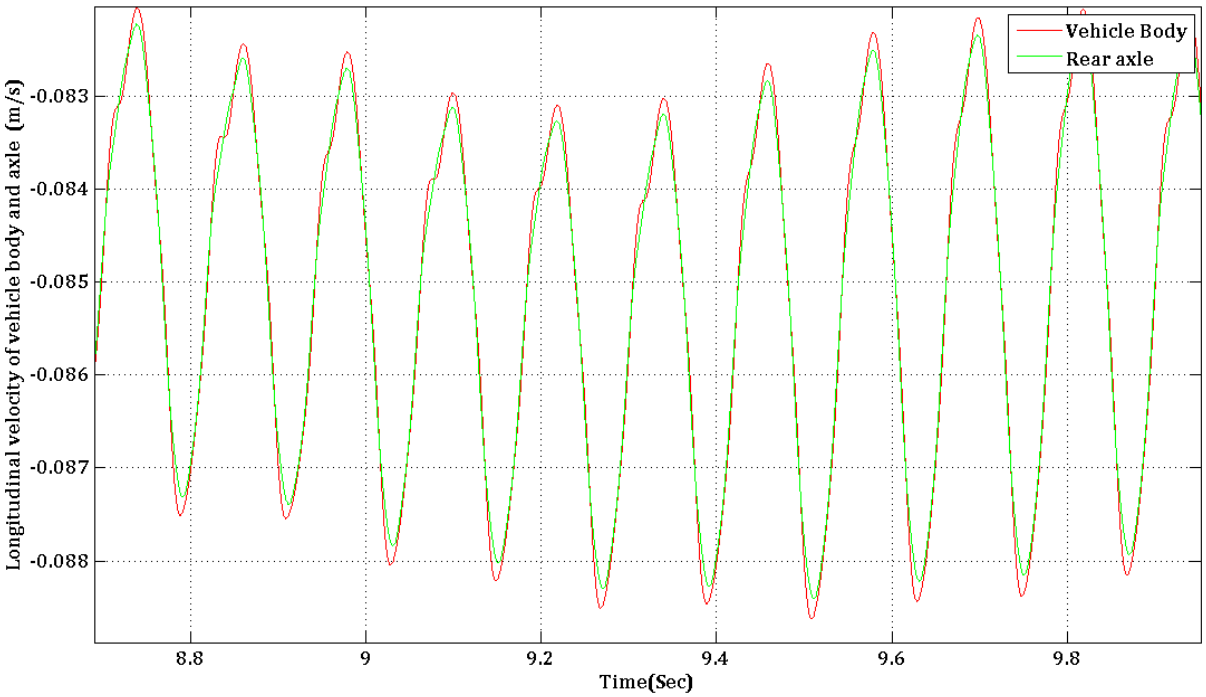

Figure 6-7, zoomed version of Figure 6-6

6.6 Studying the influence of stiffness and damping coefficients

From manufacturing view, sensitivity analysis which studies the effects of different parameter values has a significant importance. Moreover there are a variety of structural optimization techniques to find the optimum value of each parameter in any kind of system, this can be regarded as a future work for this thesis, here we will only change stiffness and damping coefficients and resolve the equations of the vehicle system to see the influence on the output results.

In Figure 6-8 and Figure 6-9, damping coefficients of the system are decreased notably which result to great higher amplitude in torsional and longitudinal velocities of driving wheels and vehicle body, respectively. Low damping may also generate instability in system output response since the dissipated energy is not enough in comparison to the added nonlinear longitudinal force,

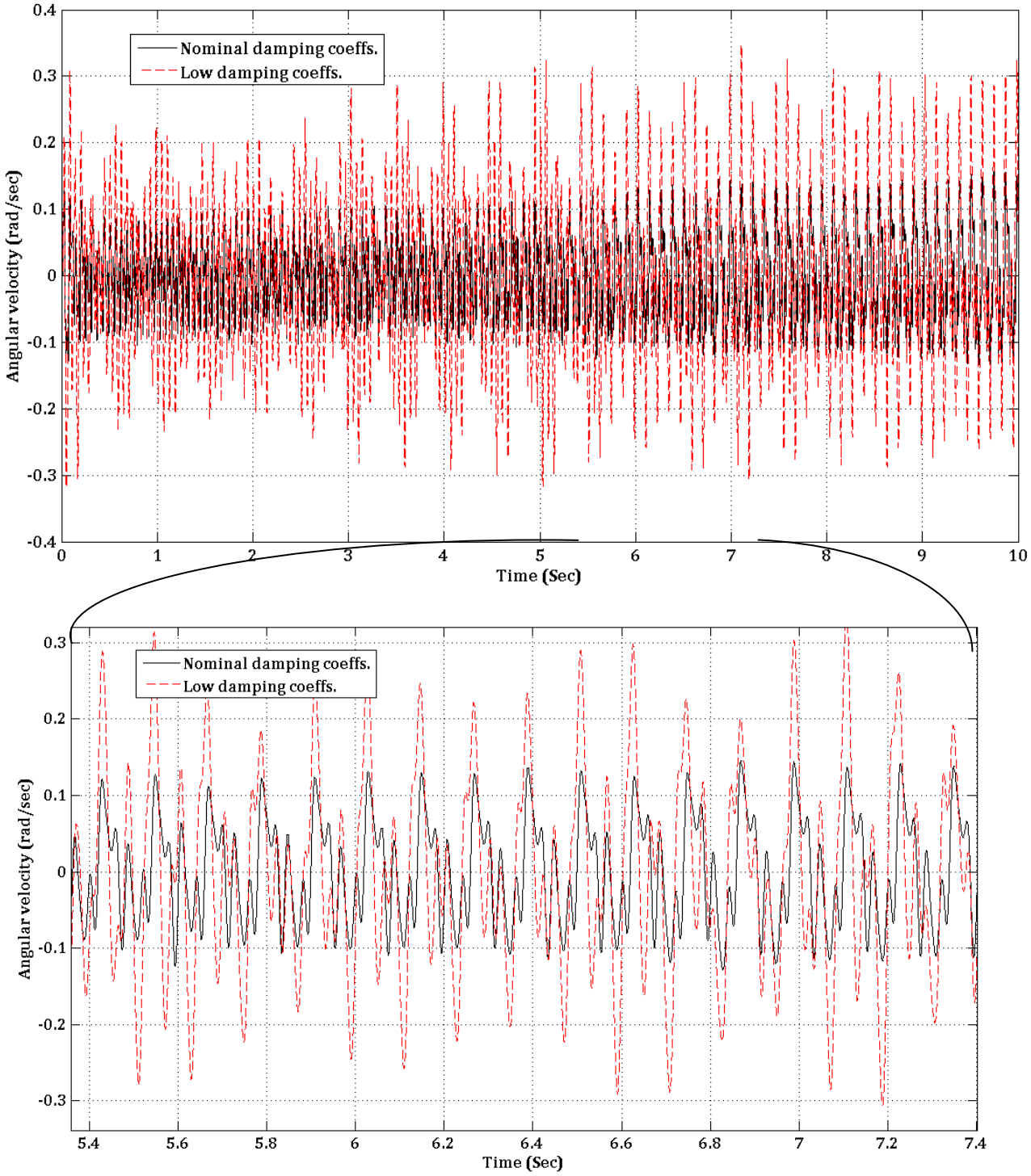

Figure 6-8, torsional velocity of driving wheels with low damping

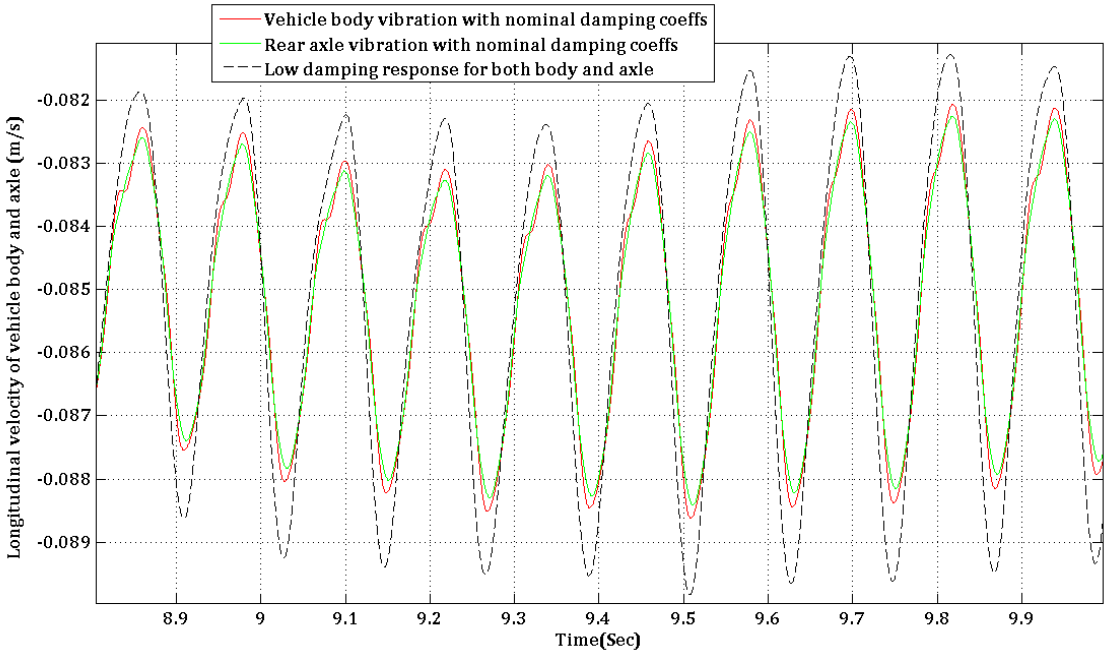

Figure 6-9, Longitudinal velocities of vehicle body and axle with low damping

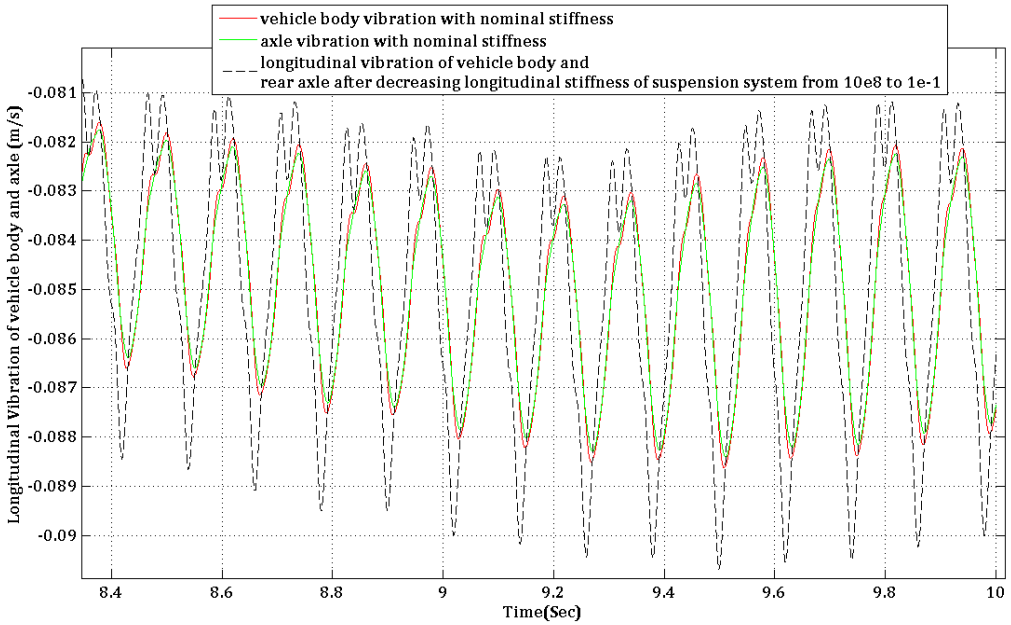

Figure 6-10, Longitudinal velocities of vehicle body and axle with low suspension system stiffness

It should be noted that the solution method may not be enough powerful to show accurate sensitivity to the data value change.

In Figure 6-10, Longitudinal velocities of vehicle body and axle with low suspension system stiffness the suspension system stiffness value has been reduced to see the influence on the longitudinal vibration of the vehicle body and axle. According to Figure 6-10, decreasing suspension system longitudinal stiffness may cause to vibration increase of the vehicle body (sprung mass) subject to engine excitation torques, which is not desired. On the other hand, appropriate suspension system vertical stiffness coefficient, as it will be seen in the next chapter, when the input excitation is from the ground[1], depends on the range of force frequency as well, and consequently high or low vertical stiffness may be required.

[1] road surface non-uniformities

7 Chapter 7

Vehicle suspension system response due to ground input using quarter-car model

7.1 Introduction

The results of previous chapter and this one will be used in ride comfort diagrams to study the level of induced discomfort due to engine oscillatory torques and road irregularities.

7.2 Quarter-car model and performance of suspension system

In order to evaluate ride quality of normal passenger cars, it is necessary to consider the possibility for different kinds of vibration which may occur in vehicle body (sprung mass)[1] system as well as front and rear wheels (unsprung mass)[2] mechanisms. it is useful to note that aerodynamic, driveline and engine forces are applied to the sprung mass, however ground non-uniformities input excitation is applied to the tire and consequently suspension system. For the 18-degrees of freedom overall vehicle model in section 6.4, longitudinal and vertical vibrations of the sprung an un-sprung masses were studied due to engine excitations torques since the goal was investigating the coupled behavior of the driveline torsional vibration and tire/suspension system. The aim of this chapter is looking more specifically into suspension system response subject to the ground input and finding the effects of raising/reducing stiffness and damping coefficients to have better performance of suspension mechanisms in automobiles. a simple two-degrees of freedom quarter–car model which is suitable for our study is represented in . In this model, sprung and unsprung masses are denoted respectively by m_2 and m_1 while all the corresponding parameter values are given in Table 7-1, using Table 6-1, *Overall vehicle properties* ,

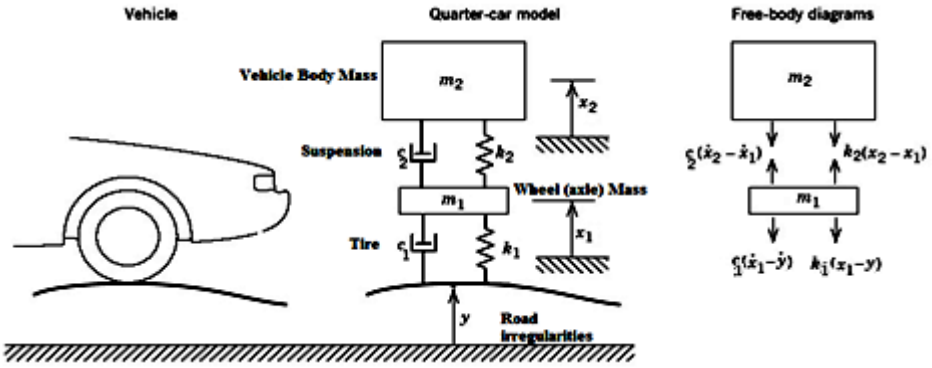

Figure 7-1, Two-degrees of freedom model vehicle

[1] pitch, bounce and roll
[2] bounce and roll

Table 7-1, Tire/suspension properties [3]

Vehicle body mass (m_2) : sprung mass = 1800/4 kg (quarter of the whole body mass) **Wheel (axle) mass : Unsprung mass = 90 kg**			
Suspension		**Tire**	
Stiffness : k_2 (N/m)	9e6	**Stiffness : k_1 (N/m)**	4e5
Damping : c_2 (N.s/m)	4000	**Damping : c_1(N.s/m)**	600

the equations of motion for the above system in vertical direction are found according to Newton's law and free body diagram of the separate masses (Figure 7-1):

$$m_1\ddot{x}_1 = -c_1\dot{x}_1 - k_1x_1 - c_2\dot{x}_1 - k_2x_1 + c_2\dot{x}_2 + k_2x_2 + c_1\dot{y}_1 + k_1y_1 \quad 7.1$$

$$m_2\ddot{x}_2 = -c_2\dot{x}_2 - k_2x_2 + c_2\dot{x}_1 + k_2x_1 \quad 7.2$$

The undamped natural frequencies of the quarter car model for sprung (vehicle body) and un-sprung masses (wheels) are as follows (Table 7-1):

$$f_{ns} = \frac{1}{2\pi}\sqrt{\frac{{}^{k_1k_2}/_{(k_1+k_2)}}{m_2}} = 2.033 \text{ Hz} \quad 7.3$$

$$f_{n-us} = \frac{1}{2\pi}\sqrt{\frac{k_1+k_2}{m_1}} = 11.74\text{Hz} \quad 7.4$$

as it is seen, there is a wide difference between natural frequencies of the vehicle body and tire/wheels assembly, therefore in the case of high excitation frequency (such as the input impulse by a bumpy road), according to Figure 7-2, since the frequencies ratio $(f_{\text{excitation}}/f_{\text{natural}})_{\text{sprung mass}}$ is high, transmissibility will be very low and consequently we will achieve desired vibration isolation for vehicle body with the aid of suspension mechanism. On the other hand, when the excitation frequency is low and near to vehicle body natural frequency (in the situation of traveling over an undulating surface), the transmitted force is equal to the input or even could be amplified, and hence a conventional suspension system with fixed properties has not good performance in this case. This is the reason for a huge amount of research activities in the field of active suspension system[1] (in contrast to passive system) which has variable stiffness and damping[2] regarding to the input frequency.

[1] Hydraulic systems which is now available in the new vehicles to have active suspension system

[2] In order to attain desired high or low natural frequency, stiff or soft properties are required for the suspension mechanism

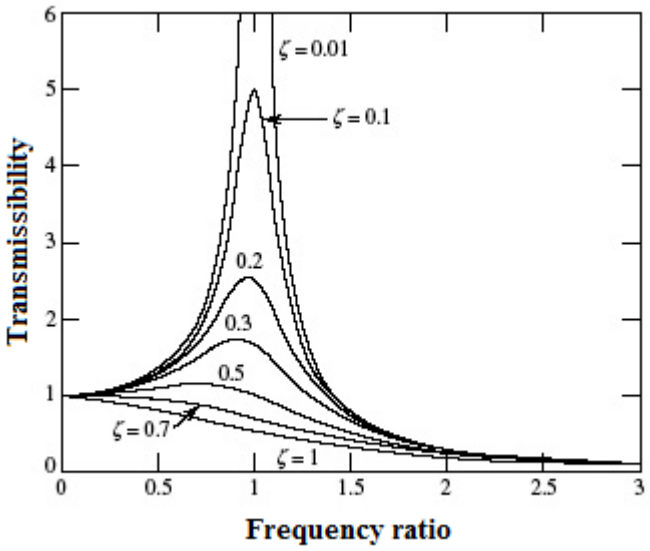

Figure 7-2, Transmissibility as a function of frequency ratio for a single-degree of freedom system

As it was already known, vertical acceleration of vehicle body is important in ride comfort diagrams and it is related to the level of isolation by the suspension system which was described precisely in previous paragraph, however the passenger will not feel vehicle body motion but rather the displacement of his seat, thus we use the model suggested in reference [2] in this thesis and it is shown in Figure 7-3, the necessary steps to find corresponding transfer functions for obtaining output responses are explained as follows:

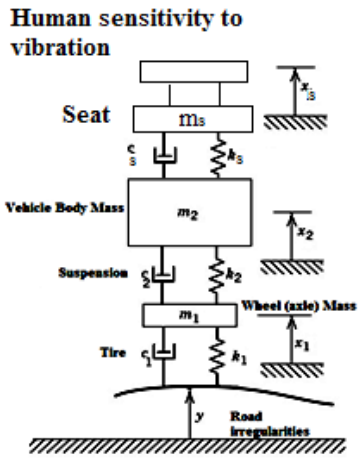

Figure 7-3, Modified quarter-car model including seat displacement

- first, it is necessary to convert the equations 7.1 and 7.2 to Laplace domain:

$$(m_1 s^2 + c_1 s + k_1 + c_2 s + k_2)X_1(s) - (c_2 s + k_2)X_2(s) = (c_1 s + k_1)Y(s) \qquad 7.5$$

$$-(c_2 s + k_2)X_1(s) + (m_2 s^2 + c_2 s + k_2)X_2(s) = 0 \qquad 7.6$$

- now the only unknowns are $X_1(s)$ and $X_2(s)$, by applying Cramer's rule and substituting $s=i\,\omega$ in equations 7.5 and 7.6, we have:

$$H_{x1}(\omega) = \frac{x_1}{y} = \frac{(c_1 i\omega + k_1)(-m_2\omega^2 + c_2 i\omega + k_2)}{(m_1\omega^2 - c_1 i\omega - k_1 - c_2 i\omega - k_2)(m_2\omega^2 - c_2 i\omega - k_2) - (c_2 i\omega + k_2)^2} \quad 7.7$$

$$H_{x2}(\omega) = \frac{x_2}{y} = \frac{(c_2 i\omega + k_2)(c_1 i\omega + k_1)}{(m_1\omega^2 - c_1 i\omega - k_1 - c_2 i\omega - k_2)(m_2\omega^2 - c_2 i\omega - k_2) - (c_2 i\omega + k_2)^2} \quad 7.8$$

- there are different versions of transfer functions :Receptance, Mobility and Accelerance, expressions 7.7 and 7.8 are receptances, now to determine the mobilities and accelerances we have the following converting relations:

$$\text{Mobility} \rightarrow H_{\dot{x}1}(\omega) = \frac{\dot{x}_1}{y} = i\omega H_{x1}(\omega) \quad 7.9$$

$$\text{Accelerance} \rightarrow H_{\ddot{x}1}(\omega) = \frac{\ddot{x}_1}{y} = -\omega^2 H_{x1}(\omega) \quad 7.10$$

- now according to random process theory [24], for a stationary[1] random input (such as Gaussian function which will be later considered as ground excitation for the suspension mechanism in) in the case of linear system, there is a well-known formula in order to attain power spectral density of output response by using power spectral density (PSD) of input and the appropriate transfer function among the above three:

$$S_{\cdot}(\omega) = |H_{\cdot}(\omega)|^2 S_y(\omega) \quad 7.11$$

where $S_{\cdot}(\omega)$ is the PSD of desired system point displacement, velocity or acceleration, $|H_{\cdot}(\omega)|^2$ is the corresponding transfer function, and $S_y(\omega)$ is the PSD of input force,

- Using the same approach, the complex transfer function between x_2 and x_s is:

$$H_s(\omega) = \frac{x_s}{x_2} = \frac{(c_s i\omega + k_s)}{(m_s\omega^2 - c_s i\omega - k_s)}$$

where from reference [2] for a normal passenger car, we have $\zeta_s = \frac{c_s}{2m_s\omega_s} = 0.3$ and $\omega_s = \sqrt{k_s/m_s} = 5\pi$ rad/sec and consequently we arrive into:

$$\ddot{x}_s = H_s(\omega) H_{\ddot{x}2}(\omega) y \quad 7.12$$

$$S_{\ddot{x}s}(\omega) = |H_s(\omega)|^2 |H_{\ddot{x}2}(\omega)|^2 S_y(\omega) \quad 7.13$$

One important point is that: *we cannot change the suspension system stiffness and damping coefficients, to reach desired vibration isolation, without taking into consideration two other aspects of suspension mechanism which are important in its performance: road holding[2] and suspension working space[3]*, these parameters are to be considered as

[1] Stationary random process: for this type of random data, mean value and variance are constant and independent of time

[2] it is important for a safe ride that the contact forces between the wheels and the road are so large that horizontal forces on the vehicle can be balanced by frictional forces at the wheels [2]

[3] practically, the working space of vehicle suspension system is limited [2]

constraints in the problem of finding optimum values of suspension damping and stiffness which can be studied in a future work.

7.3 Road roughness classification by ISO and the recommended single-sided vertical amplitude power spectral density

As it was already explained, in section 1.3, by assuming the availability of three conditions, we can use the road surface profile which is recommended by ISO in a form of single-sided power spectral density as follows [4]:

$$S_y(n) = S(n_0)\left(\frac{n_0}{n}\right)^2, \quad n \le n_0$$

$$S_y(n) = S(n_0)\left(\frac{n_0}{n}\right)^{1.5}, n \ge n_0 \qquad 7.14$$

where n_0 is a fixed datum spatial frequency equal to $1/(2\pi)$ cycles/m and $S(n_0)$ is attained according to road roughness classification proposed by ISO which is also represented in Table 7-2 using reference [4]. In the analysis of vehicle vibration, it is more practical to work with temporal frequency in Hz rather than spatial frequency in cycles/m. if the car travels with a constant speed v (m/s), then $S_y(f) = S_y(n)/v$ where$f = vn$, accordingly we reach to:

$$S_y(f) = \frac{S_y(n_0)}{v}\left(\frac{f_0}{f}\right)^2, f \le vn_0 = f_0$$

$$S_y(f) = \frac{S_y(n_0)}{v}\left(\frac{f_0}{f}\right)^2, f \ge vn_0 = f_0 \qquad 7.15$$

Table 7-2, Classification of road roughness proposed by ISO [4]

Road Class	Degree of roughness $S(n_0)$, 10^{-6}m^2/cycles/m	
	Range	Geometric mean
A (very good)	<8	4
B (good)	8-32	16
C (average)	32-128	64
D (poor)	128-512	256
E (very poor)	512-2048	1024
F	2048-8192	4096
G	8192-32768	16384
H	>32768	

7.4 Typical passenger car driver RMS acceleration to an average road roughness

We are interested in RMS vertical acceleration of the car seat which is obtainable by knowing power spectral density of the seat acceleration and using the following formula[1]:

$$\text{RMS acceleration} = \left[\int_{0.89f_c}^{1.12f_c} S_{\ddot{x}s}(f)df \right]^{1/2} \qquad 7.1$$

where $S_{\ddot{x}s}(f)$ is found from equation 7.13 by substituting$\omega = 2\pi f$, we assume that the travelling velocity of the vehicle is 80 Km/hr (22.22 m/s) and thus the value of the f_0=vn_0=3.5368 Hz. Figure 7-4 demonstaretes RMS acceleration (m/s^2) graph of a typical passenger car seat in a certain frequency range, an average road roughness class is picked, therefore $S(n_0) = 64*10^{-6}$m^2/cycles/m.

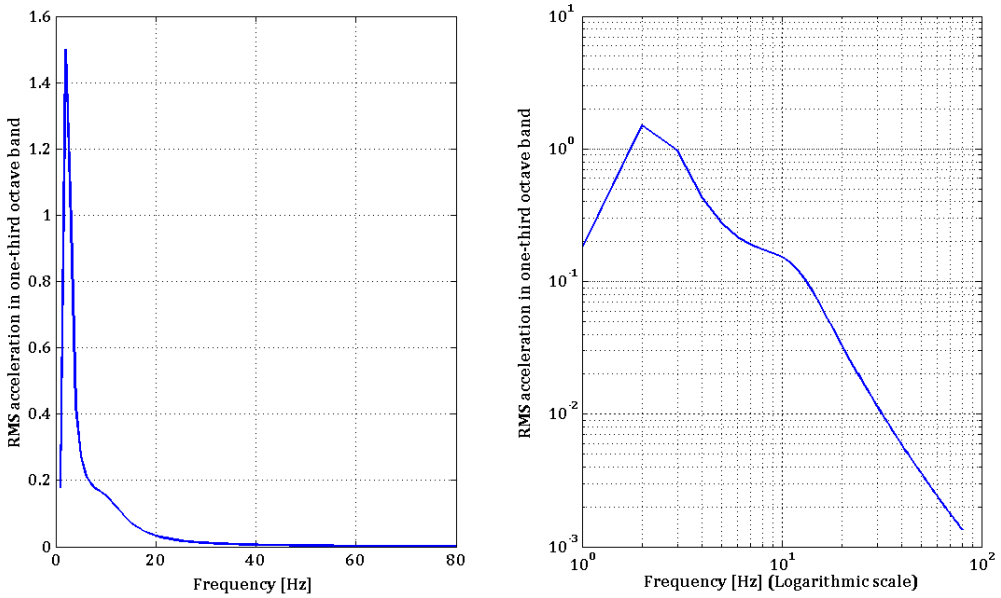

Figure 7-4, Measured vertical acceleration of a passenger car seat traveling at 80 Km/hr over an average road

As it is seen in Figure 7-4, the peak value of the car seat RMS acceleration plot happens around frequency 2 Hz which is the natural frequency of the sprung/vehicle body mass (first mode frequency), hence it can be concluded that one of the road surface input excitation frequencies is in the region of 2 Hz. further in order to control the system response amplitude for this class of road roughness and avoid high acceleration, the natural frequency of the suspension system have to be regularized[2] with respect to input force frequency by taking into account road holding and suspension working space limitations at the same time.

Now, for checking the solution method[3] accuracy, the effects of passenger seat is ignored in equation 7.13 and the represented model in is applied to obtain the vehicle body vertical acceleration power spectral density subject to surface irregularities. In this case, it is possible to compare the result with the plot which is given in reference [4]. Figure 7-5 illustrates the

[1] f_c is the center frequency, and the RMS value is calculated in one-third octave band, it is necessary to accumulate the spectrum between the lower and upper bands [24].
[2] by changing stiffness or damping coefficient in an active suspension system
[3] the procedure of finding power spectral density of the output

sprung/vehicle body mass RMS vertical acceleration in similar conditions with Figure 7-4. The plot shape has a good agreement with Fig. 7.32 in reference [4], however the acceleration amplitude is somehow greater due to different road surface conditions and suspension system characteristics. In contrast to Figure 7-4, in Figure 7-5 two peaks exist: one "at the sprung mass natural frequency around 2 Hz (1st modal frequency)" and the second one "at unsprung mass natural frequency around 10 Hz (2nd modal frequency)". The reason for this phenomenon is that if we include passenger seat mass in the model, it will perform as a absorber which is a very important subject in vibration theory, in other words passenger seat mass has absorbed the movement of unsprung mass in the region of resonance frequency and consequently no peak will occur in the 2nd modal frequency around 10 Hz[1].

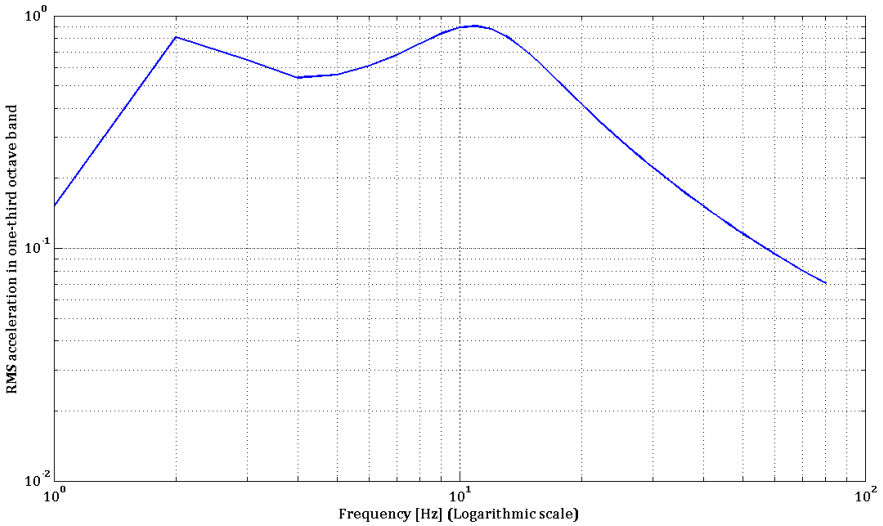

Figure 7-5, vehicle body vertical acceleration subject to an average road roughness with 80 Km/hr traveling speed

.

[1] Although this function for the absorber is strongly related to the mass ratio and if it was not in the appropriate region, then absorber has negative influence which happened in the current system for the 1st modal frequency (2Hz) and the amplitude of acceleration is greater in Figure 7-4 compare to Figure 7-5

8 Chapter 8

Evaluation of typical passenger car comfort with respect to ride quality criteria

8.1 Introduction

This chapter is devoted to use the proposed results in Figure 7-4 and Figure 6-6 in ride quality diagrams for evaluating drivability of the typical passenger car with the given overall vehicle properties in Table 6-1, Overall vehicle properties.

8.2 International Standard ISO 2631-1:1985

According to ISO 2631-1:1985 [19], four physical factors have significant effects on human response to applied vibration: the strength (power), frequency, direction and interval of exposure, there are also three different issues which are important to evaluate the human reaction to the vibratory displacements [3]:

- preservation of working efficiency
- preservation of health or safety
- preservation of comfort

In Figure 8-1 and Figure 8-2, the fatigue-decreased proficiency boundaries for various exposure times are represented in vertical (along the z_2- axis in) and longitudinal (along the x_2- axis in) directions, respectively. As it is clear in the proposed diagrams, the comfort boundary will decrease by rising the vibration duration. It should be mentioned that also the human body is more sensitive to vibration in some frequency ranges than in others, for example according to the following figures, for vertical vibration the critical frequency region is 4 to 8 Hz while for longitudinal vibration this frequency area is less than 2 Hz.

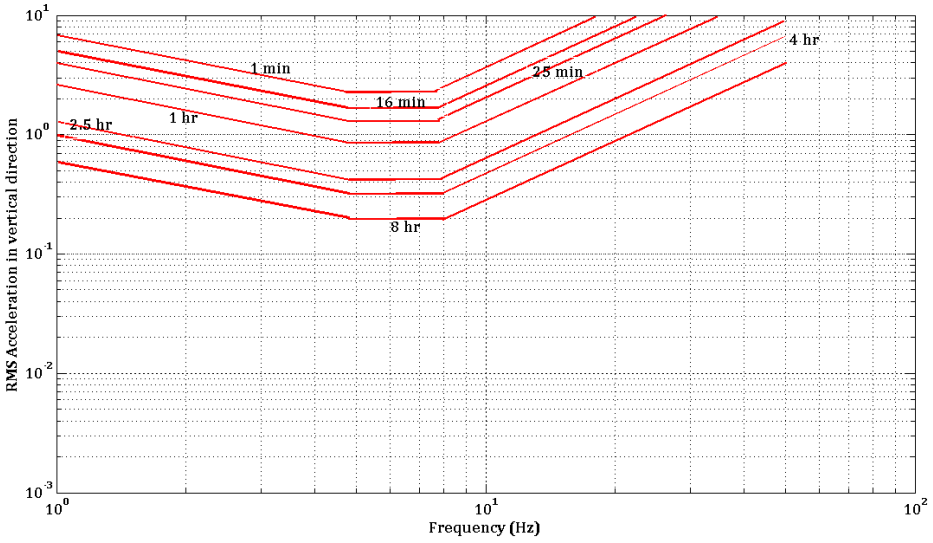

Figure 8-1, ISO 2631-1:1985 "fatigue-decreased proficiency boundary": vertical acceleration limits as a function of frequency and exposure time [4]

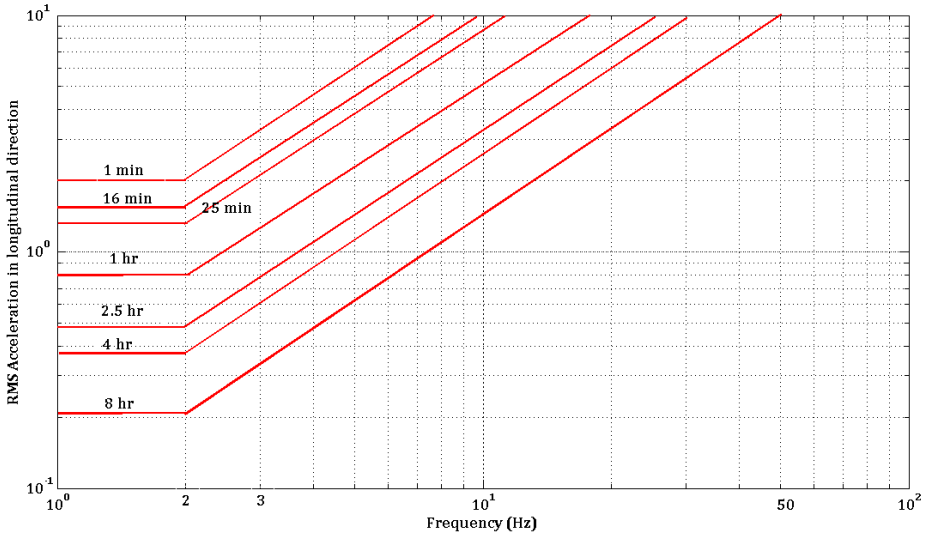

Center frequency of one-third octave band

Figure 8-2, ISO 2631-1:1985 "fatigue-decreased proficiency boundary": longitudinal acceleration limits as a function of frequency and exposure time [4]

8.3 Results and Discussion

This section of the report contains appropriate figures in order to evaluate ride comfort of a typical passenger car[1] at a certain frequency interval by using the sprung mass responses[2] and the ISO criteria which are shown in the previous section.

Measured vertical RMS acceleration of the vehicle body, with 80 Km/hr traveling speed on an average road roughness, is shown again in Figure 8-3 but together with ISO fatigue-decreased boundaries to investigate the level of comfort for this specific passenger car,

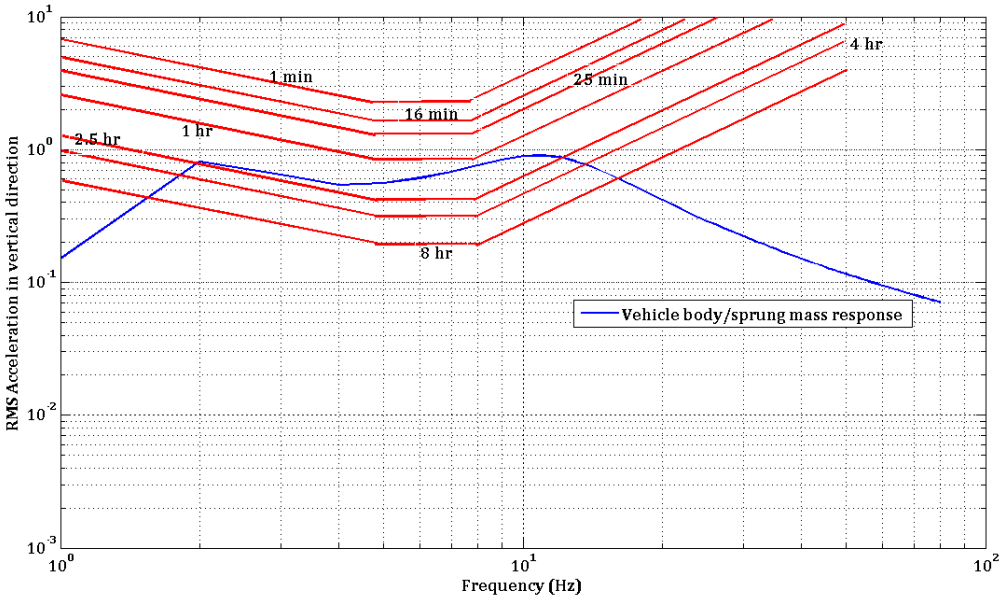

Figure 8-3, vehicle body vertical acceleration due to road excitation in comparison with ISO ride comfort boundaries

[1] with the given properties in Table 6-1

[2] which have been obtained already for different directions in chapters 6 and 7 (Figure 6-6, Figure 7-4 and Figure 7-5) subject to engine and road irregularities excitations.

Regarding Figure 8-3, it can be concluded that for this type of passenger car and passive suspension system properties, in the situation of average road roughness, it is desired to have exposure time less than 2.5 hours, however if the vibration duration is more than 2.5 hours, the vertical RMS acceleration is beyond the limitations, specifically around the modal frequencies or in the other words low frequency region, consequently the ride quality level is low. one good suggestion is moving the second modal frequency to the outside of the critical region for human sensitivity (4-8 Hz), thus it will exist wider band to the allowed boundaries.

Now, the longitudinal RMS acceleration of the vehicle body due to engine excitations is compared to ISO proposed boundaries to evaluate the ride comfort in lateral direction. to achieve this goal first, "it is necessary to differentiate the velocity data in Figure 6-6 and obtain time history for longitudinal acceleration using MATLAB command gradient", secondly, "we have to determine acceleration power spectral density in order to calculate RMS value in equation 7.16[1], one-third octave band rule is again utilized for each frequency in the interval 0f 1-80 Hz". Figure 8-4 illustrates the corresponding longitudinal RMS acceleration of the vehicle body.

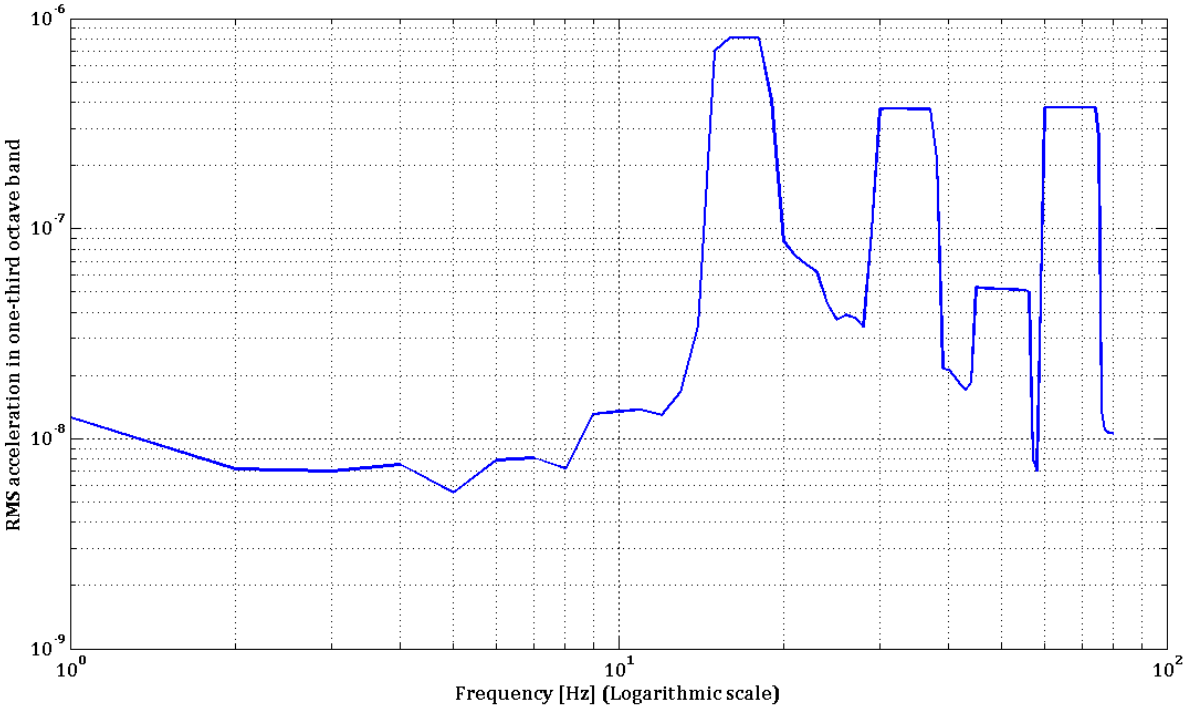

Figure 8-4, Measured longitudinal acceleration of a passenger car body due to engine excitation torques

As it was already explained, for high frequency force input, suspension system has good vibration isolation, and since the engine excitation frequencies are high in comparison with natural frequency of the sprung mass (in longitudinal direction), the acceleration amplitude is too low in Figure 8-4, which is strongly desired, and completely below the allowed ISO fatigue-decreased boundaries which is shown in Figure 8-2.

[1] In order to obtain RMS value from discrete-time power spectral density, we have to sum up the PSD values in the desired interval [24].

8.4 Thesis conclusion

In this report, two main excitation resources of a passenger car were studied in order to evaluate drivability of the specified vehicle according to ISO ride quality criteria:
1-"torsional vibration of the driveline system" due to engine oscillatory torques which was modeled by using 14-degrees of freedom system, and further the influence of driveline excitation on the longitudinal displacement of the vehicle body was investigated with the aid of coupled driveline and tire/suspension 18-degress of freedom mechanism.
2-"road surface non-uniformities vertical input force" effects on the vehicle body were attained by using two-degrees of freedom quarter-car model including suspension and tire assembly vertical properties.

Regarding the achieved results in Figure 8-3 and Figure 8-4, and by considering the specific assumptions[1] which have been described in the introductory chapter, the produced vertical RMS acceleration of the vehicle body subject to road surface irregularities (low and high frequency content) is much greater than the longitudinal acceleration of sprung mass due to engine excitation (high frequency content), and furthermore in some frequency region vertical response of the system is beyond the ISO limitations. Therefore, since the desired performance of suspension system is dependent to various input excitations, and noting that for a vehicle, there exist different input forces with different frequency content at the same time, it can be concluded that a passive suspension system with fixed stiffness and damping coefficients is not proper and an active mechanism is required. Although, it should be mentioned that the importance of driveline torsional oscillation modeling and knowing its natural frequencies is not only for the corresponding influence on the vehicle body vibration and induced noise, but also for dangerous damages which may occur for different driveline components due to high vibration amplitude and resonance phenomenon. Consequently it is necessary to obtain the response sensitivity of each driveline part to high or low parameter values as it was done in section 6.6, *Studying the influence of stiffness and damping coefficients* .

The fourth order Runge-kutta numerical approach which was used for solving 14-degrees and 18-degrees of freedom mechanical systems in Chapter 4 and Chapter 6, is a powerful iterative method for solving ordinary differential equations and it was functional here since the non-proportional damping matrix prevents from using Modal analysis method to find the system response. The problem is that, this method is not sensitive enough for showing the effects of changing different parameter values.

8.5 Future works

There exist different subjects that may be considered as a future work for this master thesis while a few numbers of them are explained in the following items:

- The effects of engine mounts, which have been ignored here. Nowadays, in new car generations, engine mounts are very helpful in order to reduce the unwanted transmitted vibration of the engine and it would be practical to model and optimize their structure.
- As it was already noted in chapter 7, it is required to introduce an appropriate optimization technique for determining suspension system optimum parameter values in order to have the best vibration isolation with taking into account the

[1] We are only studying the engine vibratory pressure torques not the effects of reciprocating parts of the engine and, moreover we ignore the nonlinear generated torques by Hooke's joints and the other possible components.

suspension working space and road holding constraints. Furthermore, investigating about an active suspension system is needed.

- It is necessary to find more powerful numerical method to solve the system and decrease the level of instability, however in some cases the lack of reference data to evaluate the accuracy of numerical solution results to requirement of analytical method, thus recently a lot of research activities have been focused on analytical approaches for liner and nonlinear systems.
- Modeling nonlinear effects of different parts in driveline system has a primary interest, since they may cause to harmful phenomenon due to corresponding chaotic behaviors.

9 References

[1]. D.Gillespie, Thomas. *Fundamentals of vehicle dynamics.* Warrendale,PA: Society of Automotive Engineers, Inc.

[2]. Dahlberg, T. "Ride Comfort and Road Holding of a 2-DOF Vehicle Travelling on a Randomly Profiled Raod." *Journal of Sound and vibration*, (1978) 58 (2): 179-187.

[3]. El-Adl Mohammed Aly Rabeih, BSc. & M. Sc. *Torsional Vibration Analysis of Automotive Driveline.* PhD thesis, Leeds, UK: Mechanical Engineering Department, the university of Leeds, 1997.

[4]. Wong, J. Y. *Theory of Ground Vehicles.* New Jersey: John Wiley & Sons, Inc., 2008.

[5]. Reik, W. "Torsional Vibrations in the Drive train of Motor Vehicles, principle considerations." *4th International Symposium.* Baden-Baden, 1990. 5-28.

[6]. Zhanoi, W., et al. "Research on the Coupling Power Train Torsional Vibration With Body Fore-Aft and Vertical Vibration of a 4x2 Vehicle." *IMechE,C3 89/450, Vol. 2, Paper No. 925067.* 1992. 219-223.

[7]. Parkins, D. W. "Automobile Drive-Line Vibration and Internal Noise." *Annual Conf. of the stress Analysis Group of the Inst. of physics, "Stress, Vibration and Noise Analysis in Vehicles".* 165-179.

[8]. Healy, S. P., et al. "An Experimental Study of Vehicle Driveline Vibrations." *IMechE, Paper No. C 13 2/79.* 1979. 69-81.

[9]. Exner, W. and Ambom, P. "Noise and Vibration in the Driveline of Passenger Cars." *IMechE Automotive Congress, Seminar 37, Paper No. C 427/37/025.* 1991. 8 pages.

[10]. J.H. Walls, J. C. Houbolt and H. Press. *Some measurements and power spectra of runway roughness.* NACA Technical Note 3305, 1954.

[11]. Houbolt, J. C. "Runway roughness studies in the Aeronautical field." *Journal of the Air Transport Division Proceedings, American Society of Civil Engineers 87, AT-1,* 1961.

[12]. Colledge, A. Craggs and R. B. *Random vibration analysis applied to road surface measurement and vehicle suspension performance.* Motor Industries Research Association Report MIRA , 1964/69.

[13]. Bender, E. K. *Optimization of the random vibration characteristics of vehicle suspensions using random process theory.* ScD Thesis, MIT, Cambridge, MA, 1967.

[14]. Hrovat, D. "Application of optimal control to advanced automotive suspension design." *Journal of dynamical systems, measurements and control*, (1993) 115: 328-342.

[15]. Rill, G. "The influence of correlated random excitations processes on dynamics of vehicles." *proceedings of the eighth IAVSD symposium on the dynamics of vehicles on road and railway tracks.* 1983. 449-459.

[16]. Turkey, S. and Akcay, H. "A study of random vibration characteristics of the quarter car model." *Journal of sound and vibration*, (2005) 282: 111-124.

[17]. Van Deusen, B.D. "Human response to vehicle vibration." *SAE transactions* , 1969 vol.77: paper 680090.

[18]. Society of automotive engineers, "Ride and vibration ata manual." *SAE J6a*, 1965.

[19]. International Standard ISO, 2631/1-1985. "Evaluation of human exposure to whole-body vibration, part1: General requirements." *International Organization for standardization*, 1985.

[20]. Hillier, V.A.W. *Fundamentals of motor vehicle technology.* Cheltenham, UK: Nelson Thornes Ltd, fourth edition, 2001.

[21]. Den Hartog, J. P. *Mechanical Vibrations.* Newyork & London: McGRAW-Hill Boo Company, 1947.

[22]. Ph. Couderc, J. Callenaere, J. Der hagopian and G. Ferraris. "Vehicle Driveline Dynamic Behaviour: Experimentation and Simulation." *Journal of Sound and Vibration*, (1998) 218(1): 133-157.

[23]. Pacejka, H. B. "Tire factors and front wheel vibrations." *International journal of vehicle design*, 1980: 97-119.

[24]. Brandt, A. *Introductory noise and vibration analysis.* Saven Edu Tech Ab, Täby, Sweden.

10 Appendix

10.1 LTI object

[x,t]=lsim(sys,f) where sys is an LTI object[1], sys=tf(1,[m(1,j),c(1,j),k(1,j)]) and f is the input data.

10.2 Driveline Modeling MATLAB code

```
clc
clear all
% close all
global i A F M H

K=[7000 0 -5000 0 0 0 0 0 0 0 0 0 0 0. 0 7000 -5000 0 0 0 0 0 0 0 0 0 0
0.-5000 -5000 210000 -200000 0 0 0 0 0 0 0 0 0 0.0 0 -200000 300000 -
100000 0 0 0 0 0 0 0 0 0 0.0 0 0 -100000 200000 -100000 0 0 0 0 0 0 0 0.0 0
0 0 -100000 1100000 -1000000 0 0 0 0 0 0 0.0 0 0 0 0 -1000000 3000000 -
2000000 0 0 0 0 0 0.0 0 0 0 0 0 -2000000 2050000 -50000 0 0 0 0 0.0 0 0 0
0 0 0 -50000 1050000 -1000000 0 0 0 0.0 0 0 0 0 0 0 0 -1000000 2000000 -
1000000 0 0 0.0 0 0 0 0 0 0 0 0 -1000000 2000000 -1000000 0 0.0 0 0 0 0 0
0 0 0 0 -1000000 2000000 -1000000 0.0 0 0 0 0 0 0 0 0 0 0 -1000000 1200000
-200000.0 0 0 0 0 0 0 0 0 0 0 0 -200000 200000].
K1=rot90(K,2).



M=[0.3 0 0 0 0 0 0 0 0 0 0 0 0 0.0 0.03 0 0 0 0 0 0 0 0 0 0 0 0.0 0 0.03 0
0 0 0 0 0 0 0 0 0 0.0 0 0 0.03 0 0 0 0 0 0 0 0 0 0.
0 0 0 0 0.03 0 0 0 0 0 0 0 0 0 0.0 0 0 0 0 0 1 0 0 0 0 0 0 0 0 0.0 0 0 0 0 0
0.05 0 0 0 0 0 0 0 0.0 0 0 0 0 0 0 0.03 0 0 0 0 0 0 0.
0 0 0 0 0 0 0 0 0 0.05 0 0 0 0 0 0.0 0 0 0 0 0 0 0 0 0 0.02 0 0 0 0 0. 0 0 0 0 0 0
0 0 0 0 0 0.02 0 0 0. 0 0 0 0 0 0 0 0 0 0 0 0 0.3 0 0.
0 0 0 0 0 0 0 0 0 0 0 0 0 2 0. 0 0 0 0 0 0 0 0 0 0 0 0 0 0 2].


C=[3 -3 0 0 0 0 0 0 0 0 0 0 0 0.-3 5 0 0 0 0 0 0 0 0 0 0 0 0.0 0 2 0 0 0 0
0 0 0 0 0 0 0.0 0 0 2 0 0 0 0 0 0 0 0 0 0.
0 0 0 0 2 0 0 0 0 0 0 0 0 0 0.0 0 0 0 0 0 4.42 -4.42 0 0 0 0 0 0 0.0 0 0 0 0 -
4.42 5.42 0 0 0 0 0 0 0.
0 0 0 0 0 0 0 1 0 0 0 0 0 0 0.0 0 0 0 0 0 0 0 1 0 0 0 0 0 0.0 0 0 0 0 0 0 0 0
1.8 0 0 0 0. 0 0 0 0 0 0 0 0 0 0 0 1.8 0 0 0 0.
0 0 0 0 0 0 0 0 0 0 0 0 2 0 0.0 0 0 0 0 0 0 0 0 0 0 0 0 10 0.0 0 0 0 0 0 0 0 0 0
0 0 0 0 10].
```

[1] According to MATLAB help, LTI object is a tool to define transfer function for differential equation of a Linear Time Invariant systems, for example You can create transfer function (TF) models by specifying numerator and denominator coefficients.

```
num = [1 0].
den = [1 2 1].
sys = tf (num,den)

Transfer function:
      s
-------------
s^2 + 2 s + 1
```

```
A=zeros(14,14).
A(1:14,15:28)=eye(14,14).
A(15:28,1:14)=-M^(-1)*K1.
A(15:28,15:28)=-M^(-1)*C.


[U,w2]=eig(K1,M).
omega=sqrt(w2).
f=omega/(2*pi).
for j=1:14
    U(:,j)=U(:,j)/max(U(:,j)).
end
for j=1:14
    m(1,j)=U(:,j)'*M*U(:,j).
    k(1,j)=U(:,j)'*K1*U(:,j).
    c(1,j)=U(:,j)'*C*U(:,j).
end

for j=1:14
    gamma(1,j)=1/sqrt(m(1,j)).
    U1(:,j)=gamma(1,j)*U(:,j).
end



load neda2000rpm100nm_110210

t1=linspace(0,(1279999/128000),1280000).
w=2000*2*pi/60.
degree=w*t1*180/pi.

torque1=hp1433_convdata.p_cyl_1*0.043.*(sin(w*t1)+1/4*sin(w*t1).*cos(w*t1)
)'*pi*0.086^2/4*10^5.

% t_sample = t1(2). % time sample step length
% n = 1. % order
% fn = 500. % [Hz] cutoff frequency
% Wn = fn/(2*pi)*t_sample.
% [b,a] = butter(n,Wn).
% torque1= filtfilt(b, a, torque1).


mean1=mean(torque1).
torque1_fluc=torque1-mean1.

torque2=-
hp1433_convdata.p_cyl_2*0.043.*(sin(w*t1)+1/4*sin(w*t1).*cos(w*t1))'*pi*0.
086^2/4*10^5.


% t_sample = t1(2). % time sample step length
% n = 1. % order
% fn = 500. % [Hz] cutoff frequency
% Wn = fn/(2*pi)*t_sample.
% [b,a] = butter(n,Wn).
% torque2= filtfilt(b, a, torque2).

mean2=mean(torque2).
torque2_fluc=torque2-mean2.
```

```
torque3(1:3841)=torque2(3841:7681).
torque3(3842:7681)=torque2(1:3840).
torque3=torque3'.
for j=1:165
torque3((7681*j)+1:(j+1)*7681)=torque3(1:7681).
end
torque3(1275047:1280000)=0.
mean3=mean(torque3).
torque3_fluc=torque3-mean3.

torque4(1:3841)=torque1(3841:7681).
torque4(3842:7681)=torque1(1:3840).
torque4=torque4'.
for j=1:165
torque4((7681*j)+1:(j+1)*7681)=torque4(1:7681).
end
torque4(1275047:1280000)=0.
mean4=mean(torque4).
torque4_fluc=torque4-mean4.

Force(1,1:1280000)=0.
Force(2,1:1280000)=torque1_fluc.
Force(3,1:1280000)=torque2_fluc.
Force(4,1:1280000)=torque3_fluc.
Force(5,1:1280000)=torque4_fluc.
for j=6:14
    Force(j,1:1280000)=0.
end

F=zeros(28,1280000).
F(15:28,1:1280000)=M^(-1)*Force.


N=U'*Force.
for j=1:14
sys=tf(1,[m(1,j),c(1,j),k(1,j)]).
sys_ss = ss(sys).
[x(:,j),t1]=lsim(sys_ss,N(j,:),t1,[0.0]).

end

x=x'.
response=U1*x.

fs=128000.
```

Runge-kutta integration

```
tsol=zeros(1,1280000).
zsol=zeros(28,1280000).

t=0. z(1:14)=0.z(15:28)=0.
tstop=10.
h=1/fs*2.
[tsol,zsol]=runkut4_driveline(t,z,tstop,h).

          function [tsol,zsol]=runkut4_driveline(t,z,tstop,h)
          global F A i M
          if size(z,1)>1. z=z'. end
```

```
tsol=zeros(1280002,1).zsol=zeros(1280002,length(z)).
tsol(1)=t.zsol(1,:)=z.

F1=zeros(1,28).

i=1.
while t<tstop

F1(1:28)=A*z'+F(1:28,i).
     h=min(h,tstop-t).
    K1=h*F1.
    z1=z+K1/2.

F1(1:28)=A*z1'+F(1:28,i).

    K2=h*F1.
    z2=z+K2/2.

F1(1:28)=A*z2'+F(1:28,i).
    K3=h*F1.
    z3=z+K3.

F1(1:28)=A*z3'+F(1:28,i).

    K4=h*F1.
    z=z+(K1+2*K2+2*K3+K4)/6.
    t=t+h.
    i=i+1
    tsol(i)=t.zsol(i,:)=z.
end
```

10.3 Power spectral density function

```
function [Pxx,f_v] = psd(x,Fs,nfft,noverlap)
%PSD Power Spectral Density estimate.
%   PSD has been replaced by SPECTRUM objects.  PSD still works but may be
%   removed in the future. Use SPECTRUM (or its functional form PWELCH)
%   instead. Type help SPECTRUM for details.
%
%   See also SPECTRUM.

%   Author(s): T. Krauss, 3-26-93
%   Copyright 1988-2005 The MathWorks, Inc.
%   $Revision: 1.12.4.5 $  $Date: 2007/12/14 15:05:42 $

%   NOTE 1: To express the result of PSD, Pxx, in units of
%           Power per Hertz multiply Pxx by 1/Fs [1].
%
%   NOTE 2: The Power Spectral Density of a continuous-time signal,
%           Pss (watts/Hz), is proportional to the Power Spectral
%           Density of the sampled discrete-time signal, Pxx, by Ts
%           (sampling period). [2]
%
%               Pss(w/Ts) = Pxx(w)*Ts,     |w| < pi. where w = 2*pi*f*Ts

%   References:
%     [1] Petre Stoica and Randolph Moses, Introduction To Spectral
%         Analysis, Prentice hall, 1997, pg, 15
%     [2] A.V. Oppenheim and R.W. Schafer, Discrete-Time Signal
%         Processing, Prentice-Hall, 1989, pg. 731
%     [3] A.V. Oppenheim and R.W. Schafer, Digital Signal
```

```
%         Processing, Prentice-Hall, 1975, pg. 556

% error(nargchk(1,7,nargin,'struct'))
% x = varargin{1}.
% [msg,nfft,Fs,window,noverlap,p,dflag]=psdchk(varargin(2:end),x).
% if ~isempty(msg), error(generatemsgid('SigErr'),msg). end
dflag='none'.
% compute PSD

window = flattopwin(nfft).
n = length(x).          % Number of data points
nwind = length(window). % length of window
if n < nwind            % zero-pad x if it has length less than the window
length
    x(nwind)=0.  n=nwind.
end
% Make sure x is a column vector. do this AFTER the zero-padding
% in case x is a scalar.
x = x(:).

k = fix((n-noverlap)/(nwind-noverlap)). % Number of windows
                                        %k = fix(n/nwind). %for
noverlap=0

%   if 0
%       disp(sprintf('   x        = (length %g)',length(x)))
%       disp(sprintf('   y        = (length %g)',length(y)))
%       disp(sprintf('   nfft     = %g',nfft))
%       disp(sprintf('   Fs       = %g',Fs))
%       disp(sprintf('   window   = (length %g)',length(window)))
%       disp(sprintf('   noverlap = %g',noverlap))
%       if ~isempty(p)
%           disp(sprintf('   p        = %g',p))
%       else
%           disp('   p        = undefined')
%       end
%       disp(sprintf('   dflag    = ''%s''',dflag))
%       disp('   --------')
%       disp(sprintf('   k        = %g',k))
%   end
index = 1:nwind.
KMU = k*norm(window)^2. % Normalizing scale factor ==> asymptotically
unbiased
% KMU = k*(sum(window))^2.% alt. Nrmlzng scale factor ==> peaks are about
right

Spec = zeros(nfft,1). % Spec2 = zeros(nfft,1).
for i=1:k
    if strcmp(dflag,'none')
        xw = window.*(x(index)).
    elseif strcmp(dflag,'linear')
        xw = window.*detrend(x(index)).
    else
        xw = window.*detrend(x(index),'constant').
    end
    index = index + (nwind - noverlap).
    Xx = abs(fft(xw,nfft)).^2.
    Spec = Spec + Xx.
%     Spec2 = Spec2 + abs(Xx).^2.
end
```

```
% Select first half
if ~any(any(imag(x)~=0)),   % if x is not complex
    if rem(nfft,2),    % nfft odd
        select = (1:(nfft+1)/2)'.
    else
        select = (1:nfft/2+1)'.
    end
    Spec = Spec(select).
%     Spec2 = Spec2(select).
%    Spec = 4*Spec(select).     % double the signal content - essentially
% folding over the negative frequencies onto the positive and adding.
%    Spec2 = 16*Spec2(select).
else
    select = (1:nfft)'.
end
f_v = (select - 1)*Fs/nfft.

% find confidence interval if needed
% if (nargout == 3) || ((nargout == 0) && ~isempty(p)),
%     if isempty(p),
%         p = .95.    % default
%     end
%     % Confidence interval from Kay, p. 76, eqn 4.16:
%     % (first column is lower edge of conf int., 2nd col is upper edge)
%     confid = Spec*chi2conf(p,k)/KMU.
%
%     if noverlap > 0
%         disp('Warning: confidence intervals inaccurate for NOVERLAP >
0.')
%     end
% end

Pxx = Spec*(2/KMU).   % normalize

% set up output parameters
% if (nargout == 3),
%    Pxx = Spec.
%    Pxxc = confid.
%    f = freq_vector.
% elseif (nargout == 2),
%    Pxx = Spec.
%    Pxxc = freq_vector.
% elseif (nargout == 1),
%    Pxx = Spec.
% elseif (nargout == 0),
%    if ~isempty(p),
%        P = [Spec confid].
%    else
%        P = Spec.
%    end
%    newplot.
%    plot(freq_vector,10*log10(abs(P))), grid on
%    xlabel('Frequency'), ylabel('Power Spectrum Magnitude (dB)').
% end
```

10.4 Vehicle modeling MATLAB codeATLAB code

```
clc
clear all
% close all
global A F i
```

```
k=[7000 0 -5000 0 0 0 0 0 0 0 0 0 0 0. 0 7000 -5000 0 0 0 0 0 0 0 0 0 0
0.-5000 -5000 210000 -200000 0 0 0 0 0 0 0 0 0 0.0 0 -200000 300000 -
100000 0 0 0 0 0 0 0 0 0.0 0 0 -100000 200000 -100000 0 0 0 0 0 0 0 0.0 0
0 0 -100000 1100000 -1000000 0 0 0 0 0 0 0.0 0 0 0 0 -1000000 3000000 -
2000000 0 0 0 0 0 0.0 0 0 0 0 0 -2000000 2050000 -50000 0 0 0 0 0.0 0 0 0
0 0 0 -50000 1050000 -1000000 0 0 0 0.0 0 0 0 0 0 0 0 -1000000 2000000 -
1000000 0 0 0.0 0 0 0 0 0 0 0 0 -1000000 2000000 -1000000 0 0.0 0 0 0 0 0
0 0 0 0 -1000000 2000000 -1000000 0.0 0 0 0 0 0 0 0 0 0 0 -1000000 1200000
-200000.0 0 0 0 0 0 0 0 0 0 0 0 -200000 200000].
K3=rot90(k,2).


K=K3(1:12,1:12).
K(13:18,13:18)=zeros(6,6).
K(12,13)=-10000.
K(13,12)=-10000.
K(13,13)=10000.
K(13,14)=-.3^2*5e5.
K(13,16)=-0.03*.3*4e5.
K(14,16)=-0.03*.3*4e5.
K(15,14)=.3*5e5.
K(15,15)=1e8.
K(15,16)=0.03*4e5.
K(15,17)=-1e8.
K(16,16)=49e4.
K(16,18)=-9e4.
K(17,15)=-1e8.
K(17,17)=1e8.
K(18,16)=-9e4.
K(18,18)=9e4.



M=[0.3 0 0 0 0 0 0 0 0 0 0 0 0 0.0 0.03 0 0 0 0 0 0 0 0 0 0 0 0.0 0 0.03 0
0 0 0 0 0 0 0 0 0 0.0 0 0 0.03 0 0 0 0 0 0 0 0 0 0.
0 0 0 0 0 0.03 0 0 0 0 0 0 0 0 0 0.0 0 0 0 0 0 1 0 0 0 0 0 0 0 0 0.0 0 0 0 0 0 0
0.05 0 0 0 0 0 0 0 0.0 0 0 0 0 0 0 0 0.03 0 0 0 0 0 0 0.
0 0 0 0 0 0 0 0 0 0.05 0 0 0 0 0 0.0 0 0 0 0 0 0 0 0 0 0 0.02 0 0 0 0 0. 0 0 0 0 0 0
0 0 0 0 0 0.02 0 0 0. 0 0 0 0 0 0 0 0 0 0 0 0 0 0.3 0 0.
0 0 0 0 0 0 0 0 0 0 0 0 0 2 0. 0 0 0 0 0 0 0 0 0 0 0 0 0 0 0 2].

M=M(1:12,1:12).
M(13:18,13:18)=zeros(6,6).
M(13,13)=4.12.
M(13,14)=0.12.
M(14,13)=0.12.
M(14,14)=0.12.
M(15,15)=180.
M(16,16)=180.
M(17,17)=1800.
M(18,18)=1800.


C=[3 -3 0 0 0 0 0 0 0 0 0 0 0 0.-3 5 0 0 0 0 0 0 0 0 0 0 0 0 0.0 0 2 0 0 0 0
0 0 0 0 0 0 0.0 0 0 2 0 0 0 0 0 0 0 0 0 0 0.
0 0 0 0 2 0 0 0 0 0 0 0 0 0 0 0.0 0 0 0 0 0 4.42 -4.42 0 0 0 0 0 0 0.0 0 0 0 0 0 -
4.42 5.42 0 0 0 0 0 0 0.
```

```
0 0 0 0 0 0 0 1 0 0 0 0 0 0.0 0 0 0 0 0 0 0 1 0 0 0 0 0.0 0 0 0 0 0 0 0 0
1.8 0 0 0 0. 0 0 0 0 0 0 0 0 0 0 0 1.8 0 0 0.
0 0 0 0 0 0 0 0 0 0 0 2 0 0.0 0 0 0 0 0 0 0 0 0 0 0 0 10 0.0 0 0 0 0 0 0 0 0
0 0 0 0 10].

C=C(1:12,1:12).
C(13:18,13:18)=zeros(6,6).
C(13,14)=-0.3^2*4000.
C(13,16)=-0.03*0.3*600.
C(14,16)=-0.03*0.3*600.
C(15,14)=0.3*4000.
C(15,15)=100000.
C(15,16)=0.03*600.
C(15,17)=-100000.
C(16,16)=4600.%
C(16,18)=-4000.%
C(17,15)=-100000.
C(17,17)=100000.
C(18,16)=-4000.%4->2
C(18,18)=4000.%


A=zeros(18,18).
A(1:18,19:36)=eye(18,18).
A(19:36,1:18)=-M^(-1)*K.
A(19:36,19:36)=-M^(-1)*C.


load neda2000rpm100nm_110210.mat

t1=linspace(0,(1279999/128000),1280000).
w=2000*2*pi/60.
degree=w*t1*180/pi.


t_sample = t1(2). % time sample step length
n = 1. % order
fn = 1000. % [Hz] cutoff frequency
Wn = fn/(2*pi)*t_sample.
[b,a] = butter(n,Wn).
pres1= filtfilt(b, a, hp1433_convdata.p_cyl_1).


torque1=pres1*0.043.*(sin(w*t1)+1/4*sin(w*t1).*cos(w*t1))'*pi*0.086^2/4*10
^5.
mean1=mean(torque1).
torque1_fluc=torque1-mean1.


t_sample = t1(2). % time sample step length
n = 1. % order
fn = 1000. % [Hz] cutoff frequency
Wn = fn/(2*pi)*t_sample.
[b,a] = butter(n,Wn).
pres2= filtfilt(b, a, hp1433_convdata.p_cyl_2).
torque2=-
pres2*0.043.*(sin(w*t1)+1/4*sin(w*t1).*cos(w*t1))'*pi*0.086^2/4*10^5.
mean2=mean(torque2).
torque2_fluc=torque2-mean2.
```

```
torque3(1:3841)=torque2(3841:7681).
torque3(3842:7681)=torque2(1:3840).
torque3=torque3'.
for j=1:165
torque3((7681*j)+1:(j+1)*7681)=torque3(1:7681).
end
torque3(1275047:1280000)=0.
mean3=mean(torque3).
torque3_fluc=torque3-mean3.

torque4(1:3841)=torque1(3841:7681).
torque4(3842:7681)=torque1(1:3840).
torque4=torque4'.
for j=1:165
torque4((7681*j)+1:(j+1)*7681)=torque4(1:7681).
end
torque4(1275047:1280000)=0.
mean4=mean(torque4).
torque4_fluc=torque4-mean4.

Force(1,1:1280000)=0.
Force(2,1:1280000)=torque1_fluc.
Force(3,1:1280000)=torque2_fluc.
Force(4,1:1280000)=torque3_fluc.
Force(5,1:1280000)=torque4_fluc.
for j=6:18
    Force(j,1:1280000)=0.
end
F=zeros(36,1280000).
F(19:36,1:1280000)=M^(-1)*Force.


fs=128000.

% tsol=zeros(1,1280000).
% zsol=zeros(36,1280000).
%runge-kutta integration

t=0. z(1:18)=0.z(19:36)=0.
tstop=10.
h=1/fs*2.
[tsol,zsol]=runkut4(t,z,tstop,h).

acc_axle_long=gradient(zsol(1:640002,33)).
acc_vehicle_long=gradient(zsol(1:640002,35)).

x1=acc_vehicle_long.
[Pxx_ovp,f_ovp]=psd_1(x1,2^18,fs,hann(2^18),2^17).
Pxx_ovp=Pxx_ovp/fs.
[n,m]=min(abs(f_ovp-0.89*(33))).
[n1,m1]=min(abs(f_ovp-1.12*(33))).
Pxx_sum=sum(Pxx_ovp(m:m1)).
RMS_psd=sqrt(Pxx_sum*fs/(2^18))
```